# EFFECT OF NANO-CLAY AND SURFACTANT ON THE ABIOTIC AND BIOTIC DEGRADATION OF POLY(LACTIC ACID) FILMS

By

Pooja C. Mayekar

# A THESIS

Submitted to
Michigan State University
in partial fulfillment of the requirements
for the degree of

Packaging – Master of Science

2019

#### **ABSTRACT**

# EFFECT OF NANO-CLAY AND SURFACTANT ON THE ABIOTIC AND BIOTIC DEGRADATION OF POLY(LACTIC ACID) FILMS

By

### Pooja C. Mayekar

The abiotic and biotic degradation of poly(lactic acid) – PLA film and PLA films compounded with two nanoclays - montmorillonite (MMT) and organomodified MMT (OMMT), and a surfactant - stearyl bis(2-hydroxyethyl) methyl ammonium chloride (QAC) was evaluated in inoculated and non-inoculated vermiculite, and a simulated compost environment ( $58 \pm 2^{\circ}$ C, 50  $\pm$  5% RH). All films were produced in-house with approximately the same number average molecular weight  $(M_n)$ , crystallinity, and thickness. After full thermal, morphological and physical characterization, the  $M_n$  and evolved CO<sub>2</sub> were used as the key parameters to track the evolution of the abiotic and biotic processes, respectively. The abiotic stage was not significantly altered due to the presence of nanoclays, and the biodegradation rates of the PLA and PLA nanocomposite films were not modified as opposed to the claims made by the studies conducted before. There was no reduction in lag time of PLA due to the addition of nanoclays. The biodegradation test in a simulated compost environment showed higher mineralization for PLA films with QAC as compared to PLA films with MMT and OMMT, due to the presence of two alkyl (tallow) tails imparting more hydrophilicity and plasticization effect. Similar results were seen in the inoculated and non-inoculated vermiculite. The hydrolysis experiment was conducted to decouple the abiotic/ hydrolytic phase of biodegradation at  $58 \pm 2$ °C, and the addition of nanoclays did not improve the degradation of PLA. Overall, the inclusion of nanoclays did not enhance the hydrolytic degradation or biodegradation of PLA films.

Copyright By POOJA C. MAYEKAR 2019 Dedicated to my parents, Chandrashekhar and Chhaya Mayekar brother, Prasad

#### **ACKNOWLEDGMENTS**

One of the most challenging things when you write a thesis, is writing the acknowledgment which reminds me of my advisor's quote, "It's never about the destination, but it's about the journey", and what a journey this has been. I would like to start off my acknowledgment by thanking my advisor, Dr. Rafael Auras for his unending support, guidance and faith in me throughout this journey. Not only is he an amazing advisor but also a great role model. From giving us the freedom to work at our own pace to checking on us if we got enough sleep as graduate students, he truly exceeded the duties of an advisor. I would also like to extend my gratitude towards my committee members, Dr. Susan Selke (School of Packaging, Michigan State University) and Dr. Ramani Narayan (College of Engineering, Michigan State University) for their support and constructive feedback throughout my research.

Any research would not be feasible without proper lab equipments and a great lab manager to go with that. Hence, I would like to thank my lab manager, Mr. Aaron Walworth (School of Packaging, Michigan State University) for letting me use the lab resources. Next, I would like to thank my research group members: Uruchaya, Fabiola, Anibal especially Edgar Castro and Wanwarang Limsukon for their constant guidance and support.

I would also like to thank my friends Sonal, Gauri, Aditya, Jiyon, Dhwani, Rishabh and office 105 for their constant encouragement and who turned out to be a family away from home. A special thanks to Akshay Asaithambi for his care and never ending support that he has provided me. Finally, I would like to thank my parents, my brother and my cousin for their love and support without whom all this would have not been possible. Finally, I would like to express my gratitude towards God for giving me the strength and blessing me with this opportunity to be a Spartan!

# TABLE OF CONTENTS

LIST OF TABLES	viii
LIST OF FIGURES	ix
CHAPTER 1	1
INTRODUCTION	1
1.1 Background and motivation	
1.2 Overall goal and objectives	
1.3 Hypothesis	
1.4 Structure of thesis	
REFERENCES	6
CHAPTER 2	11
LITERATURE REVIEW	11
2.1 Introduction	11
2.2 Poly(lactic acid) - PLA	
2.3 Synthesis of PLA	13
2.4 Polymer degradation	17
2.5 Biodegradation	18
2.5.1 Evaluation of Biodegradation	20
2.6 Hydrolytic degradation of PLA	22
2.6.1 Mechanism of Hydrolysis	
2.6.2 Parameters dominating the hydrolytic degradation	25
2.6.2.1 pH	
2.6.2.2 Temperature	29
2.6.2.3 Molecular weight	30
2.6.2.4 Crystallinity	
2.7 PLA nanocomposites	35
2.7.1 Characteristic	37
2.7.1.1 Montmorillonite structure	37
2.7.1.2 Surface modification of clay	
2.7.1.3 Morphology	43
2.7.1.4 Advantages of PLA nanocomposite	
2.7.1.5 Effect of nanoclay on PLA biodegradation	
REFERENCES	49
CHAPTER 3	
MATERIALS & METHODS	
3.1 Direct Measurement Respirometric & Hydrolysis Materials	
3.2 Production of Masterbatches	67
3.3 Production of Nanocomposite Films	68
3.4 Material characterization	69
3.4.1 Differential scanning calorimetry (DSC)	69

3.4.2 Thermogravimetric Analysis (TGA)	70
3.4.3 Carbon, Hydrogen & Nitrogen analysis (CHN Analyzer)	
3.4.4 Size Exclusion Chromatography (SEC)	
3.4.5 Digital Micrometer.	72
3.4.6 Scanning Electron Microscopy (SEM)	
3.4.7 X-ray diffraction study (XRD)	
3.5 Biodegradation Test	
3.5.1 Moisture Analyzer	
3.5.2 Preparation of inoculum solution	74
3.5.3 Biodegradation in compost	
3.5.4 Biodegradation in vermiculite	
3.6 Hydrolysis Test	
REFERENCES	
CHAPTER 4	80
RESULTS & DISCUSSIONS	80
4.1 Initial characterization of the films	
4.1.1 Initial Molecular weight	80
4.1.2 Initial Thickness	
4.1.3 Crystallinity	82
4.1.4 Amount of Nanoclay	
4.1.5 Characterization of PLA OMMT films	
4.2 Biodegradation: CO <sub>2</sub> evolution and mineralization	87
4.2.1 Biodegradation in Compost	
4.2.2 Biodegradation in Non-inoculated & Inoculated vermiculite	
4.3 Molecular weight	
4.3.1 Molecular Weight distribution	
4.4 Hydrolysis	
4.4.1 Molecular Weight	
4.5 Crystallinity evolution during hydrolysis	109
REFERENCES	113
CHAPTER 5	117
CONCLUSIONS & RECOMMENDATIONS	
5.1 Conclusions	117
5.2 Recommendations	119
REFERENCES	120

# LIST OF TABLES

Table 2.1. Type and causes of polymer degradation, adapted from [33]
Table 2.2. Commonly modified montmorillonites used for producing PLA nanocomposites, adapted from [17]
Table 3.1. Physical data of organomodified clay [1]
Table 3.2. Processing conditions for cast film extrusion
Table 3.3. Detailed composition of 1L mineral solution
Table 4.1. Initial molecular weight of PLA, PLA-OMMT & PLA-MMT & PLA-QAC films 80
Table 4.2. Micrometer and SEM thickness t for all the films
Table 4.3. Crystallinity χc (%) for all the films
Table 4.4. Amounts of carbon, hydrogen & nitrogen content determined by CHNS/O Elemental Analyzer (%)
Table 4.5. Thermal properties of PLA, PLA-QAC, PLA-MMT and PLA-OMMT films 84
Table 4.6. presents the rate constant k (d-1) for PLA, PLA-OMMT, PLA-MMT and PLA-QAC exposed to different medias
Table 4.7. Rate constants for PLA, PLA-QAC, PLA-OMMT & PLA-MMT films in water at 60°C
Table 4.8. Crystallinity for PLA, PLA-QAC, PLA-OMMT & PLA-MMT films in water at 60°C at end of hydrolysis (45 days)

# LIST OF FIGURES

Figure 2.1. Number of research reports published between 1995 and 2018 (from Web of Science®Core Collection search results with title key-words "PLA", "PLLA", "PDLA", "polylactic acid", "polylactide", and "poly(lactic acid)"
Figure 2.2. Chemical structure of L-(+)-lactic acid (left) and D-(-)Lactic acid (right), adapted from [17]
Figure 2.3. Manufacturing process to produce high molecular weight PLA, adapted from [17]
Figure 2.4. PLA synthesis by ring-opening polymerization [27]
Figure 2.5. Schematic representation of Biodegradation mechanism, adapted from [98] 20
Figure 2.6. Hydrolysis and cleavage of ester linkage, adapted from [76]
Figure 2.7. Schematic representation of bulk erosion (top) and surface erosion (bottom), adapted from [84]
Figure 2.8. Hydrolytic degradation mechanism in : (A) alkaline and (B) basic media, adapted from [99]
Figure 2.9. Change in M <sub>n</sub> during hydrolytic degradation (37°C) in phosphate buffered solutions, adapted from [112,142]
Figure 2.10. Hydrolytic degradation for PLLA films with different molecular weights in a phosphate-buffered solution at 37°C, adapted from [143]
Figure 2.11. Diffusion of water is restricted to the crystalline regions as opposed to amorphous regions, adapted from [84]
Figure 2.12. Change in PLA structure (a) before and (b) after hydrolysis, adapted from [145]
Figure 2.13. Different types of nanoscale materials, adapted from [150]

Figure 2.14. Categorization of natural clay, adapted from [161]
Figure 2.15. Structure of montmorillonite (2:1 phyllosilicates). Reproduced from [158] 39
Figure 2.16. Surface modification of clay using quaternary ammonium, adapted from [157]
Figure 2.17. Different morphologies obtained from the nanoclay polymer interaction, adapted from [163]
Figure 3.1. Hydrolysis setup in the lab and migration cell, partially reproduced from [7] 77
Figure 4.1. SEM micrographs of a) PLA, b) PLA-MMT, c) PLA-QAC and d) PLA-OMMT
Figure 4.2. DSC curve for PLA OMMT film
Figure 4.3. TGA of PLA, PLA-QAC, PLA-MMT and PLA-OMMT films
Figure 4.4. XRD spectra for OMMT and MMT clay powder ,PLA-OMMT, PLA-MMT and PLA films
Figure 4.5. CO2 evolution (a) and % Mineralization (b) of PLA, PLA-OMMT, PLA-MMT and PLA-QAC films in compost
Figure 4.6. CO2 evolution (a) and % Mineralization (b) of PLA, PLA-OMMT, PLA-MMT and PLA-QAC films in non-inoculated vermiculite
Figure 4.7. CO2 evolution (a) and % Mineralization (b) of PLA, PLA-OMMT, PLA-MMT and PLA-QAC films in inoculated vermiculite
Figure 4.8. Initial molecular weight distribution for PLA, PLA-OMMT, PLA-MMT and PLA-QAC films

Figure 4.9. Change in molecular weight distribution for PLA film in Compost
Figure 4.10. Deconvolution of PLA peaks at days a) 5, b) 10, c) 15, d) 20 in Compost media
Figure 4.11. a) Mn and b) area fraction as function for PLA in compost after performing deconvolution
Figure 4.12. Molecular weight reduction as a function of time for PLA, PLA-OMMT, PLA-MMT and PLA-QAC films in (a) compost media, (b) inoculated vermiculite and (c) non-inoculated vermiculite. Fitting of first order reaction: $Mn = Mno \ exp(-kt)$ , where Mn is the number average molecular weight at time $t$ , $Mno$ is the initial Mn and k is the rate constant
Figure 4.13. Change in molecular weight distribution for a) PLA b) PLA-OMMT c) PLA-
MMT and d) PLA-QAC films in compost
Figure 4.14. Molecular weight reduction as a function of time for PLA, PLA-OMMT, PLA-MMT and PLA-QAC films in water at 60°C. Fitting of first order reaction: $M_n = M_{no} \exp(-kt)$ , where Mn is the number average molecular weight at time $t$ , $M_{no}$ is the initial $M_n$ and $k$ is the rate constant
Figure 4.15. Change in molecular weight distribution for a) PLA b) PLA-OMMT c) PLA-MMT and d) PLA-QAC films in water at 60°C
Figure 4.16. DSC thermograms of a) PLA b) PLA-OMMT c) PLA-MMT and d) PLA-QAC in water at 60°C (1st cycle). The numbers on the thermogram indicate the day immersed 110

#### CHAPTER 1

#### INTRODUCTION

#### 1.1 Background and motivation

As per the U.S. Environmental Protection Agency (EPA), around 262 million tons of municipal solid waste (MSW) was generated in the United States in 2015. More than 137 million tons of MSW (52.5%) ended up in landfill whereas only 8.9% ended up in composting facilities. Plastics formed around 13.1% of the total waste generated of which only 4.6% was recovered. Of the 138 million tons going to landfill, plastics accounted for 18.9%. Packaging generated the highest amount of MSW, around 78 million tons [1]. The huge amount of plastic accumulating in the landfill, is an alarming concern for the environment, leading to problems such as greenhouse gas emissions, global warming etc.

Worldwide production of plastics was estimated over 322 million tons in 2015 [2], due to rising economy globally. Therefore to curb the problems of waste disposal of plastics after use, reduce the dependence on non-renewable fossil based fuels and create a sustainable environment by adopting ecofriendly solutions, industries have turned to bioplastics, particularly due to their biodegradable nature [3]. Biodegradable plastics like polylactic acid (PLA), thermoplastic starch (TPS), polyhydroxyalkanoate (PHA) and poly(butylene adipate-co-terephthalate) can be diverted to an additional end of life scenario (composting) [4]. Additionally, the transition from conventional plastics to bioplastics can be backed up by the numbers from the extensive market research conducted by Germany's nova-Institute, hinting towards an upward trend showing increase in global bioplastic production capacity from 3.5 million tonnes in 2011 to around 12 million tonnes in 2020 [5].

PLA, a biobased biodegradable thermoplastic polyester, has turned out to be a major player in the market due to exhibiting reasonable properties, which mimics its conventional counterparts, such as high clarity, optimal strength, compostable, non-toxic, ease of processing [6–11]. These appealing benefits can be translated as PLA has captivated the global market, valued at USD 698.27 million in 2017. It is estimated to reach USD 2091.29 million in 2023, lodging a compound annual growth rate (CAGR) of 20.06%, with packaging dominating the market share [12].

PLA, however, has few drawbacks such as its inherent brittleness, which is manifested in less impact strength and toughness, easy degradation at substantially high temperatures, low flexibility, which has limited its potential reach to few sectors [13–15]. There have been several studies spanning over the past two decades, which focused on improving PLA's properties by incorporating fillers or by blending PLA with other biodegradable and conventional polymers [16–20]. Addition of nanoparticles has a huge potential since they bring significant improvement in the shortcomings of PLA by producing PLA nanocomposites. The PLA properties can be tailored by achieving good dispersion and facilitating the interfacial interaction between the nanofillers and the polymer matrix, thus reaping the benefits of the individual components by inducing optical clarity, barrier to gases and water, surface morphology, high moduli [21–23].

Among the nanoparticles, inorganic layered silicates or nanoclays have achieved a breakthrough due to their low cost, easy availability and the significant enhancement they bring when added in low concentrations [24]. Montmorillonite (MMT) is one such nanoclay, which received great attention from industry and academia since it exhibits dramatic improvement in mechanical, thermal and barrier properties in PLA, for loadings as low as 5%. Surface modification of MMT is essential to draw on to this advantages and to facilitate the integration of nanoparticles in the polymer matrix [25]. Ample research in PLA nanocomposites based on organomodified

montmorillonite (OMMT) have shown improvement in tensile modulus, flexural strength, barrier to permeants properties in comparison to pure PLA [26–28].

Apart from the property shortcomings, one another disadvantage of biodegradable polymers such as PLA is that it degrades at a slower pace as compared to other organic wastes in composting environment, which affects their admittance into industrial composting facilities [29]. Studies have identified that inclusion of OMMT enhances the biodegradation rate of biodegradable polymers as compared to their respective pristine polymer. In retrospect, incorporation of nanoclays not only improves the performance of polymer, but it also provides an added advantage of enhanced biodegradability in composting facilities [29–41].

Albeit so much research has been conducted, it is still not clear how the nanoclays and the organomodifiers (surfactant) affect the hydrolytic degradation and biodegradation (abiotic and biotic phase) of PLA, especially since nanoclays are known to increase chain scission of PLA during processing and to reduce the molecular weight when added to PLA. The specific role of unmodified clay, organomodified clay and surfactant has still not been investigated in depth pertaining to the changes it brings in molecular weight, which is an important factor tracked throughout the biodegradation process.

# 1.2 Overall goal and objectives

The overall goal of this research is to understand the role of nanoclays and surfactant and their effect on the hydrolytic degradation and biodegradation of PLA and PLA nanocomposites. Work done by previous researchers have claimed OMMT, as responsible for faster and higher biodegradation, but no control was exercised over the main characteristics of the fabricated nanocomposite like initial molecular weight, crystallinity, amount of clay and thickness of the samples [42]. The comparison between PLA and PLA nanocomposites has been two different starting points due to the difference in the initial molecular weight thereby giving edge to PLA nanocomposites. To answer this question whether nanoclays really enhance the biodegradation of biodegradable polymers, PLA with unmodified clay (MMT), organomodified clay (OMMT) and surfactant (QAC) will be used as reference model system to test biodegradation in simulated composting conditions.

The main goal was further divided into different specific objectives as outlined below:

- To produce PLA, PLA-MMT, PLA-OMMT and PLA-QAC films having same characteristics such as molecular weight, crystallinity and thickness with an experimental variation of not more than 10%.
- To evaluate the effect of nanoclays and surfactant on the hydrolytic degradation of PLA nanocomposites to understand and decouple the abiotic phase of biodegradation.
- 3. To gain in depth knowledge and investigate the effect of nanoclays and surfactant on the biodegradation rate of PLA in simulated compost environment.

To bridge this missing gap, hydrolysis and biodegradation tests will be conducted as per their respective standards [43,44].

# 1.3 Hypothesis

This research aspires to test the general hypothesis: "Abiotic and biotic degradation of biodegradable polymers are affected by the presence of nanoclays".

# 1.4 Structure of thesis

The first chapter of the thesis establishes the logical reasoning as to the need of conducting this research. Chapter 2 provides a thorough literature background shedding light on PLA, nanocomposites and surfactant, influence of nanoclay on the biodegradation of PLA nanocomposites, and parameters influencing the hydrolysis process. The manufacturing of samples, material description and experimental setup is detailed in Chapter 3. Chapter 4 discusses the results from the hydrolysis and biodegradation tests and provides insights on the role and impact of nanoclays and surfactant on PLA degradation rate. Chapter 5 summarizes all the work conducted and the experimental findings deduced and concludes with future work recommendations.

**REFERENCES** 

#### REFERENCES

- [1] EPA, "Advancing Sustainable Materials Management: 2015 Fact Sheet," 2018.
- [2] Eric Beckman, "Production, use, and fate of all plastics ever made," 2018.
- [3] S. M. Emadian, T. T. Onay, and B. Demirel, "Biodegradation of bioplastics in natural environments," *Waste Manag.*, vol. 59, pp. 526–536, 2017.
- [4] R. Auras, B. Harte, and S. Selke, "An overview of polylactides as packaging materials," *Macromol. Biosci.*, vol. 4, no. 9, pp. 835–864, 2004.
- [5] A. S. Mirabal, L. Scholz, and M. Carus, "Market study on Bio-based Polymers in the World Capacities, Production and Applications: Status Quo and Trends towards 2020," 2013.
- [6] R. Sikkema, H. M. Junginger, W. Pichler, S. Hayes, and A. P. C. Faaij, "Present and future development in plastics from biomass," *Biofuels, Bioprod. Biorefining*, vol. 4, no. 1, pp. 132–153, 2010.
- [7] D. Notta-Cuvier *et al.*, "Tailoring polylactide (PLA) properties for automotive applications: Effect of addition of designed additives on main mechanical properties," *Polym. Test.*, vol. 36, pp. 1–9, 2014.
- [8] P. Sanglard, V. Adamo, J.-P. Bourgeois, T. Chappuis, E. Vanoli, and E. Vanoli, "Poly(lactic acid) Synthesis and Characterization," *Chimia (Aarau)*., vol. 66, no. 12, pp. 951–954, 2012.
- [9] Y. Li, "Biodegradable Poly(Lactic Acid) Nanocomposites: Synthesis And Characterization," 2011.
- [10] K. Hamad, M. Kaseem, H. W. Yang, F. Deri, and Y. G. Ko, "Properties and medical applications of polylactic acid: A review," *Express Polym. Lett.*, vol. 9, no. 5, pp. 435–455, 2015.
- [11] Y. Hu, W. A. Daoud, K. K. L. Cheuk, and C. S. K. Lin, "Newly Developed Techniques on Polycondensation, Ring-Opening Polymerization and Polymer Modification: Focus on Poly(Lactic Acid).," *Mater. (Basel, Switzerland)*, vol. 9, no. 3, Feb. 2016.
- [12] Research and Markets, "Global Polylactic Acid Market Segmented by Raw material, Form, Application and Geography Growth, Trends and Forecasts (2019-2024)." [Online]. Available: https://www.mordorintelligence.com/industry-reports/polylactic-acid-market.
- [13] A. P. Gupta and V. Kumar, "New emerging trends in synthetic biodegradable polymers-Polylactide: A critique," *Eur. Polym. J.*, vol. 43, no. 10, pp. 4053–4074, 2007.

- [14] R. A. Auras, "Investigation of polylactide as packaging material," 2004.
- [15] Niclis Robert Kouloungis, "Aerobic Biodegradability Of Citrate Ester Plasticizers And Plasticized PLA Films In Simulated Soil And Compost Environments," 1999.
- [16] H. Liu and J. Zhang, "Research progress in toughening modification of poly(lactic acid)," *J. Polym. Sci. Part B Polym. Phys.*, vol. 49, no. 15, pp. 1051–1083, 2011.
- [17] H. Balakrishnan, A. Hassan, M. Imran, and M. Uzir Wahit, "Toughening of Polylactic Acid Nanocomposites: A Short Review," *Polym. Plast. Technol. Eng.*, vol. 51, no. 2, pp. 175–192, 2012.
- [18] H. Tsuji, R. Auras, L.-T. Lim, and S. Selke, *Poly(lactic acid): synthesis, structures, properties, processing and applications.* Wiley, 2011.
- [19] S. S. Karkhanis, L. M. Matuana, N. M. Stark, and R. C. Sabo, "Effect Of Compounding Approaches On Fiber Dispersion And Performance Of Poly(Lactic Acid)/Cellulose Nanocrystal Composite Blown Films," 2017.
- [20] M. Raja, S. H. Ryu, and A. M. Shanmugharaj, "Macromolecular Nanotechnology Thermal, mechanical and electroactive shape memory properties of polyurethane (PU)/poly (lactic acid) (PLA)/CNT nanocomposites," *Eur. Polym. J.*, vol. 49, no. 11, pp. 3492–3500, 2013.
- [21] D. N. Bikiaris, "Nanocomposites of aliphatic polyesters: An overview of the effect of different nanofillers on enzymatic hydrolysis and biodegradation of polyesters," *Polym. Degrad. Stab.*, vol. 98, no. 9, pp. 1908–1928, Sep. 2013.
- [22] S. S. Ray and M. Okamoto, "Polymer/layered silicate nanocomposites: a review from preparation to processing," *Prog. Polym. Sci*, vol. 28, no. 11, pp. 1539–1641, 2003.
- [23] S. Pavlidou and C. D. Papaspyrides, "A review on polymer-layered silicate nanocomposites," *Prog. Polym. Sci.*, vol. 33, no. 12, pp. 1119–1198, 2008.
- [24] H. M. C. de Azeredo, "Nanocomposites for food packaging applications," *Food Res. Int.*, vol. 42, no. 9, pp. 1240–1253, 2009.
- [25] S. Kango, S. Kalia, A. Celli, J. Njuguna, Y. Habibi, and R. Kumar, "Surface modification of inorganic nanoparticles for development of organic-inorganic nanocomposites-A review," *Prog. Polym. Sci.*, vol. 38, no. 8, pp. 1232–1261, 2013.
- [26] S. Sinha Ray, P. Maiti, M. Okamoto, K. Yamada, and K. Ueda, "New polylactide/layered silicate nanocomposites. 1. Preparation, characterization, and properties," *Macromolecules*, vol. 35, no. 8, pp. 3104–3110, 2002.
- [27] S. Sinha Ray, K. Yamada, M. Okamoto, and K. Ueda, "New polylactide-layered silicate nanocomposites. 2. Concurrent improvements of material properties, biodegradability and melt rheology," *Polymer (Guildf).*, vol. 44, no. 3, pp. 857–866, 2002.

- [28] S. S. Ray, K. Yamada, M. Okamoto, A. Ogami, and K. Ueda, "New polylactide/layered silicate nanocomposites, 4. Structure, properties and biodegradability," *Compos. Interfaces*, vol. 10, no. 4–5, pp. 435–450, 2003.
- [29] P. Stloukal *et al.*, "Kinetics and mechanism of the biodegradation of PLA/clay nanocomposites during thermophilic phase of composting process," *Waste Manag.*, vol. 42, no. April, pp. 31–40, 2015.
- [30] T. Wu, T. Xie, and G. Yang, "Preparation and characterization of poly(\varepsilon-caprolactone)/Na +-MMT nanocomposites," *Appl. Clay Sci.*, vol. 45, no. 3, pp. 105–110, 2009.
- [31] M. C. S. Corrêa, M. C. Branciforti, E. Pollet, J. A. M. Agnelli, P. A. P. Nascente, and L Avérous, "Elaboration and Characterization of Nano-Biocomposites Based on Plasticized Poly(Hydroxybutyrate-Co-Hydroxyvalerate) with Organo-Modified Montmorillonite," *J. Polym. Environ.*, vol. 20, no. 2, pp. 283–290, 2012.
- [32] N. F. Magalhães and C. T. Andrade, "Thermoplastic corn starch/clay hybrids: Effect of clay type and content on physical properties," *Carbohydr. Polym.*, vol. 75, no. 4, pp. 712–718, 2008.
- [33] Sang-Rock Lee *et al.*, "Microstructure, tensile properties, and biodegradability of aliphatic polyester/clay nanocomposites," *Polymer (Guildf).*, vol. 43, no. 8, pp. 2495–2500, 2002.
- [34] M. A. Paul, C. Delcourt, M. Alexandre, P. Degée, F. Monteverde, and P. Dubois, "Polylactide/montmorillonite nanocomposites: Study of the hydrolytic degradation," *Polym. Degrad. Stab.*, vol. 87, no. 3, pp. 535–542, 2005.
- [35] Y. H. Lee *et al.*, "Electrospun dual-porosity structure and biodegradation morphology of Montmorillonite reinforced PLLA nanocomposite scaffolds," *Biomaterials*, vol. 26, no. 16, pp. 3165–3172, Jun. 2005.
- [36] A. Araújo, M. Oliveira, R. Oliveira, G. Botelho, and A. V. Machado, "Biodegradation assessment of PLA and its nanocomposites," *Environ. Sci. Pollut. Res.*, vol. 21, no. 16, pp. 9477–9486, 2014.
- [37] P. K. Roy, M. Hakkarainen, and A.-C. Albertsson, "Nanoclay effects on the degradation process and product patterns of polylactide," *Polym. Degrad. Stab.*, vol. 97, no. 8, pp. 1254–1260, 2012.
- [38] S. Molinaro *et al.*, "Effect of nanoclay-type and PLA optical purity on the characteristics of PLA-based nanocomposite films," *J. Food Eng.*, vol. 117, no. 1, pp. 113–123, 2013.
- [39] P. M. S. Souza, A. R. Morales, M. A. Marin-Morales, and L. H. I. Mei, "PLA and Montmorilonite Nanocomposites: Properties, Biodegradation and Potential Toxicity," *J. Polym. Environ.*, vol. 21, no. 3, pp. 738–759, 2013.
- [40] A. V. Machado, A. Araújo, and M. Oliveira, "Assessment of polymer-based nanocomposites biodegradability," *Biodegrad. Polym. Vol. 1 Adv. Biodegrad. Study Appl.*,

- pp. 166-196, 2015.
- [41] M. P. Balaguer, C. Aliaga, C. Fito, and M. Hortal, "Compostability assessment of nanoreinforced poly(lactic acid) films," *Waste Manag.*, vol. 48, pp. 143–155, 2016.
- [42] M. Pluta, A. Galeski, M. Alexandre, M.-A. Paul, and P. Dubois, "Polylactide/montmorillonite nanocomposites and microcomposites prepared by melt blending: Structure and some physical properties," *J. Appl. Polym. Sci.*, vol. 86, no. 6, pp. 1497–1506, Nov. 2002.
- [43] ASTM International, "ASTM Standard D4754-18, Standard Test Method for Two-Sided Liquid Extraction of Plastic Materials Using FDA," 2003.
- [44] ASTM International, "ASTM D5338-15: Standard Test Method for Determining Aerobic Biodegradation of Plastic Materials Under Controlled Composting Conditions, Conditions, Incorporating Thermophilic Temperatures," in *ASTM Standards*., 2015, pp. 1–7

#### **CHAPTER 2**

# LITERATURE REVIEW

#### 2.1 Introduction

A literature review was conducted to understand the effect of nanoclays and surfactant on the hydrolysis and biodegradation process of poly(lactic acid) PLA. The review focuses on the role of nanoclays and surfactant, their effect on the molecular weight and in turn the effect on the abiotic and biotic degradation process.

# 2.2 Poly(lactic acid) – PLA

Bio-based polymers that are biodegradable and sustainable, in recent times have garnered great interest in the scientific community, as an alternative to the ever-growing demand of petroleum based conventional polymers due to several economic, social and environmental issues like plastic waste management, global warming and limited availability of fossil fuels [1].

PLA is an aliphatic polyester which is biodegradable and compostable in nature. Due to its compostable nature and lower environmental footprint, than the traditional petroleum based fossil derived polymers, PLA has attracted a lot of attention and is considered as a favorable replacement to the ever growing plastics waste disposal issue [2,3]. The fermentation of corn, cassava starch and potato sugar yields lactic acid, which is the precursor for PLA [4,5]. The interest in PLA has increased by leaps and bounds Figure 2.1 illustrates the number of research studies published in the past two decades about PLA and related subject.

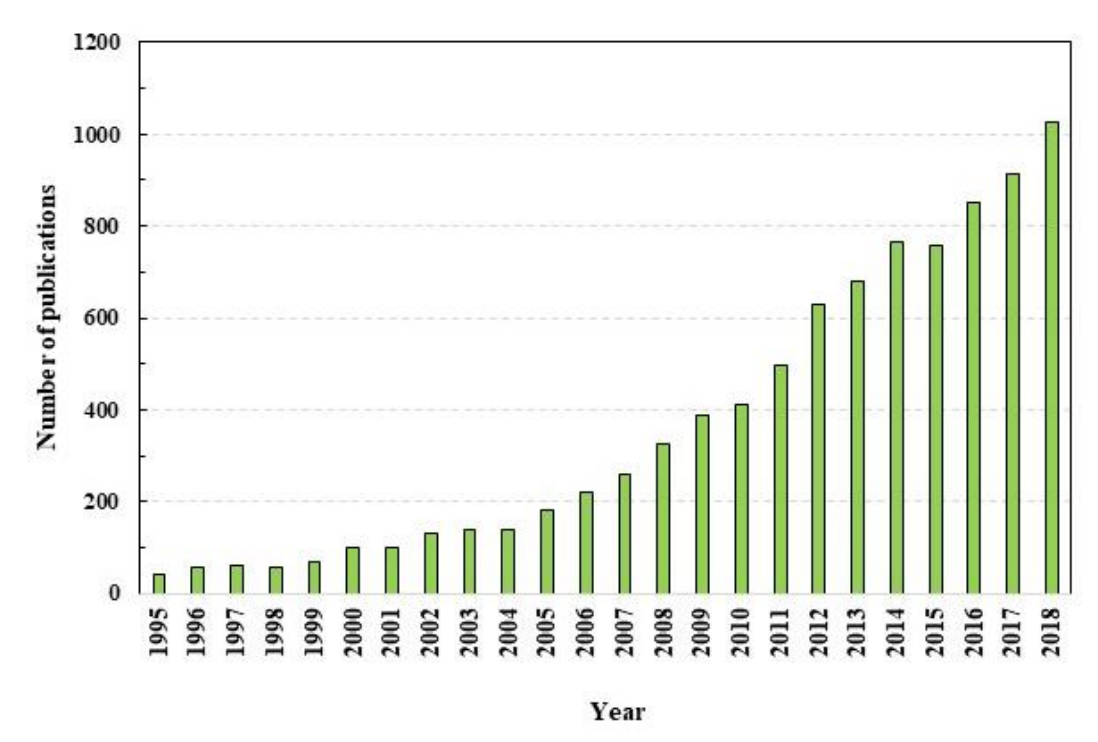


Figure 2.1. Number of research reports published between 1995 and 2018 (from Web of Science®Core Collection search results with title key-words "PLA", "PLLA", "PDLA", "polylactic acid", "polylactide", and "poly(lactic acid)".

During the 1960s, the use of PLA was mainly restricted to the medical field due to the particular interest in its hydrolysable structures. Lower mass production, high cost of lactic acid and low molecular weight hampered PLA's reach to other markets and commodity applications [6,8]. But later in the late 1980s, due to rapid advancements in the lactic acid production technique, a higher molecular weight PLA was finally produced. The biodegradability combined with the production from renewable sources along with the excellent properties provided at a low cost opened a whole new arena for PLA applications. Nowadays, PLA is used in the healthcare and medical industry to prepare a range of devices as degradable sutures, medical implants, tissue engineering porous scaffolds, drug delivery systems due to its biocompatibility with human body and packaging containers [9,11]. The U.S. Food and Drug Administration have approved PLA as Generally Recognized as Safe (GRAS) polymer to use in contact with food. Commonly in

packaging industries, PLA is used in the form of films, drinking cups, blister packages, sundae and salad cups and rigid thermoformed containers [12,13]. PLA is used for producing industrial textiles, filtration fabrics, geotextiles, military textiles in the textile industry [14], as mulch films in the agricultural sector [15] and structural applications such as high end automotive parts and electrical components [16].

# 2.3 Synthesis of PLA

Lactic acid (LA), a chiral molecule is the building block/monomer of PLA. It is also known as 2-hydroxypropionic acid and has two enantiomers: L- and D-lactic acid. Figure 2.2 shows the different chemical structures of these isomers.

Figure 2.2. Chemical structure of L-(+)-lactic acid (left) and D-(-)Lactic acid (right), adapted from [17].

Production of lactic acid is carried out either by the fermentation or chemical synthesis [17]. Among the two, the sought-after route is by bacterial fermentation of sugar and starches into lactic acid using a strain of *Lactobacillus* [18]. The popularity of this method can be gauged by the fact that 90% of the total lactic acid produced globally is by bacterial fermentation and is being put to advantage by big market players like NatureWorks LLC and Carbion<sup>®</sup>, while the rest is produced synthetically by hydrolysis of lactonitrile. Other chemical synthesis routes by which lactic acid can be produced are detailed elsewhere but are preposterous costwise [19,20]. The

chemical synthesis has major restrictions like inability to produce only the desired L-lactic acid and finite production capacity [19].

PLA with fluctuating molecular weights can be manufactured using lactic acid. Majorly, high molecular weight PLA finds applications in high value textile, fiber and packaging industries. Figure 2.3 depicts the three ways in which polymerization of LA to high molecular weight PLA can be obtained: (1) direct condensation polymerization of lactic acid (2) azeotropic dehydration condensation reaction of lactic acid (3) ring opening polymerization (ROP) of lactide.

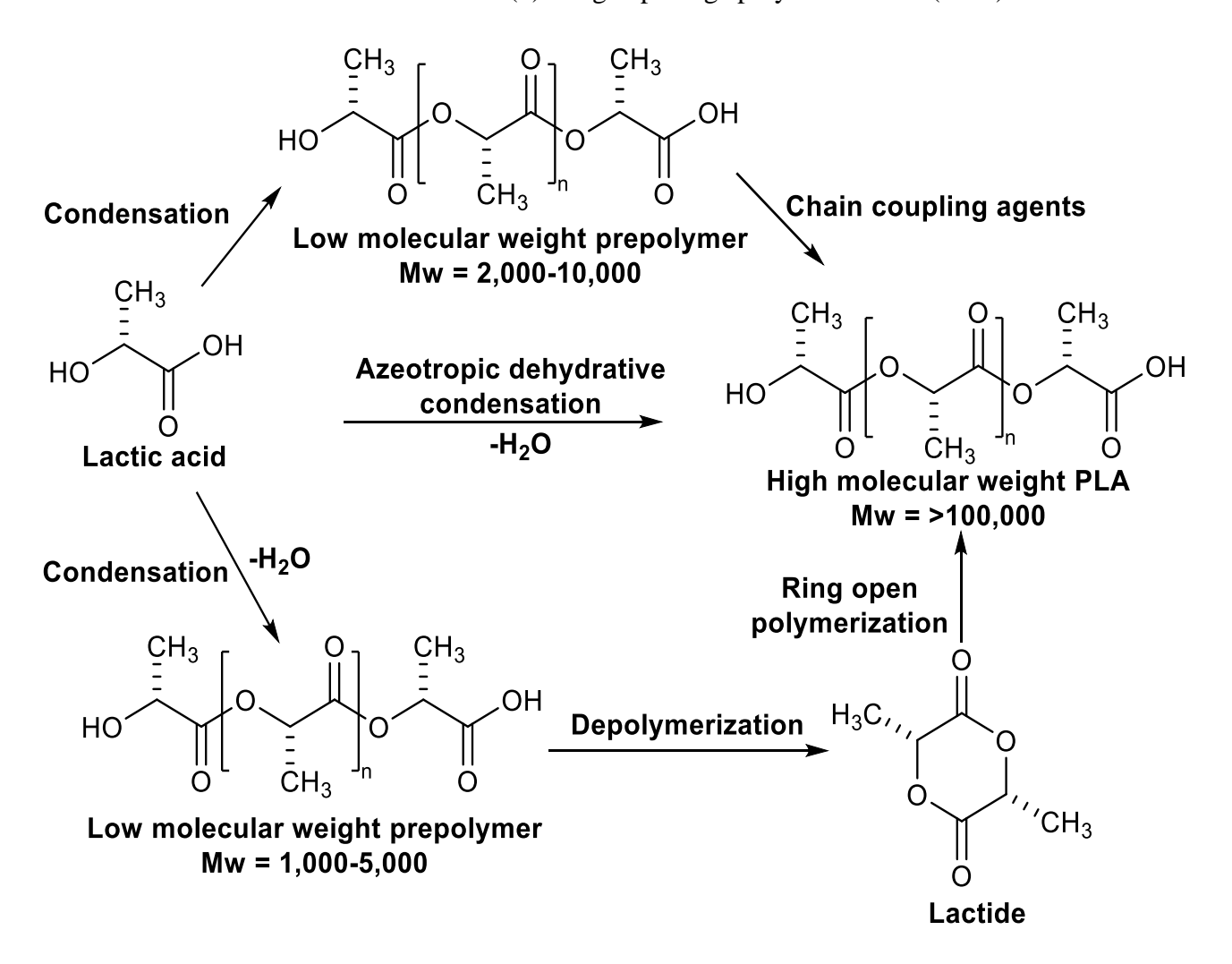


Figure 2.3. Manufacturing process to produce high molecular weight PLA, adapted from [17].

The 1<sup>st</sup> method is generally considered to be the least expensive route to produce high molecular weight PLA. It is based on the esterification of monomers, with the help of some solvents coupled with efflux of water under gradual vacuum and high temperatures. It is difficult to obtain a solvent free high molecular weight polylactic acid and usually the method results in low to intermediate molecular weight (<50,000 g·mol<sup>-1</sup>). To obtain a high molecular weight, the use of coupling agents such as isocyanates, epoxides or adjuvants *e.g.*, bis (tri-chloromethyl) carbonate, carbonyl diimidazole is indisputable. This in turn results in low quality PLA having poor mechanical properties, along with reaction by-products such as water and alcohols, which need to be eliminated, leading to higher reaction times and cost thereby increasing the complexity of the process [20–23].

In azeotropic dehydrative condensation polymerization, high molecular weight PLA is obtained from lactic acid, without the use of chain extenders or adjuvants. An azeotrope can be defined as a mixture of two or more liquids in a ratio such that their fractions cannot be varied during the process of distillation. This happens because when an azeotrope is boiled, the resulting vapor has the same fraction of constituents as the original. This method involves efficient removal of water using azeotropic solvents. The equilibrium between the polymer and its monomer is exploited in organic solvents (*e.g.*, toluene, xylene or diphenyl ether) to produce high molecular weight polymer in a single step. The Chinese company Mitsui Toatsu Chemicals has patented this process [24].

Ring-opening polymerization is a form of addition polymerization (chain growth), wherein the terminal end of the polymer acts a reactive center. A long polymer chain is formed through ionic propagation wherein more cyclic monomers react by opening its ring structure [25,26]. This method is comprised of three steps: formation of low molecular weight PLA from

polycondensation of LA, depolymerization of PLA into lactide and catalytic ring-opening polymerization of the lactide intermediate. Lactic acid is first condensed to form low molecular weight oligomers, then lactide is produced from the thermal cracking of low molecular weight PLA oligomer under high temperature and low pressure in the presence of catalyst. The cyclic dimer of LA namely lactide (3,6 dimethyl 1,4-dioxane 2,5-dione), is the monomer for PLA. Since LA has two enantiomers: L- and D- lactic acid, the resulting lactide has three stereoisomeric forms: DD-, LL- or DL-lactide [27]. The obtained crude lactide has different impurities such as water, lactic acid and oligomers which can hinder with the polymerization reaction and increase the population of low molecular weight species. Therefore, lactide is thoroughly purified by vacuum distillation. The ring of the purified lactide then opens to form a high molecular weight polymer grade PLA as shown in Figure 2.4 [28].

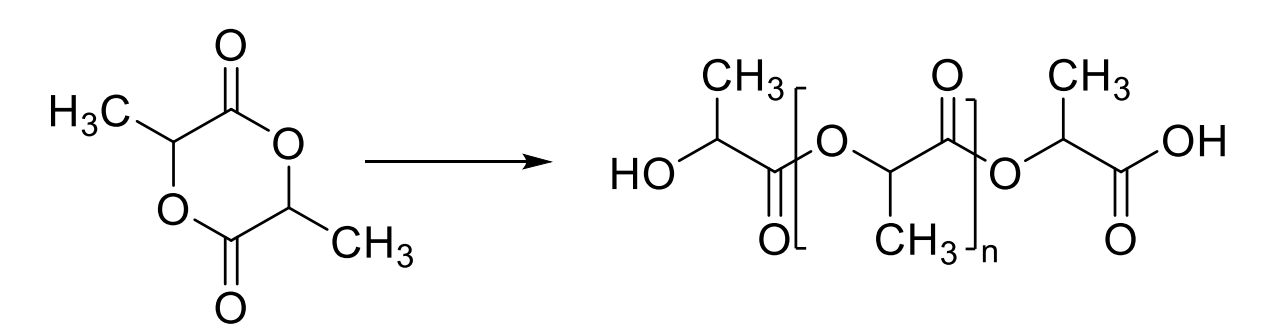


Figure 2.4. PLA synthesis by ring-opening polymerization [27].

This is the long established route for the large scale industrial manufacturing of PLA. This can be verified from the fact that NatureWorks LLC, the major producer of high molecular weight PLA has abused this ROP method to produce around 300 million pounds of Ingeo PLA per year [29]. ROP helps exercise control over the chemistry to produce high molecular weight PLA by altering various parameters like residence time, temperature and type of catalyst used. The

resulting PLA thus has controlled desirable properties such as refractive index, high molecular weight without the use of azeotropic system, which can be varied to broaden the application fields for PLA.

In comparison to the conventional polymers like polypropylene (PP), poly (ethylene terephthalate) (PET) and polystyrene (PS), high molecular weight PLA exhibits similar properties such as mechanical, grease and oil resistance, good heat sealability and excellent barrier to aroma and flavor [30,31]. However, it has certain drawbacks like brittleness, low melt viscosity, low resistance to conditions of high temperature and humidity, low flexibility, poor mechanical, gas barrier and thermal properties which limits its access to commercial application in many sectors of packaging [32–34]. To overcome these limitations, ample amount of studies have been conducted focusing on improving PLA properties and expanding its applications. This has been achieved by blending it with different polymers (biodegradable and non-biodegradable), or via composites and nanocomposites inclusion such as cellulose nanocrystals, nanoclays, fibers into the PLA matrix [35–40].

# 2.4 Polymer degradation

Degradation can be defined as deviation in the desirable traits of materials from the desired set point due to the impact produced by environmental factors such as light, temperature, water, oxygen, biological organisms or chemicals [41,42]. The degradation process involve a lot of physical and chemical processes which results in irreversible structural changes and remarkable deterioration in the quality, rendering the polymeric materials useless for applications [43].

The degradation of polymers results in the cleavage of ester bonds, backbone chain scission creating low molecular weight fragments, monomers or oligomers etc. Table 2.1 encapsulates the

different types of degradation and the factors responsible. Detailed information regarding the different degradation types can be found elsewhere [44–49]. Hydrolytic degradation and biodegradation will be discussed in detail in the further sections.

Table 2.1. Type and causes of polymer degradation, adapted from [33].

Causes/Environmental factors
Ultraviolet and visible light
Heat and temperature
Oxygen, ozone
Acids, alkalis, salts, water
Microorganisms, enzymes
Stress, fatigue

# 2.5 Biodegradation

Biodegradation is the chemical breakdown in which organic substances are broken down into smaller compounds due to the enzymatic action, when microorganisms such as bacteria, fungi and algae use this substances as a source of carbon and energy [50,51]. It can be of two types: aerobic degradation or anaerobic degradation characterized by the presence or absence of oxygen [88]. The main end products formed at the end of biodegradation are biomass, water (H<sub>2</sub>O) and carbon dioxide (CO<sub>2</sub>) (aerobic) or methane (CH<sub>4</sub>) (anaerobic) [52]. Biodegradation can also take place in two different environments: solid (compost, soil) and aquatic [53].

As per the ASTM standard, a biodegradable plastic is defined as "a degradable plastic in which the degradation results from the action of naturally occurring microorganisms such as

bacteria, fungi, and algae" while a compostable plastic is "a plastic that undergoes degradation by biological processes during composting to yield CO<sub>2</sub>, water, inorganic compounds, and biomass at a rate consistent with other known compostable materials and leave no visible, distinguishable or toxic residue" [54]. The biodegradation mechanism can take place only in a conducive environment and proceeds via chain scission. For instance, there can be a highly efficient biodegradation mechanism available in one environment, whereas the same mechanism might not work at par and with so much efficiency in another environment due to inadequate conditions [55]. The biodegradability of the polymers is heavily influenced by many important factors such as: 1) Polymer composition: this includes polymer characteristics such as nature of the chemical bonds present, molecular weight and molecular weight distribution; 2) Higher order structure details: such as chain arrangement, stereochemistry, crystallinity, glass transition temperature; 3) Surface conditions: this pertains to the surface area available, hydrophilic and hydrophobic properties; 4) Environmental conditions: the environment to which the polymer is exposed to such as temperature, moisture level, oxygen and pH. Factors specific to microorganisms such as bioavailability (amount of substrate physiochemically available), the availability of enzyme to degrade the polymer substrate, metabolic pathways to produce those specific enzymes, concentration, presence of nutrients to support and nurture their growth, presence of inhibitors which might arrest their growth [56–58].

Biodegradation proceeds in principally into two steps: primary degradation and ultimate degradation as seen in Figure 2.5. Primary degradation usually involves the breaking down of polymer chains due to hydrolysis or oxidation initiated by chemical or microbial enzymes resulting in low molecular weight fragments. Once this low molecular weight fragments are formed, ultimate degradation takes place by microorganisms digesting the polymer chains. This

step is also termed as mineralization. Mineralization can be defined as the process of converting biodegradable materials into CO<sub>2</sub>, methane, water and residual biomass via microbial assimilation [59,60].

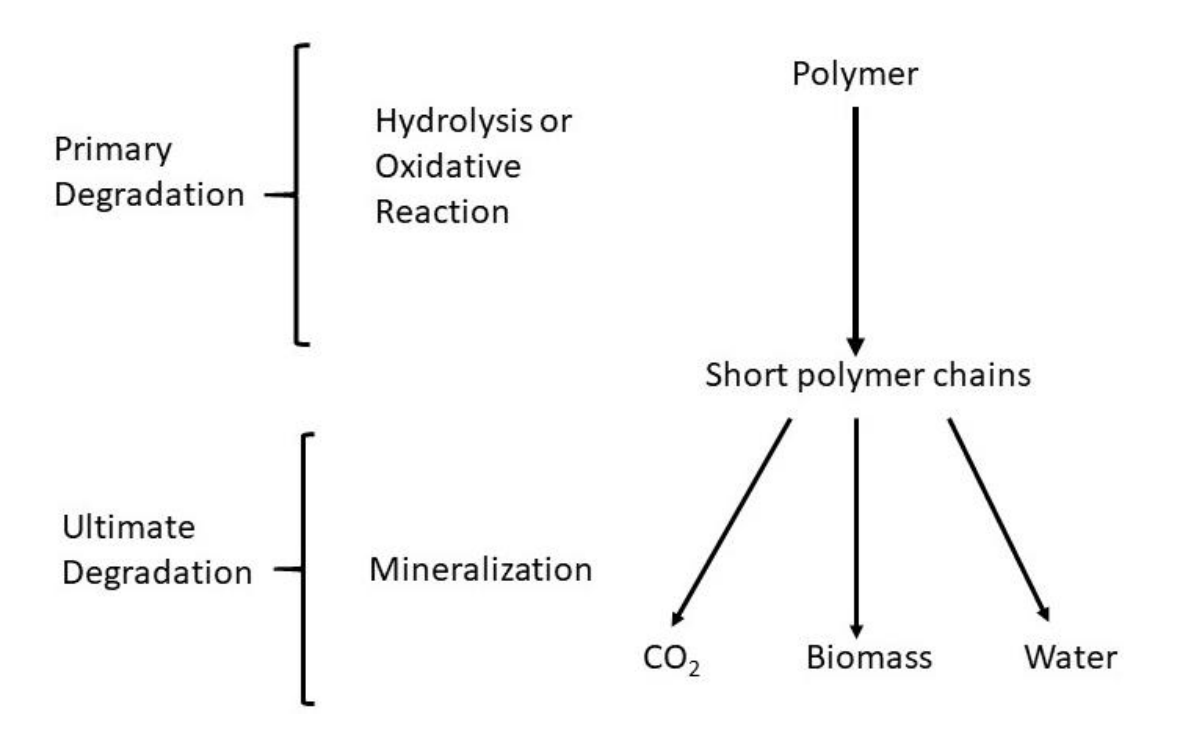


Figure 2.5. Schematic representation of Biodegradation mechanism, adapted from [98].

# 2.5.1 Evaluation of Biodegradation

There are different testing methods available to evaluate biodegradation, directly or indirectly. These include visual observations, decrease in the mechanical properties, reduction of molecular weight -etc. [61].

Visual measurements take into account surface modification which can be considered as a first indication that a microbial attack has been initiated. This involves change in the polymer surface such as surface irregularities, discoloration, formation of holes and cracks, surface roughness, embrittlement, formation of biofilm, fragmentation etc [62]. Weight loss measurements

are widely used as an indicator to imply that degradation is under way. As the name suggests, it is based on the reduction in the polymer weight due to deterioration. Declining rheological and mechanical properties are often associated to the degradation event taking place. Change in tensile strength, elasticity, elongation at break coupled with weight loss and product formation is an indicator of degradation [63]. Though these are some of the most fundamental approaches used to identify degradation, but they necessarily do not confirm the presence of the event, since they can be evidence of fragmentation and degradation but not biodegradation.

There are different modes available that can be used to figure out the biodegradability of polymers. This incorporates laboratory test methods such as fourier transform infrared spectroscopy (FTIR), UV-visible spectroscopy, gel permeation chromatography (GPC), scanning electron microscopy (SEM) and nuclear magnetic response (NMR). Although, this techniques aid in the evaluation of biodegradation, respirometric methods are usually favored to measure the biodegradation of polymeric materials in laboratory settings due to their accuracy, reliability, reproducibility and ability to simulate real life conditions and help demonstrating that if biodegradation is in process or not, which is a major drawback for all the methods mentioned above [53–64].

The respirometric methods use a respirometer or respirometric system which measures and monitors the respiration activity of the microorganisms either through evolution of carbon

$$C_{polymer} + O_2 \longrightarrow CO_2 + H_2O + C_{residue} + C_{biomass} + salts$$
 Equation 1

dioxide or consumption of oxygen. A number of studies have shown that the conversion of solid carbon to carbon dioxide follows a first order reaction as seen in Equation 1 [65–67].

In this method, the carbon dioxide evolution can be measured in continuous or discrete way, and the residual remaining from the samples can be analyzed using the characterization techniques mentioned above [68]. ASTM D5338 and ISO 14855 standards are of the most importance for evaluating the aerobic biodegradation of polymeric materials under simulated composting conditions by analysis of evolved CO<sub>2</sub> [69]. More details regarding the standards and their comparison can be found elsewhere [70].

# 2.6 Hydrolytic degradation of PLA

The hydrolytic degradation of PLA is known to occur through the chain scission (decomposition of polymer chains) of ester bonds by reaction with water, which results in formation of low molecular weight fragments, oligomers and monomers [71]. This can be simply illustrated by the reaction below:

$$-COO + H_2O \rightarrow -COOH + HO-$$
 Equation 2

The hydrolytic degradation of polyesters occurs in following stages as widely reported:

- 1) Water diffusion into the material
- 2) Hydrolysis of the amorphous regions, due to feeble resistance to water attack
- 3) Hydrolytic cleavage of ester bonds resulting in the attenuation of molecular weight along with formation of water-soluble compounds.

4) Increase in the concentration of carboxylic chain ends and accumulation of acidic degradation products leading to an autocatalytic mechanism thus making hydrolysis a self-sustaining reaction [56,72–75] as seen in Figure 2.6.

Figure 2.6. Hydrolysis and cleavage of ester linkage, adapted from [76].

# 2.6.1 Mechanism of Hydrolysis

During hydrolytic degradation, the chain cleavage occurs favorably in the amorphous region thereby increasing the polymer crystallinity due to the diffusion of water [77,78]. The amorphous regions are more prone to attack due to their larger void volume and disorganized structural arrangement as compared to the crystalline regions, water can also penetrate easily in such spaces. Subsequently, the population of carboxyl groups increases due to the chain rupture in water which catalytically alters the rate at which hydrolytic degradation of PLA takes place. The

reduction of pH of the degradation media, due to the generation of polylactic acid oligomers makes hydrolysis a self-maintaining and self-catalyzed process [79].

The hydrolytic degradation of PLA and PLA based matrices generally proceeds via two routes either (1) surface / heterogenous erosion and (2) bulk / homogenous erosion Figure 2.7. The diffusion route of water molecules into PLA matrix and hydrolysis rate of ester bonds determine whether surface or bulk erosion phenomena comes into play [80]. Water plays a dual role in the process of hydrolysis, firstly by diffusing into the polymer matrix and severing the ester bonds; thereby releasing carboxyl and hydroxyl end groups and secondly, by diffusion of water soluble oligomers and monomers. Water also assists by inducing a plasticization effect, thus increasing the free volume and leading to weight loss. This phenomena is termed as erosion [81]. Surface erosion takes place when the rate of water diffusion is lower than the hydrolytic degradation rate of ester bonds. The surface erosion occurs mainly at the near-surface regions wherein the watersoluble oligomers closer to the surface leach out and not within the polymer matrix, hence the term heterogenous [82]. The thickness, dimensions of the specimens accompanied with weight loss have an insignificant effect on the rate at which it proceeds [83]. On the other hand, when the ingress of water into the matrix is higher than the degradation rate, bulk erosion phenomena occurs. Bulk erosion takes place homogenously and demands a reduction in molecular weight throughout the material over the degradation time [84]. Homogenous / bulk erosion can be classified into following stages: 1) rapid water uptake into the PLA matrix 2) diminution in molecular weight due to cleavage of ester bonds 3) creation of hollow core due to the release of water-soluble and low molecular weight monomers [80,85–86].

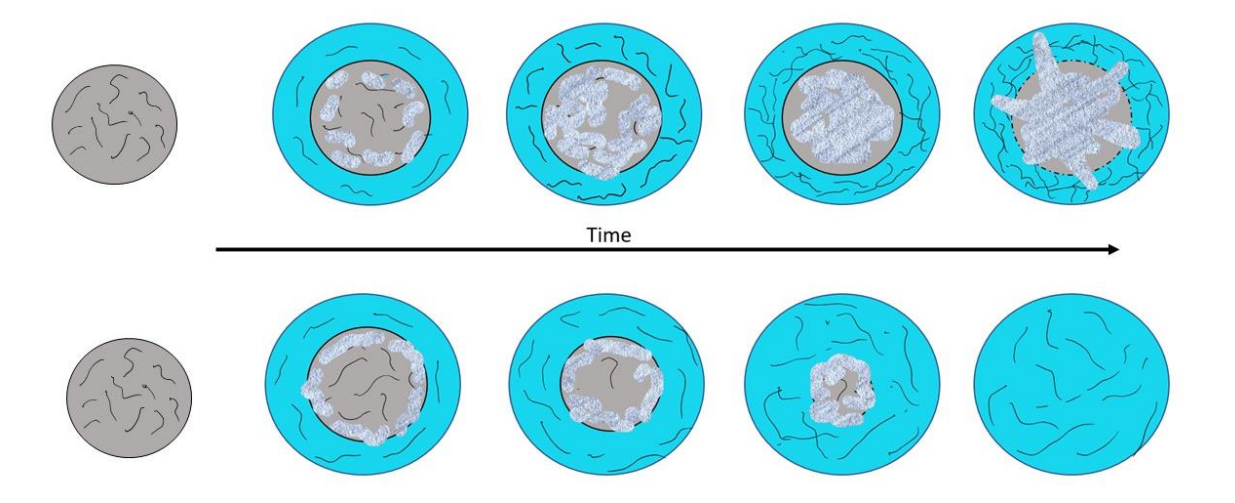


Figure 2.7. Schematic representation of bulk erosion (top) and surface erosion (bottom), adapted from [84].

The rate at which hydrolytic degradation mechanism advances is determined by many factors, such as shape and thickness of the specimen, conditions under which hydrolysis is taking place like temperature [88] and pH [89,90], polymers associated factors such as molecular weight, crystallinity, morphology, chemical structure, L-lactide content, etc. [91–93]. A thickness of lower than 0.5-2 mm and higher than 7.4 mm is said to be favorable for bulk and surface erosion respectively [94].

# 2.6.2 Parameters dominating the hydrolytic degradation

# 2.6.2.1 pH

pH plays a significant role in the hydrolysis of PLA, since it affects both the rate kinetics and the degradation mechanisms. Hydrolysis rates can vary enormously at different values of pH [95,96]. Depending on the pH of the media, different degradation mechanisms take place due to

the difference in the reactivity of ester groups in the lactic acid oligomers as seen in Figure 2.8 [81,90,97,98].

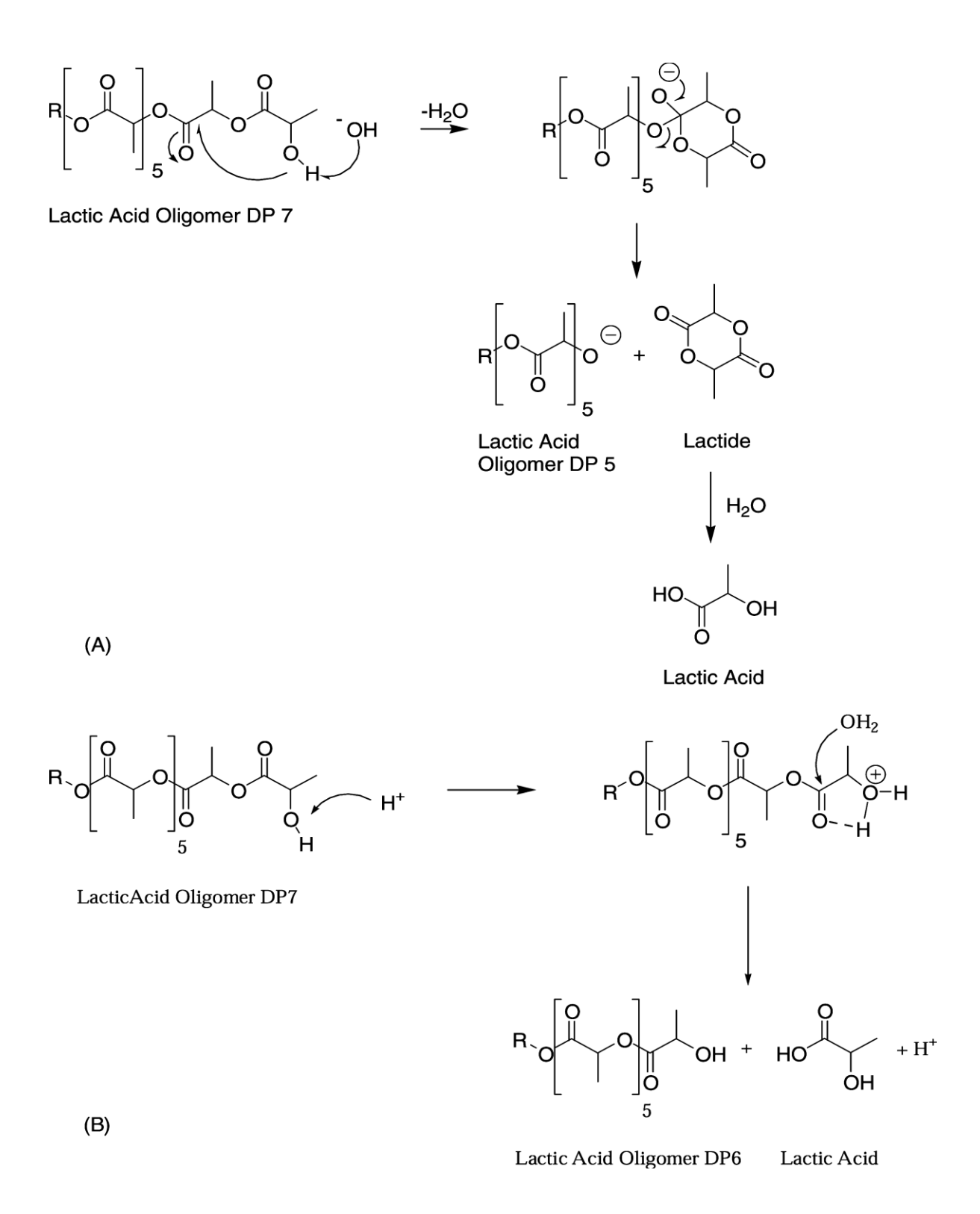


Figure 2.8. Hydrolytic degradation mechanism in : (A) alkaline and (B) basic media, adapted from [99].

The hydrolytic degradation usually prevails favorably through backbiting reactions, resulting in the generation of cyclic dimer of lactic acid at higher pH i.e. alkaline media whereas for lower pH i.e. acidic media, the hydrolysis progress through chain scission of the terminal polymer ends ("unzipping") [100–102]. The chain scission kinetic constant of the terminal ends was found to be manifold larger than that of the internal ester groups [103,104]. The presence of hydronium (H<sub>3</sub>O<sup>+</sup>) and hydroxide (OH<sup>-</sup>) ions contribute to the cleavage of ester bonds during the hydrolysis process [105]. In alkaline media, the hydroxide ions attack the carbonyl atoms and a huge reduction in molecular weight along with weight loss is observed [106]. This translates to quick drop in the properties of the polymer [107]. Albeit in acidic media, the chain end scission fosters a substantial drop in the average molecular weight and not much weight loss in the initial stage. However, as the hydrolysis proceeds weight loss increases rapidly, and molecular weight decreases slowly [108]. Acidic pH leads to autocatalytic effects, that leads to faster polymer degradation by release of soluble oligomers closer to the surface and reducing the pH of the core [108].

For neutral aqueous medium, studies have shown that the hydrolytic degradation proceeds via bulk erosion and is responsible for weight loss and decrease in molecular weight over time [109–111]. Researchers have conducted studies quantifying the effect of pH on PLA hydrolytic degradation at different temperatures [96,112–115]. Very few papers mention the change in the degradation kinetics at very specific pH [116–118]. Effect of nanofillers and additives in controlling the pH of the hydrolyzing media and in turn modulating the kinetics of hydrolysis process is also investigated [79,119–123].

### 2.6.2.2 Temperature

Temperature of the media to which PLA is exposed to plays a crucial role in the hydrolytic degradation of PLA [104]. As the temperature increases, the rate at which chain scission of ester bonds occur, also increases [124–132]. For temperatures above the glass transition temperature  $(T_g)$ , the degradation rate is intensified due to the physical changes taking place in PLA . Above  $T_g$ , the mobility of the chains increases thereby increasing the free volume available making it easier for the diffusion of water molecules into the polymer matrix. This increases the rate at which hydrolysis reaction takes place, breaking down the long massive chains and increasing the concentration of carboxyl groups which further aid in the degradation [133].

Various characteristics of PLA such as molecular weight, mechanical and thermal properties change dramatically from below to above ( $T_g$ ) [17,134,135]. Ho and Pometto [136] analyzed the effect of a range of temperatures on PLA degradation and found that the weight average molecular weight ( $M_w$ ) loss and the degradation rate was highest for 55°C followed by 40°C and 25°C in the end. This is attributed to the glass transitional temperature range (55-60°C) [137] due to increased mobility of polymer chains. Mitchell and Hirt [138] reported that at 60°C, PLA displayed a higher polydispersity index in comparison to 40°C, due to rapid degradation of amorphous regions. A reduction in  $T_g$ , was attributed to the modifications materializing from the change in the degree of plasticization, due to perforation action of water in the polymer matrix. The low molecular weight oligomers produced from the hydrolysis reactions, diffuse into the water further aiding to the weight loss and the slow rearrangement of amorphous regions into crystalline ones further reduce the  $T_g$  [114]. The breakdown of long polymer chains into shorter ones, lowering molecular weight and the amorphous regions responsiveness towards hydrolysis and easy

reorganization into crystalline regions result in shifting of  $T_m$  and the crystallization temperature  $(T_{cc})$  also shift to lower temperatures [139].

#### 2.6.2.3 Molecular weight

Molecular weight is seen as another crucial parameter affecting the hydrolytic degradation of PLA [92,140,141]. As the molecular weight reduces, the rate at which the degradation proceeds increases. Lower the molecular weight, higher the chain flexibility. The diffusion of water molecules into the polymer matrix can be viewed as infiltration into voids i.e. free spaces, thereby increasing the population of hydrophilic terminal carboxyl and hydroxyl groups which further help in degrading the polymer. As hydrolysis proceeds, the rate at which the low molecular weight chains and oligomers are formed increases.

Shah and Tsuji [146] investigated the effects of molecular weight and D-lactide units ( $X_D$ ) on the hydrolytic degradation behavior of PLLA, by exposing the films to phosphate-buffered solution at 37°C. Three films of different molecular weights  $M_n = 4.09 \times 10^5$  g/mol and  $X_D = 0\%$ ,  $M_n = 1.22 \times 10^5$  g/mol and  $X_D = 1.2\%$  and  $M_n = 8.07 \times 10^4$  g/mol and  $X_D = 0.2\%$  were tested for hydrolysis. The incorporation of small amounts of D-lactide units was found to enhance the hydrolysis in the first stage (0-32 weeks). They found that the rate constant for hydrolytic degradation (k) increased with the increasing content of  $X_D$ . On the other hand, both crucial parameters  $X_D$  and  $M_n$  didn't produce any significant difference for the determination of k. In another study on hydrolysis by Shah and Tsuji [142], PLLA films with different ratios of L and D-lactide [P(LLA-DLA)](77-23) was used Figure 2.9. They concluded that the hydrolytic degradation rate constant was higher for P(LLA-DLA) than PLLA films due to their hydrophilicity. The rate constant was found to increase with the increase in water absorption.

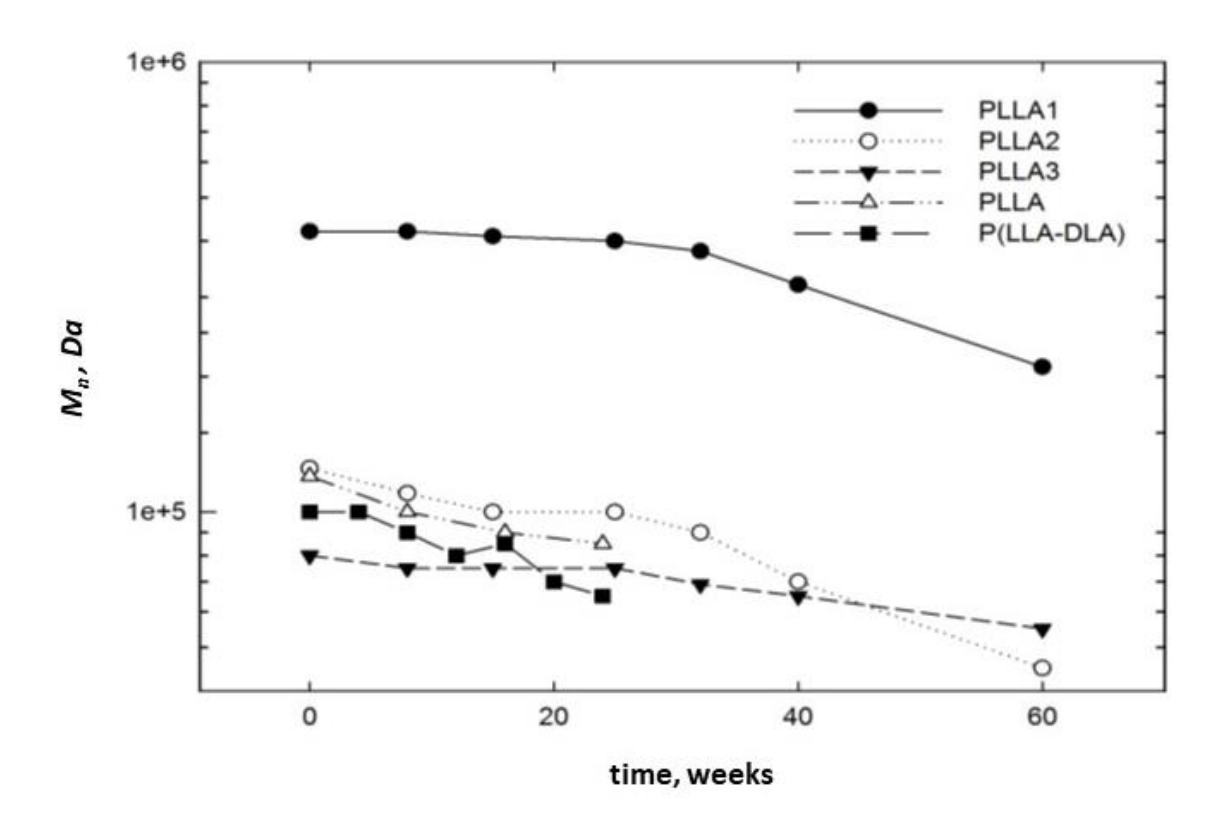


Figure 2.9. Change in  $M_n$  during hydrolytic degradation (37°C) in phosphate buffered solutions, adapted from [112,142].

Çelikkaya et al., studied the effect of different molecular weights ( $M_n$  = 21900, 12100 and 7300 g/mol) on the hydrolytic degradation of PLLA by calculating the degradation rates [143].

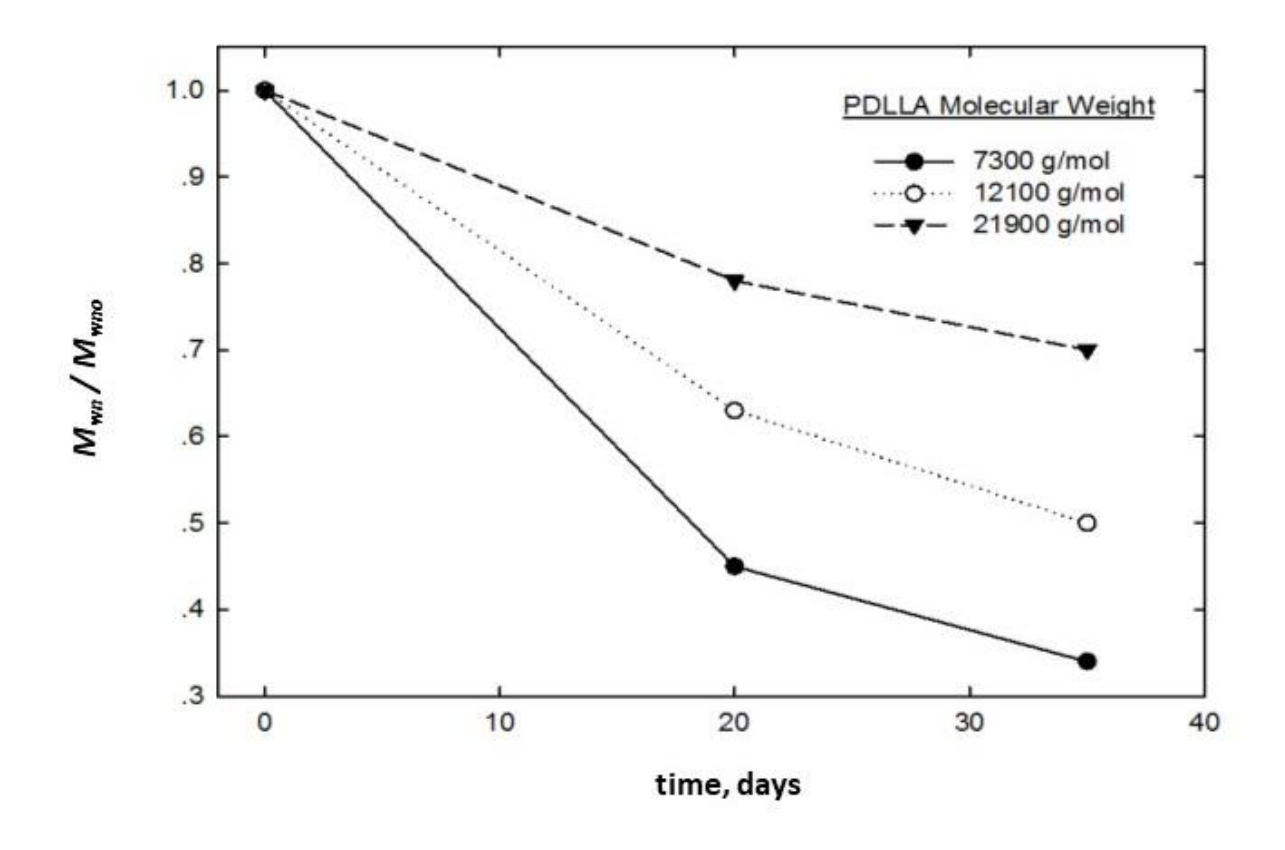


Figure 2.10. Hydrolytic degradation for PLLA films with different molecular weights in a phosphate-buffered solution at 37°C, adapted from [143].

It was found that PLLA film with lower  $M_n$  degraded faster as compared to others Figure 2.10. This behavior was observed due to the easy diffusion of water molecules into the polymer matrix. The low molecular weight chain correspond to less complexity, less entanglement, more affinity towards water due to higher density of carboxyl and terminal hydroxyl groups thereby inducing faster degradation.

#### 2.6.2.4 Crystallinity

Crystallinity and in turn, the structural configuration of PLA plays an important part in the hydrolytic degradation. The degradation mechanism calls for the hydrolysis of ester bonds and is rate dependent on the global crystallinity of PLA [144]. As compared to the crystalline regions the amorphous regions are more prone to water attack, since the access of water molecules to the inside of crystalline regions is restricted as seen in Figure 2.11. This results in preferential hydrolytic degradation of amorphous regions and this chain scission of ester bonds results in the release of water-soluble monomers and oligomers.

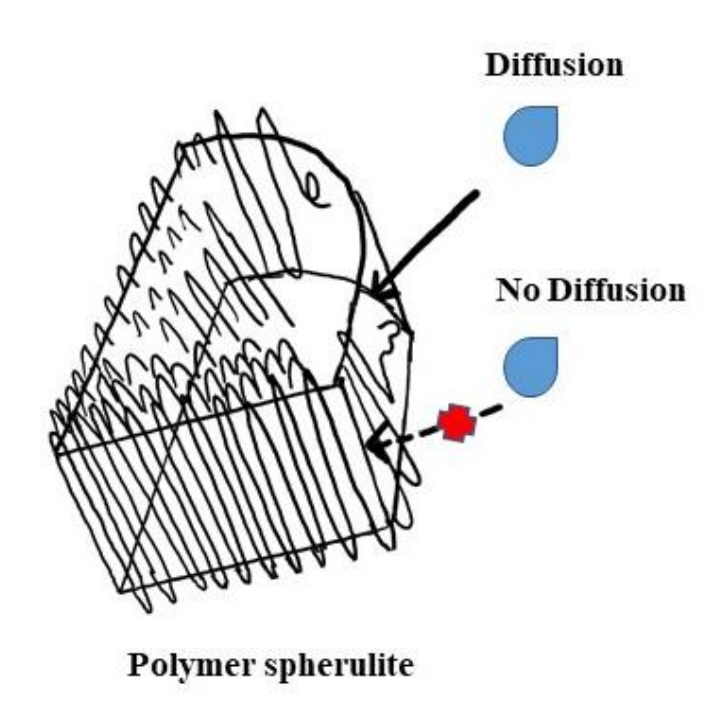


Figure 2.11. Diffusion of water is restricted to the crystalline regions as opposed to amorphous regions, adapted from [84].

The amorphous regions between the crystalline regions is called as the "restricted / restrained amorphous region" as seen in Figure 2.12. This restricted amorphus regions is made of

three types of chains as seen. "Free amorphous region" is the one external to spherulite in the completely amorphous areas[145]. Once the free amorphous region is hydrolysed, the crystalline region left back is termed as "crystalline residues", which are degraded in the end. Water swells up the amorphous phase in the polymer matrix, acting as a plasticiser and imparting just enough molecular chain mobility to induce crystallisation [146].

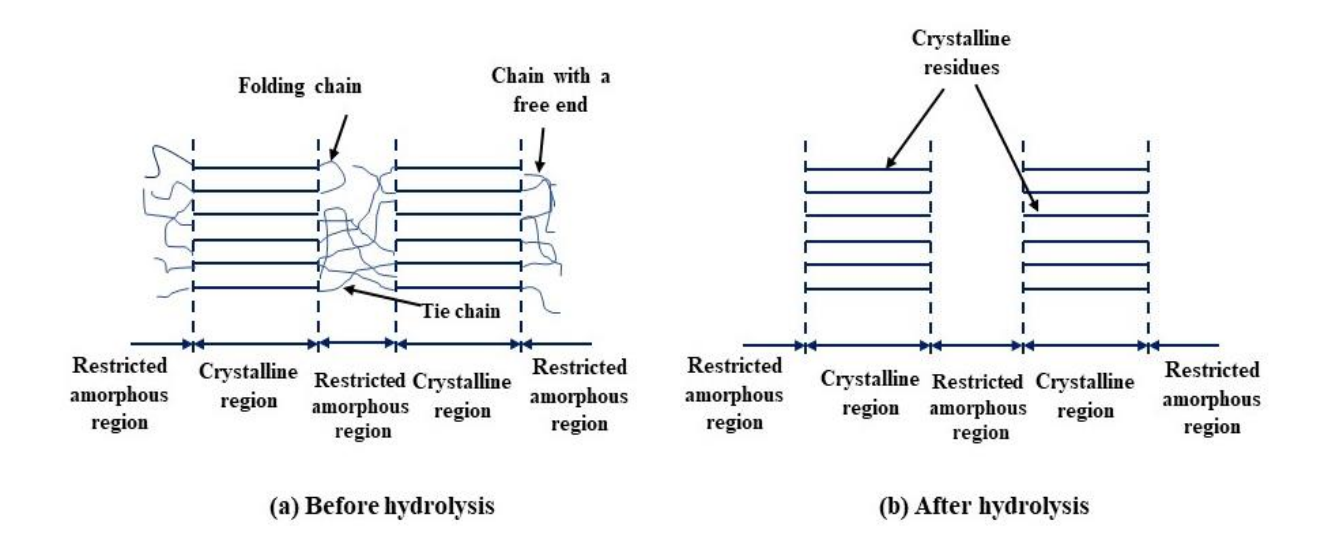


Figure 2.12. Change in PLA structure (a) before and (b) after hydrolysis, adapted from [145].

Tsuji and Ikada investigated the effect of crystallinity and found that the amorphous PLA degraded faster as compared to semi-crystalline PLA for hydrolytic degradation in a phoshpate buffered soution (pH = 4.0 and 37°C) [147]. Weight loss of around 14% was observed for amorphous PLLA with respect to its initial mass at the end of 18 weeks, whereas 19% of weight loss was detected for semicrystalline PLA at the end of 20 months when hydrolysis was performed in solution of pH = 3.4 and at 37°C [148,149]. Similar findings were obtained at (pH = 1 and 9) at 70°C [81]. This indicate that the degree of degradation for amorphous regions was higher than the crystalline regions due to attack of water on ester bonds. Zhang et al., studied the changes in the structural configuration of semicrystalline PLA (D-stereisomer content of 1.4%) and amorphous

PLA (D-stereisomer content of 12%) grades during the hydrolytic degradation [85]. It was concluded as the degradation time increased, molecular weight decreased whereas crytsallinity increased, though the amorphous PLA degraded much more rapidly as compared to semi-crytsalline PLA. Due to the decrease in molecular weight, the shorter PLA chains gain more mobility and tend to form a more crystalline structure which explains the increase in crystallinity.

## 2.7 PLA nanocomposites

Nanocomposites are the composite materials, wherein one or more components has at least one dimension in the nanoscale range (< 100 nm) [150]. This nanoparticles are used in small amounts such as 1-5 wt %., to demonstrate improvement in barrier, mechanical, thermal properties when used with a polymer matrix as compared to a conventional microcomposites [151–155]. Nanocomposites can generally be classified into three different categories as seen in Figure 2.13 [156].

- a) Nanoparticles: Also termed as isodimensional nanoparticle. These spherical particles have their three dimensions in nanometers. Example: Silica, semiconductor nanoclusters.
- b) Nanotubes: Also termed as whiskers/nanorods, nanotubes have two dimensions in the nanometer range and the third dimension larger than the other two dimensions Example: carbon nanotubes.
- c) Nanolayers: They have one dimension in nanometers. Also called as nanosheets, this plate like nanofiller have thickness in the range one to few nanometer, with an aspect ratio of 25 between other two dimensions [157]. Example: smectite clays, graphene sheets and layered double hydroxides.

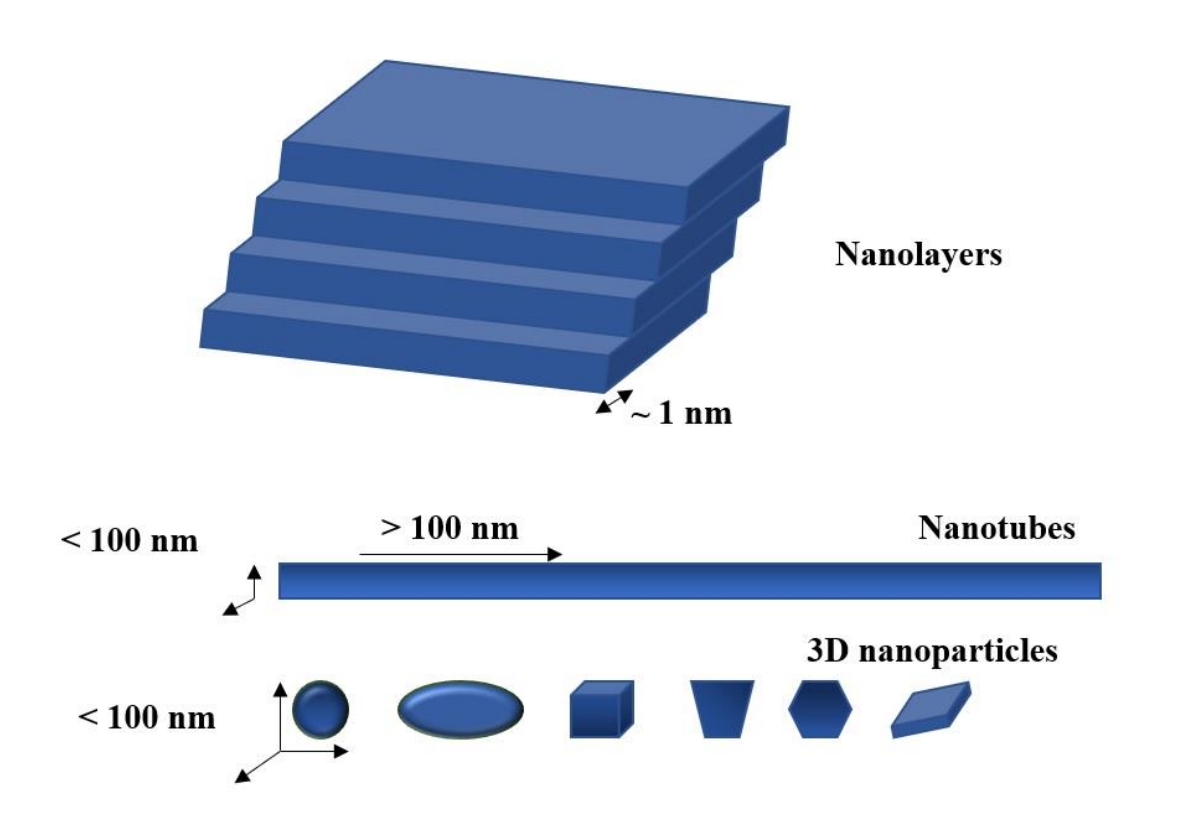


Figure 2.13. Different types of nanoscale materials, adapted from [150].

To enhance the performance of polymer, many nanofillers have been identified as possible additions to the polymer matrix, but the packaging industry has focused its attention on layered inorganic clays, because of low cost, easy availability, capability to swell and expand and the significant upgrade that they bring in the properties of the resulting nanocomposites [158–160].

Depending on their origin, nanofillers can further be classified as natural, semi-synthetic or synthetic. Natural nanoclays can be further categorized depending on the ratio of silicon dioxide ("SiO<sub>2</sub>") and "AlO<sub>6</sub>" units [161] Figure 2.14.

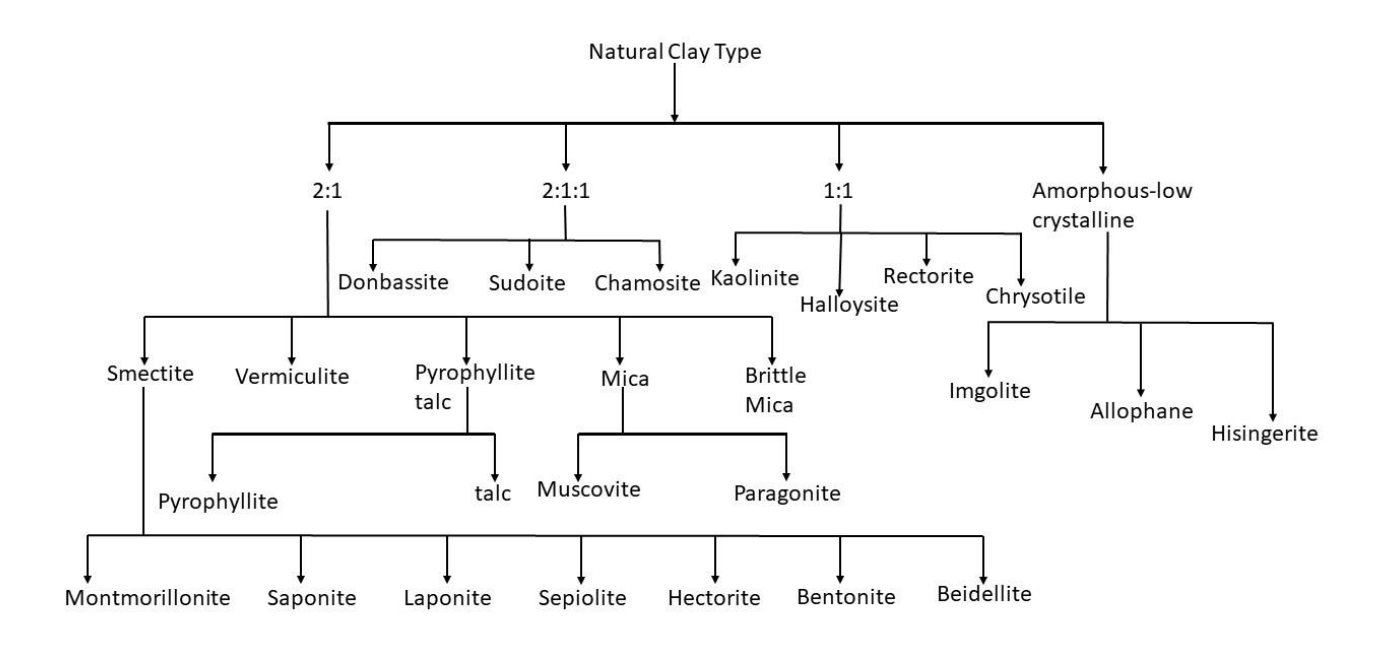


Figure 2.14. Categorization of natural clay, adapted from [161].

# 2.7.1 Characteristics

#### 2.7.1.1 Montmorillonite structure

Montmorillonite (MMT), is an extensively studied clay filler with respect to packaging (industries and academia) and is a popular choice for producing polymer nanocomposites. It falls in the smectite group belonging to the 2:1 phyllosilicates, the structural family of clays [162,163]. The crystal lattice is made of an shared octahedral sheet of alumina or magnesium hydroxide sandwiched onto two tetrahedral sheets of silica by the edge, such that the oxygen ions of the octahedral sheet are at the disposal of the tetrahedral sheets too Figure 2.15 [164,165]. The clay layers stack above each other in a repetitive pattern, with regular gap between the successive layers, thereby maintaining its platelet like structure. These anisotropic platelets are separated by thin layers of water. These layers are held together by the van der Waals forces. Interlayer spacing is the gap/spacing within the clay layer, also known as galleries and the height is approximately 1

nm. The lateral dimensions are in the range from tens of nanometers to several microns. The d-spacing ( $d_{001}$ ) also known, as the basal spacing is the thickness comprising of one clay layer and one interlayer spacing. Due to an large aspect ratio of 50-1000 and higher surface area in the range of 750 m<sup>2</sup>/g, MMT has proved to be a very effective reinforcement filler [166].

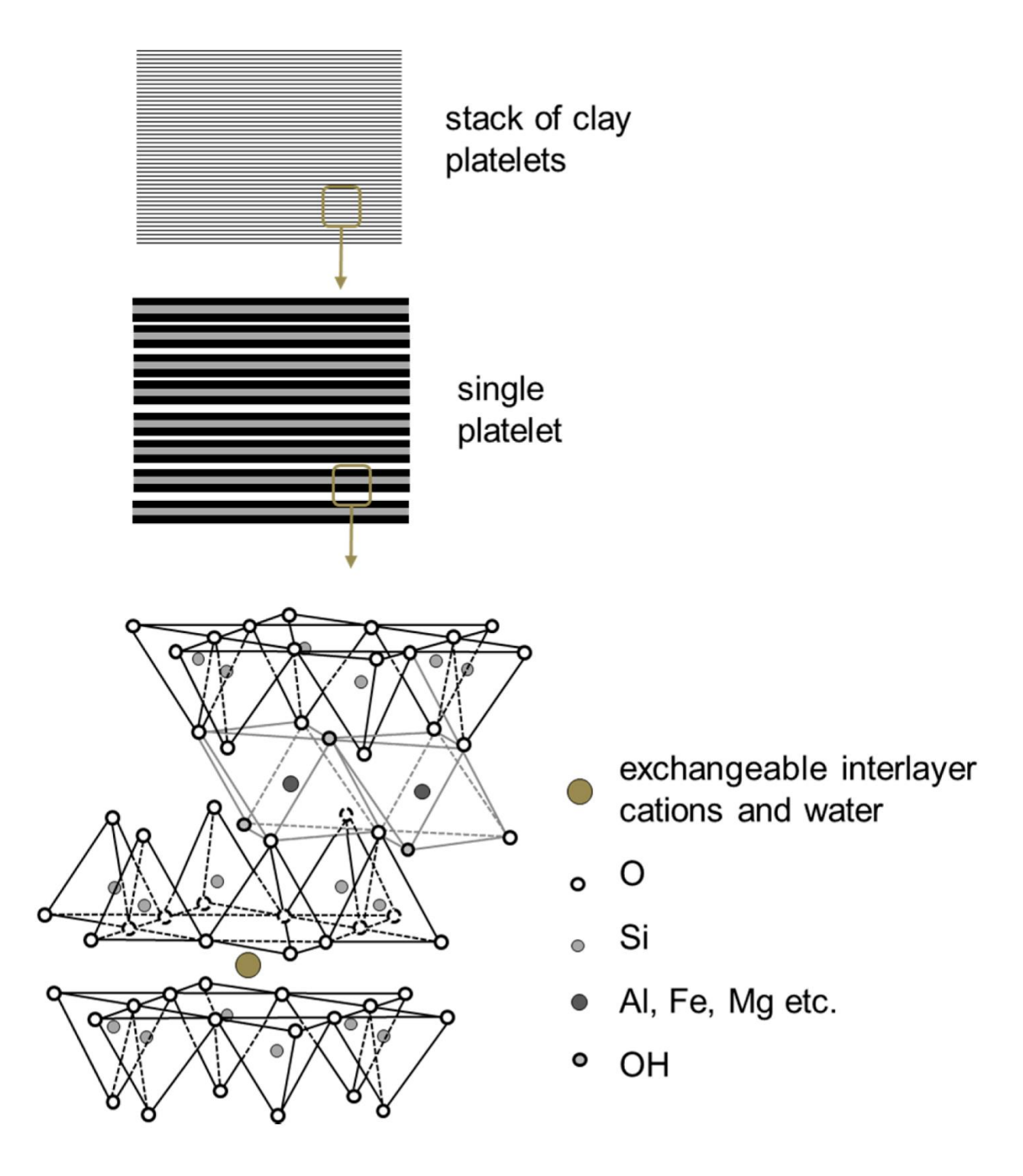


Figure 2.15. Structure of montmorillonite (2:1 phyllosilicates). Reproduced from [158].

Due to the disparity of electrons (for example, substitution of Al<sup>3+</sup> by Mg<sup>2+</sup> or Fe<sup>2+</sup>, or Mg<sup>2+</sup> by Li<sup>+</sup> within the layer), the clay layer is negatively charged but is counterbalanced by the hydrated exchangeable cations such as Na<sup>+</sup>, K<sup>+</sup>, Ca<sup>2+</sup> situated in the gallery [156]. This cations do not adhere tightly to the surface and hence are easily substituted by other compounds [167]. The general chemical formula is  $M_x(Al_{4-x}Mg_x)Si_8O_{20}(OH)_4$ •nH<sub>2</sub>O where (M = Na<sup>+</sup>, K<sup>+</sup>, Ca<sup>2+</sup>, etc.) and has an cation exchange capacity (CEC) of 80-150 meq/100 g[157,161].

## 2.7.1.2 Surface modification of clay

The presence of hydrated inorganic cations on the exchange sites makes MMT hydrophilic in nature. Due to the hydrophilic nature of MMT, the nanolayers of the clay tend to agglomerate together making it difficult for hydrophobic or less hydrophilic polymers like PLA to coexist with pure MMT [157]. The high surface energy of MMT coupled with the strong coherent interaction between individual clay layers, further hinders the incorporation of polymer chains and hampers the compatibility of the resulting polymer nanocomposite, posing a difficulty in achieving uniform dispersion of clay into the polymer matrix. The agglomeration resulting due to the hydrophilic nature MMT, also tends to nullify the properties of the individual components. In order to achieve a more favorable synergy, between the pristine MMT and the polymers, hydrophilic MMT must be converted to organophilic. This surface modification can be attained by organophilization or organic modification, a technique that focuses on reducing the surface energy of the MMT, thereby allowing individual layers to separate and disperse into the polymer matrix, thus achieving a better inclusion of polymer chains into MMT [163,168–170].

Organomontmorillonite (OMMT) is produced by exchanging the inorganic cations of

MMT (Na<sup>+</sup>, K<sup>+</sup>, Ca<sup>2+</sup> and Mg<sup>2+</sup>) for surfactant including primary, secondary, tertiary and quaternary alkylammonium or alkylphoshonium cations [161,171]. Quaternary ammonium salts are regarded as the best organo-modifiers as seen from the literature [172,173]. When the inorganic ions are substituted by organic cations, the surface energy of MMT is diminished, the long alkyl tail increases the interlayer spacing, thereby improving the wettability of the polymer matrix [174]. The result is well dispersed clay within the polymer matrix as seen in Figure 2.16. The nanoclay resulting from the surface modification is termed as organoclay, for example (MMT when surface modified is called as organomodified MMT).

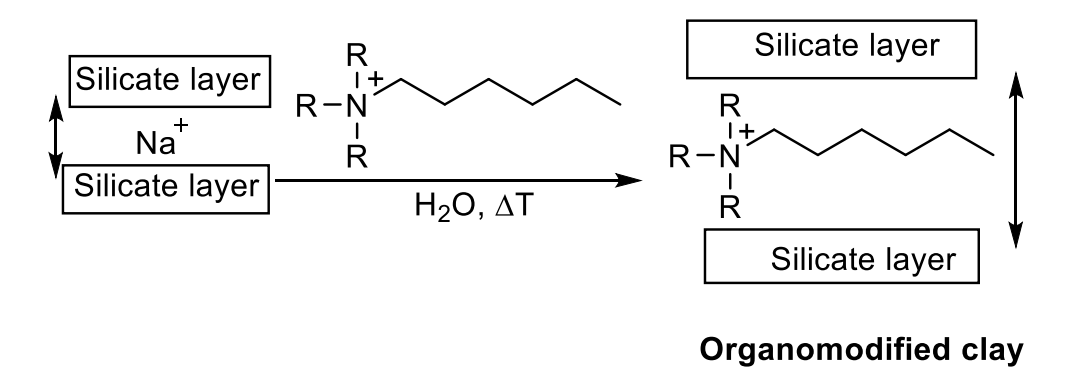


Figure 2.16. Surface modification of clay using quaternary ammonium, adapted from [157].

Table 2.2 presents the structure and commercial names of the modifiers used for producing PLA nanocomposites.

Table 2.2. Commonly modified montmorillonites used for producing PLA nanocomposites, adapted from [170].

Modifier	Modifier structure	Commercial name
Methyl, tallow, bis-2- hydroxyethyl, quaternary ammonium	CH <sub>2</sub> CH <sub>2</sub> OH I+ H <sub>3</sub> C -N-T I CH <sub>2</sub> CH <sub>2</sub> OH	Nanomer® I.34 TCN
Dimethyl, dehydrogenated tallow, 2-ethylhexyl quaternary ammonium	CH <sub>3</sub> I + H <sub>3</sub> C -N <sup>+</sup> -CH <sub>2</sub> CHCH <sub>2</sub> CH <sub>2</sub> CH <sub>2</sub> CH <sub>3</sub> I I HT CH <sub>2</sub> CH <sub>3</sub>	CLOISITE 25A/Southern Clay Products
Dimethyl, dehydrogenated tallow, quaternary ammonium	CH <sub>3</sub>  + H <sub>3</sub> C-N-HT   HT	CLOISITE 20A/Southern Clay Products CLOISITE 15A/Southern Clay Products
Methyl, dehydrogenated tallow, quaternary ammonium	H I+ H₃C−N−HT I HT	CLOISITE 93A/Southern Clay Products
Octadecyl ammonium	H   <sub>+</sub>     H—N—H     C <sub>18</sub> H <sub>37</sub>	NANOMER 1.30P/Nanocor
Stearyl dihydroxyethyl ammonium	TH + O H	NANOFIL 804/Sud-Chemie

<sup>\*</sup> T is tallow having around 65%  $C_{18}$ , 30% C16, and 5%  $C_{14}$ .

The chemical structure of the surfactant used defines how well the resulting dispersion of the nanoclay in the polymer matrix is going to be [176]. The carbonyl groups of PLA chains interact with the surfactant's hydroxyl groups and aids in the dispersion and separation of individual clay layer within the polymer matrix [177]. In addition, strong interaction of the hydroxyl groups of PLA with MMT platelet surfaces or with the hydroxyl group of the surfactant in the organomodified clay can also materialize which can further enhance the uniform dispersion [178].

#### 2.7.1.3 Morphology

The final properties of the resulting nanocomposites depend on the affinity between the hydrophilic silicate layers and the organophilic polymers, which in turn is dependent on the dispersion of the individual layers of silicates in the polymer matrix. Depending on the dispersion, three different structures as shown Figure 2.17:

- a) Microcomposite: a microcomposite structure is the structure wherein the clay and the polymer remain immiscible due to the low affinity between the two. This results in clay agglomeration (no delamination of the layers) and the resulting polymer nanocomposite has the same or even diminished properties.
- b) Intercalated nanocomposite: When affinity exists, intercalated nanocomposite is formed, wherein the polymer chains penetrate the interlayer or the galleries of the silicate layers. The intercalated nanocomposite is an ordered multilayer structure, with restricted polymer chain movements which results in material reinforcement.
- c) Exfoliated nanocomposite: When the layer structure of the clay is completely delaminated and is randomly dispersed, achieving maximum penetration into the polymer matrix, the emerging nanocomposite is exfoliated. Exfoliated nanocomposite manifests the highest potential of the layered silicates due to the optimal interaction and helps exploit the benefits of the nanocomposite.

Thus, it is of crucial importance to modify the hydrophilic surface to organophilic one to achieve agreement between the clay and polymer to capitalize on the resulting benefits of polymer nanocomposites. Mostly, the resulting nanocomposites are a mixture of both the intercalated and exfoliated morphologies called as disordered morphologies [179].

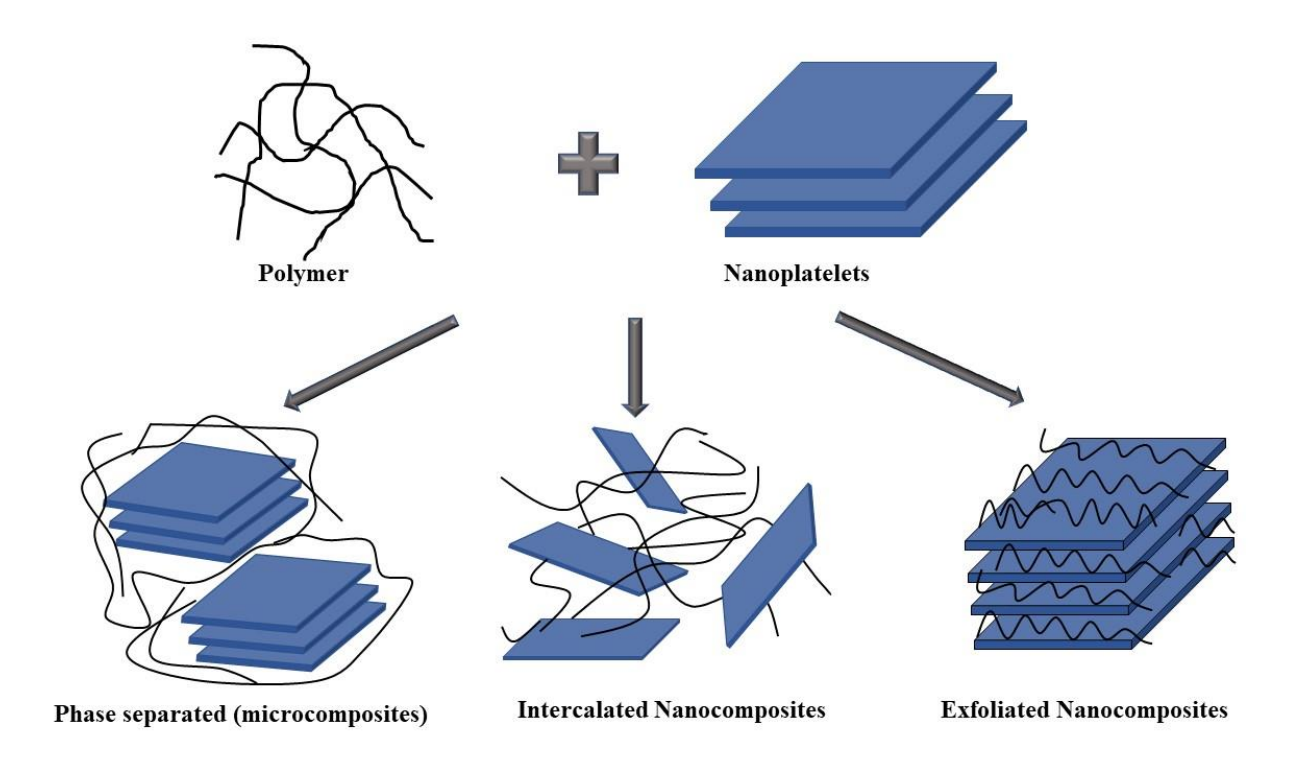


Figure 2.17. Different morphologies obtained from the nanoclay polymer interaction, adapted from [163].

### 2.7.1.4 Advantages of PLA nanocomposite

A significant improvement in the properties of PLA nanocomposites such as barrier, thermal and mechanical in comparison with pure PLA due to the addition of nanoclays. Many researchers have reported improvement in properties due to the addition of organomodified MMT in PLA [180–182]. In terms of barrier properties, the clay platelets form a maze creating a long torturous path for the permeant to trace, which increases its dwelling time and therefore improves the barrier properties at loading of as low as 0.5% [183–186]. Improvement in the mechanical properties in the PLA nanocomposites is ascribed to the presence of clay in tactoid form, which

act as nucleating agent thereby enhancing the crystallization capacity and in turn the tensile properties. Also the intercalation of PLA in the galleries of the clay along with the aspect ratio of clay dispersed, significantly improve the storage modulus and elongation at break [187–189]. Lewitus et al., observed, a 30% increase in the tensile modulus and 40% increase in elongation when films were extruded from masterbatch of PLLA with 5% OMMT loading [190]. On the same lines, Ray et al., reported improvement in biodegradability, storage modulus, flexural strength, gas permeability as compared to pure PLA [159,191,192].

## 2.7.1.5 Effect of nanoclay on PLA biodegradation

Nanoclay are incorporated into the PLA matrix, to enhance its properties. A significant improvement in mechanical and barrier properties is seen in PLA nanocomposites as compared to pure PLA [16]. One other drawback of biodegradable PLA, is the rate at which it biodegrades is still slow as compared to other organic wastes during composting [67]. Due to this, industrial composting facilities are hesitant towards accepting pure polymers. The nanoclays are known to affect the hydrolytic degradation as well as biodegradation and depending on the final application, this may or may not be beneficial.

Studies conducted by several researchers show the effect of nanoclays on the hydrolytic degradation and biodegradation of PLA nanocomposites due to the addition of MMT [193–197]. Paul et al., investigated the effect of MMT (unmodified clay) and two OMMT on the hydrolytic degradation of PLA in a phosphate buffer solution of pH 7.4 at 37°C [198]. The two OMMT had different surfactants having different nature, Cloisite<sup>®</sup>25A (low water affinity) and Cloisite<sup>®</sup>30B (high water affinity). A reduction of 41.6% was observed in  $M_n$  of unfilled PLA, while  $M_n$  loss of about 71.2% and 79.2% was observed in case of Cloisite<sup>®</sup>25A and Cloisite<sup>®</sup>30B PLA

nanocomposites after 165 days. A reduction of approximately 10°C in  $T_g$ , was observed for PLA after one month in the buffer solution, while for Cloisite®25A and Cloisite®30B the reduction was observed after two and a half months and one month respectively. This behavior is assigned to  $M_n$  reduction of PLA and plasticizing effect introduced due to the formation of lactic acid oligomers, resulting from degradation. More hydrophilic the filler, faster is the rate at which degradation occurs.

Fukushima et al., examined the consequences of two organomodified montmorillonites, namely Cloisite®30B and Nanofil 804 at 5% loading on PLA by performing biodegradation at  $40^{\circ}$ C [34]. The starting  $M_n$  for PLA, PLA- Cloisite®30B and PLA-Nanofil 804 was different and this can affect the way biodegradation proceeds. For molecular weight, in case of pure PLA, a reduction of 55% (72,743 g/mol to 32,755 g/mol) was observed. While a curtailment of around 79% and 40% was calculated for Cloisite®30B and Nanofil 804, after 17 weeks. The reduction in molecular weight in case of PLA nanocomposites was than pristine PLA, specifically more pronounced for Cloisite®30B and this can be accredited to good dispersion and the presence of hydroxylated groups in organomodified clay. In another work, Fukushima et al., [199] assessed the response of MMT and kaolinite on the biodegradation capacity of amorphous PLA (12% mol of D-Lactide) in compost at 32°C. Whitening and distortion of the PLA nanoclay film surface was noticed 6 weeks into the degradation test. DSC results demonstrated higher  $T_g$  reduction for nanocomposites. The biodegradation was found to be higher for kaolinite as compared to MMT because of the hydroxylated silicate layers of the clay.

Zhou and Xanthos studied how hydrolytic degradation is affected due to the presence of unmodified and modified clay (MMT and OMMT) for a semicrystalline PLLA (6% D-lactic acid)

and amorphous PDLLA for a temperature range of 50-70°C [79]. PDLLA and its composites underwent faster hydrolytic degradation as compared to PLLA and its composites. Due to its semicrystalline morphology, PLLA chains provided less chain mobility and free volume which is essentially necessary for higher amount of water uptake to carry out hydrolysis. The hydrolytic degradation rate constant was higher for nanocomposites followed by unmodified PLA and microcomposites was the lowest. Higher uptake of water by PLA nanocomposites was attributed to the greater extent of polymer matrix in close touch with the nanoclays edges, surface as compared to pristine PLA. The high dispersion of nanoclays heavily affected the water uptake capacity of PLA (easier water attack) which in turns exerts more influence on the rate at which hydrolysis proceeds.

Ray et al., [200] studied how biodegradation of PLA nanocomposites proceeds by simulating industrial composting norms at  $58 \pm 2^{\circ}$ C. The biodegradation rate of PLA and PLA nanocomposite sheets, made using three different organomodified clays was compared. The addition of nanoclays was shown to enhance the biodegradability of PLA nanocomposites as compared to unfilled PLA. The terminal hydroxyl groups of silicate layers of clay within PLA matrix started the heterogenous hydrolytic degradation via moisture absorption from compost. Another reason that accounted for the escalated biodegradation was the homogenous dispersion of intercalated organomodified clay in the PLA matrix. The uniform dispersion, assures maximum contact between the nanoclay edge, surface and the PLA matrix, thus increasing the likelihood of chain fragmentation and thus more degradation. Ray and Okamoto [201,159] conducted a respirometric test to scrutinize the biodegradation of PLA at  $58 \pm 2^{\circ}$ C. One study involved using varying percentage (4,7 and 10 %) of nanoclay incorporation in PLA. PLA-MMT showed enhanced biodegradation in comparison with PLA, due to the presence of hydrophilic silicate

layers or ammonium salts. Other study indicated the use of different surfactants for organomodification of clays. The mineralization ( $CO_2$  evolution) was determined for just PLA and PLA nanocomposites, PLA( $C_{18}$ -MMT) modified with octadecylammonium cations and PLA( $qC_{18}$ -MMT) modified with octadecyltrimethylammonium cations. Molecular weight reduction along with weight loss was measured and PLA( $qC_{18}$ -MMT) showed enhanced biodegradation and completely disappeared in compost.

Araújo et al. [202] introduced Cloisite®15A, Cloisite®30B, and Dellite 43B in PLA and performed biodegradation on the compression molded films at 40°C. High degradation was associated with samples containing Cloisite®15A and Cloisite®30B and barely small pieces were recovered after 6 weeks, whereas pure PLA and Dellite 43B containing samples remained intact. In conjunction, higher weight loss was observed for Cloisite®15A and Cloisite®30B. The dispersion of individual clay layers and presence of hydroxyl group in Cloisite®30B was held accountable for the catalytic hydrolysis of ester groups of PLA, thus improving the biodegradability of PLA.

Several other studies concluded the same effect of OMMT on the biodegradation of PLA, wherein nanocomposites have shown enhancement in the degradation activity as compared to pristine polymers [203–207]. The structure of the surfactant used also alters the degradation. The startling discovery among all the studies mentioned above was the different initial molecular weights before conducting the hydrolysis or biodegradation test, since low molecular weight PLA films with or without nanoclays tend to show higher degradation.

**REFERENCES** 

#### REFERENCES

- [1] F. Gironi and V. Piemonte, "Bioplastics and petroleum-based plastics: Strengths and weaknesses," *Energy Sources, Part A Recover. Util. Environ. Eff.*, vol. 33, no. 21, pp. 1949–1959, 2011.
- [2] L. Liu, S. Li, H. Garreau, and M. Vert, "Selective Enzymatic Degradations of Poly(L-lactide) and Poly(E-caprolactone) Blend Films," *Biomacromolecules*, vol. 1, no. 3, pp. 350–359, 2000.
- [3] Y. Li, "Biodegradable Poly(Lactic Acid) Nanocomposites: Synthesis And Characterization," 2011.
- [4] E. Castro-Aguirre, F. Iñiguez-Franco, H. Samsudin, X. Fang, and R. Auras, "Poly(lactic acid)—Mass production, processing, industrial applications, and end of life," *Adv. Drug Deliv. Rev.*, vol. 107, pp. 333–366, 2016.
- [5] S. S. Karkhanis, N. M. Stark, R. C. Sabo, and L. M. Matuana, "Blown film extrusion of poly(lactic acid) without melt strength enhancers," *J. Appl. Polym. Sci.*, vol. 134, no. 34, pp. 1–10, 2017.
- [6] M. Jamshidian, E. A. Tehrany, M. Imran, M. Jacquot, and S. Desobry, "Poly-Lactic Acid: Production, applications, nanocomposites, and release studies," *Compr. Rev. Food Sci. Food Saf.*, vol. 9, no. 5, pp. 552–571, 2010.
- [7] S. Domenek and D. Violette, "Characteristics and Applications of PLA," in *Biodegradable and Biobased Polymers for Environmental and Biomedical Applications*, 2016.
- [8] L. T. Sin, A. R. Rahmat, and W. A. W. A. Rahman, *Polylactic acid: PLA biopolymer technology and applications*. William Archer, 2012.
- [9] S. Farah, D. G. Anderson, and R. Langer, "Physical and mechanical properties of PLA, and their functions in widespread applications A comprehensive review," *Adv. Drug Deliv. Rev.*, vol. 107, pp. 367–392, Dec. 2016.
- [10] J. S. Bergstrom and D. Hayman, "An Overview of Mechanical Properties and Material Modeling of Polylactide (PLA) for Medical Applications," *Ann. Biomed. Eng.*, vol. 44, no. 2, pp. 330–340, 2015.
- [11] K. Hamad, M. Kaseem, H. W. Yang, F. Deri, and Y. G. Ko, "Properties and medical applications of polylactic acid: A review," *Express Polym. Lett.*, vol. 9, no. 5, pp. 435–455, 2015.
- [12] V. Siracusa, P. Rocculi, S. Romani, and M. D. Rosa, "Biodegradable polymers for food packaging: a review," *Trends Food Sci. Technol.*, vol. 19, no. 12, pp. 634–643, Dec. 2008.

- [13] R. A. Auras, "Investigation of polylactide as packaging material," 2004.
- [14] J. Lunt and A. L. Shafer, "Polylactic Acid Polymers from Corn. Applications in the Textiles Industry," *J. Coat. Fabr.*, vol. 29, no. 3, pp. 191–205, 2000.
- [15] M. VERT, G. SCHWARCH, and J. COUDANE, "Present and Future of PLA Polymers," J. Macromol. Sci. Part A Pure Appl. Chem., vol. 32, no. 4, pp. 787–796, 1995.
- [16] D. Notta-Cuvier *et al.*, "Tailoring polylactide (PLA) properties for automotive applications: Effect of addition of designed additives on main mechanical properties," *Polym. Test.*, vol. 36, pp. 1–9, 2014.
- [17] B. Gupta, N. Revagade, and J. Hilborn, "Poly(lactic acid) fiber: An overview," *Polym. Test.*, vol. 32, pp. 455–482, 2007.
- [18] M. G. Adsul, A. J. Varma, and D. V Gokhale, "Lactic acid production from waste sugarcane bagasse derived cellulose," *Green Chem.*, vol. 9, no. 1, pp. 58–62, 2007.
- [19] R. Datta and M. Henry, "Lactic acid: recent advances in products, processes and technologies a review," *J. Chem. Technol. Biotechnol.*, vol. 81, no. 7, pp. 1119–1129, 2006.
- [20] H. R. Kricheldorf:, I. Kreiser-Saunders, C. Jiirgen, and D. Wolter, "Polylactides Synthesis, Characterization and Medical Application," *Macromol. Symp.*, vol. 103, no. 1, pp. 85–102, 1996.
- [21] M. H. Hartmann, "High Molecular Weight Polylactic Acid Polymers," in *Biopolymers from Renewable Resources*, 1998, pp. 367–411.
- [22] S.-H. Hyon, K. Jamshidi, and Y. Ikada, "Synthesis of polylactides with different molecular weights," *Biomateriols*, vol. 18, no. 22, pp. 1503–1508, 1997.
- [23] Y. Zhao, Z. Wang, J. Wang, H. Mai, B. Yan, and F. Yang, "Direct Synthesis of Poly(D,L-lactic acid) by Melt Polycondensation and Its Application in Drug Delivery," *J. Appl. Polym. Sci.*, vol. 91, no. 4, pp. 2143–2150, 2004.
- [24] P. Sanglard, V. Adamo, J.-P. Bourgeois, T. Chappuis, E. Vanoli, and E. Vanoli, "Poly(lactic acid) Synthesis and Characterization," *Chimia (Aarau)*., vol. 66, no. 12, pp. 951–954, 2012.
- [25] S. Jacobsen, H.-G. Fritz, P. Degée, P. Dubois, and R. Jérôme, "New developments on the ring opening polymerisation of polylactide," *Ind. Crop. Prod.* (2000), vol. 11, no. 2–3, pp. 265–275, 2000.
- [26] O. Nuyken and S. D. Pask, "Ring-opening polymerization-An introductory review," *Polymers (Basel).*, vol. 5, no. 2, pp. 361–403, 2013.
- [27] A. P. Gupta and V. Kumar, "New emerging trends in synthetic biodegradable polymers-

- Polylactide: A critique," Eur. Polym. J., vol. 43, no. 10, pp. 4053–4074, 2007.
- [28] R. P. O'Connor *et al.*, "The Sustainability of NatureWorks<sup>TM</sup> Polylactide Polymers and Ingeo<sup>TM</sup> Polylactide Fibers: an Update of the Future," *Macromol. Biosci.*, vol. 4, no. 6, pp. 551–564, 2004.
- [29] K. Porter, "Ring Opening Polymerization of Lactide for The synthesis of Poly (Lactic Acid)," 2006.
- [30] G. Kale, T. Kijchavengkul, R. Auras, M. Rubino, S. E. Selke, and S. P. Singh, "Compostability of bioplastic packaging materials: An overview," *Macromol. Biosci.*, vol. 7, no. 3, pp. 255–277, 2007.
- [31] R. Auras, B. Harte, and S. Selke, "An overview of polylactides as packaging materials," *Macromol. Biosci.*, vol. 4, no. 9, pp. 835–864, 2004.
- [32] J. M. Lagaron and A. Lopez-Rubio, "Nanotechnology for bioplastics: Opportunities, challenges and strategies," *Trends Food Sci. Technol.*, vol. 22, no. 11, pp. 611–617, 2011.
- [33] A. P. Kumar, D. Depan, N. Singh Tomer, and R. P. Singh, "Nanoscale particles for polymer degradation and stabilization-Trends and future perspectives," *Prog. Polym. Sci.*, vol. 34, no. 6, pp. 479–515, 2009.
- [34] K. Fukushima, C. Abbate, D. Tabuani, M. Gennari, and G. Camino, "Biodegradation of poly(lactic acid) and its nanocomposites," *Polym. Degrad. Stab.*, vol. 94, no. 10, pp. 1646–1655, 2009.
- [35] S. S. Karkhanis, L. M. Matuana, N. M. Stark, and R. C. Sabo, "Effect Of Compounding Approaches On Fiber Dispersion And Performance Of Poly(Lactic Acid)/Cellulose Nanocrystal Composite Blown Films," 2017.
- [36] R. Al-Itry, K. Lamnawar, and A. Maazouz, "Improvement of thermal stability, rheological and mechanical properties of PLA, PBAT and their blends by reactive extrusion with functionalized epoxy," *Polym. Degrad. Stab.*, vol. 97, no. 10, pp. 1898–1914, 2012.
- [37] M.-P. Ho, K.-T. Lau, H. Wang, and D. Hui, "Improvement on the properties of polylactic acid (PLA) using bamboo charcoal particles," *Compos. Part B*, vol. 81, pp. 14–25, 2015.
- [38] M. Jonoobi, J. Harun, A. P. Mathew, and K. Oksman, "Mechanical properties of cellulose nanofiber (CNF) reinforced polylactic acid (PLA) prepared by twin screw extrusion," *Compos. Sci. Technol.*, vol. 70, no. 12, pp. 1742–1747, 2010.
- [39] M. Raja, S. H. Ryu, and A. M. Shanmugharaj, "Macromolecular Nanotechnology Thermal, mechanical and electroactive shape memory properties of polyurethane (PU)/poly (lactic acid) (PLA)/CNT nanocomposites," *Eur. Polym. J.*, vol. 49, no. 11, pp. 3492–3500, 2013.
- [40] J.-W. Rhim, S.-I. Hong, and C.-S. Ha, "Tensile, water vapor barrier and antimicrobial

- properties of PLA/nanoclay composite films," *Food Sci. Technol.*, vol. 42, no. 2, pp. 612–617, 2009.
- [41] N. S. Allen and M. Edge, Fundamentals of Polymer Degradation and Stabilization. 1992.
- [42] S. H. Hamid, Handbook of Polymer Degradation. 2000.
- [43] R. P. Singh, P. N. Thanki, S. S. Solanky, and S. M. Desai, "Photodegradation and stabilization of polymers," *Adv. Funct. Mol. Polym.*, vol. 4, pp. 1–19, 1995.
- [44] G. Scott and D. Gilead, "Introduction to the abiotic degradation of carbon chain polymers," in *Degradable polymers: principles and applications*, 1987, pp. 1–128.
- [45] M. Iring, T. Kelen, and F. Tudos, "Initiated Oxidation And Auto-Oxidation Of Polyethylene In Trichlorobenzene Solution," *Polym. Degrad. Stab.*, vol. 1, no. 4, pp. 297–310, 1979.
- [46] Y. A. Mikheev, G. E. Zaikov, and V. G. Zaikov, "Heterogeneous features of autooxidation of hydrocarbon polymers," *Polym. Degrad. Stab.*, vol. 72, no. 1, pp. 1–21, 2001.
- [47] X. Colin and J. Verdu, "Polymer degradation during processing," *Comptes Rendus Chim.*, vol. 9, no. 11–12, pp. 1380–1395, 2006.
- [48] J. Friedrich, I. Loeschcke, H. Frommelt, H.-D. Reiner, H. Zirnmermann, and P. Lutgen, "Ageing and Degradation of Poly(ethylene terephthalate) in an Oxygen Plasma," *Polym. Degrad. Stab.*, vol. 31, no. 1, pp. 97–114, 1991.
- [49] J. R. White and A. Turnbull, Weathering of polymers: mechanisms of degradation and stabilization, testing strategies and modelling, vol. 29. 1994.
- [50] J. G. Speight, "Transformation of Inorganic Chemicals in the Environment," in *Environmental Inorganic Chemistry for Engineers*, Butterworth-Heinemann, 2017, pp. 333–382.
- [51] Martin Alexander, "Biodegradation and Bioremediation," in *Journal of controlled release*, vol. 2, no. 67, 2000, pp. 1–418.
- [52] J. J. Kolstad, E. T. H. Vink, B. De Wilde, and L. Debeer, "Assessment of anaerobic degradation of Ingeo<sup>TM</sup> polylactides under accelerated landfill conditions," *Polym. Degrad. Stab.*, vol. 97, no. 7, pp. 1131–1141, 2012.
- [53] S. Grima, V. Bellon-Maurel, P. Feuilloley, and F. Silvestre, "Aerobic Biodegradation of Polymers in Solid-State Conditions: A Review of Environmental and Physicochemical Parameter Settings in Laboratory Simulations," *J. Polym. Environ.*, vol. 8, no. 4, pp. 183– 195, 2000.
- [54] ASTM International, "ASTM D6400 12 Standard Specification for Labeling of Plastics Designed to be Aerobically Composted in Municipal or Industrial Facilities," in *ASTM*

- Standards., 2012, pp. 1–3.
- [55] I. Kyrikou and D. Briassoulis, "Biodegradation of Agricultural Plastic Films: A Critical Review," *J. Polym. Environ.*, vol. 15, no. 2, pp. 125–150, Apr. 2007.
- [56] Y. Tokiwa and B. P. Calabia, "Biodegradability and Biodegradation of Poly(lactide)," *Appl. Microbiol. Biotechnol.*, vol. 72, no. 2, pp. 244–251, 2006.
- [57] Ken-ichi Kasuya, Ko-ichi Takagi, Shin-ichi Ishiwatari, Yasuhiko Yoshidab, and Yoshibaru Doi, "Biodegradabilities of various aliphatic polyesters in natural waters," *Polym. Degrad. Stab.*, vol. 59, no. 1–3, pp. 327–332, 1998.
- [58] Eduardo Díaz, Microbial Biodegradation: Genomics and Molecular Biology. 2008.
- [59] D. Briassoulis, C. Dejean, and P. Picuno, "Critical Review of Norms and Standards for Biodegradable Agricultural Plastics Part II: Composting," *J. Polym. Environ.*, vol. 18, no. 3, pp. 364–383, Sep. 2010.
- [60] A. Ali Shah, F. Hasan, A. Hameed, and S. Ahmed, "Biological degradation of plastics: A comprehensive review," *Biotechnol. Adv.*, vol. 26, no. 3, pp. 246–265, 2008.
- [61] E. Castro, "Design And Construction Of A Medium-Scale Automated Direct Measurement Respirometric System To Assess Aerobic Biodegradation Of Polymers," 2013.
- [62] K. Van De Velde and P. Kiekens, "Biopolymers: overview of several properties and consequences on their applications," *Polym. Test.*, vol. 21, no. 4, pp. 433–442, 2002.
- [63] N. Lucas, C. Bienaime, C. Belloy, M. Queneudec, F. Silvestre, and J.-E. Nava-Saucedo, "Polymer biodegradation: Mechanisms and estimation techniques A review," *Chemosph.*, vol. 73, no. 4, pp. 429–442, 2008.
- [64] M. Itavaara and M. Vikman, "An Overview of Methods for Biodegradability Testing of Biopolymers and Packaging Materials," *J. Environ. Polym. Degrad.*, vol. 4, no. 1, pp. 29–36, 1996.
- [65] T. Kijchavengkul, R. Auras, M. Rubino, M. Ngouajio, and R. Thomas Fernandez, "Development of an automatic laboratory-scale respirometric system to measure polymer biodegradability," *Polym. Test.*, vol. 25, no. 8, pp. 1006–1016, 2006.
- [66] Dimitris P. Komilis, "A kinetic analysis of solid waste composting at optimal conditions," *Waste Manag.*, vol. 26, no. 1, pp. 82–91, 2006.
- [67] P. Stloukal *et al.*, "Kinetics and mechanism of the biodegradation of PLA/clay nanocomposites during thermophilic phase of composting process," *Waste Manag.*, vol. 42, no. April, pp. 31–40, 2015.
- [68] V. Mittal, Characterization techniques for polymer nanocomposites. Wiley-VCH, 2012.

- [69] ASTM International, "ASTM D5338-15: Standard Test Method for Determining Aerobic Biodegradation of Plastic Materials Under Controlled Composting Conditions, Conditions, Incorporating Thermophilic Temperatures," in *ASTM Standards*., 2015, pp. 1–7.
- [70] E. Castro-Aguirre, "Increasing The Biodegradation Rate Of Poly (Lactic Acid) In Composting Conditions," 2018.
- [71] H. Tsuji, R. Auras, L.-T. Lim, and S. Selke, *Poly(lactic acid): synthesis, structures, properties, processing and applications.* Wiley, 2011.
- [72] K.Madhavan Nampoothiri, Nimisha Rajendran Nair, and Rojan Pappy John, "An overview of the recent developments in polylactide (PLA) research," *Bioresour. Technol.*, vol. 101, no. 22, pp. 8493–8501, 2010.
- [73] V. Piemonte and F. Gironi, "Lactic Acid Production by Hydrolysis of Poly(Lactic Acid) in Aqueous Solutions: An Experimental and Kinetic Study," *J. Polym. Environ.*, vol. 21, no. 1, pp. 275–279, 2013.
- [74] E. F. Craparo, B. Porsio, M. L. Bondì, G. Giammona, and G. Cavallaro, "Evaluation of biodegradability on polyaspartamide-polylactic acid based nanoparticles by chemical hydrolysis studies," *Polym. Degrad. Stab.*, vol. 119, pp. 56–67, 2015.
- [75] S. Li and S. McCarthy, "Further investigations on the hydrolytic degradation of poly (DL-lactide)," *Biomaterials*, vol. 20, no. 1, pp. 35–44, 1999.
- [76] Felix Simonovsky, "University of Washington Engineered Biomaterials :: Research : Biomaterials Tutorial." [Online]. Available: https://www.uweb.engr.washington.edu/research/tutorials/plagla.html. [Accessed: 13-Mar-2019].
- [77] M. A. Elsawy, K. H. Kim, J. W. Park, and A. Deep, "Hydrolytic degradation of polylactic acid (PLA) and its composites," *Renew. Sustain. Energy Rev.*, vol. 79, no. April, pp. 1346–1352, 2017.
- [78] M. Hakkarainen, "Aliphatic Polyesters: Abiotic and Biotic Degradation and Degradation Products," in *Degradable Aliphatic Polyesters*, Berlin, Heidelberg: Springer Berlin Heidelberg, 2002, pp. 113–138.
- [79] Q. Zhou and M. Xanthos, "Nanoclay and crystallinity effects on the hydrolytic degradation of polylactides," *Polym. Degrad. Stab.*, vol. 93, no. 8, pp. 1450–1459, 2008.
- [80] H. Antheunis, J.-C van der Meer, M. de Geus, A. Heise, and C.E. Koning, "Autocatalytic Equation Describing the Change in Molecular Weight during Hydrolytic Degradation of Aliphatic Polyesters," *Biomacromolecules*, vol. 11, no. 4, pp. 1118–1124, 2010.
- [81] E. J. Rodriguez, B. Marcos, and M. A. Huneault, "Hydrolysis of polylactide in aqueous media," *J. Appl. Polym. Sci.*, vol. 133, no. 44, pp. 1–11, 2016.

- [82] J. Siepmann, "Mathematical modeling of bioerodible, polymeric drug delivery systems," *Adv. Drug Deliv. Rev.*, vol. 48, no. 2–3, pp. 229–247, Jun. 2001.
- [83] F. Iñiguez-Franco *et al.*, "Control of hydrolytic degradation of Poly(lactic acid) by incorporation of chain extender: From bulk to surface erosion," *Polym. Test.*, vol. 67, no. February, pp. 190–196, 2018.
- [84] L. N. Woodard and M. A. Grunlan, "Hydrolytic Degradation and Erosion of Polyester Biomaterials," *ACS Macro Lett.*, vol. 7, no. 8, pp. 976–982, 2018.
- [85] X. Zhang, M. Espiritu, A. Bilyk, and L. Kurniawan, "Morphological behaviour of poly(lactic acid) during hydrolytic degradation," *Polym. Degrad. Stab.*, vol. 93, no. 10, pp. 1964–1970, 2008.
- [86] F. Von Burkersroda, L. Schedl, and A. G. Opferich, "Why degradable polymers undergo surface erosion or bulk erosion," *Biomaterials*, vol. 23, no. 21, pp. 4221–4231, 2002.
- [87] B. D. Ulery, "Molecular design of nanoparticle-based delivery vehicles for pneumonic plague," 2015.
- [88] D. K. Gilding and A. M. Reed, "Biodegradable polymers for use in surgery polyglycolic/poly(actic acid) homo-and copolymers: 1," *Polym.*, vol. 20, no. 12, pp. 1459–1464, 1979.
- [89] M. Vert, G. Schwarch, and J. Coudane, "Present and Future of PLA Polymers," *J. Macromol. Sci. Part A Pure Appl. Chem.*, vol. 32, no. 4, pp. 787–796, 1995.
- [90] C. Shih, "Chain-end scission in acid catalyzed hydrolysis of poly(D,L-lactide) in solution," *J. Control. Release*, vol. 34, no. 1, pp. 9–15, 1995.
- [91] Y. Li and T. Kissel, "Synthesis, characteristics and in vitro degradation of star-block copolymers consisting of L-lactide, glycolide and branched multi-arm poly(ethylene oxide)," *Polymer (Guildf).*, vol. 39, no. 18, pp. 4421–4427, 1998.
- [92] J. Mauduit, E. Perouse, and M. Vert, "Hydrolytic degradation of films prepared from blends of high and low molecular weight poly(DL-lactic acid)s," *J. Biomed. Mater. Res.*, vol. 30, no. 2, pp. 201–207, Feb. 1996.
- [93] H. Fukuzaki, M. Yoshida, M. Asano, and M. Kumakura, "Synthesis Of Copoly(D,L-Lactic Acid) With Relatively Low Molecular Weight And In Vitro Degradation," *Eur. Poluymer J.*, vol. 25, no. 10, pp. 1019–1026, 1989.
- [94] L. Lu, C. A. Garcia, and A. G. Mikos, "In vitro degradation of thin poly(DL-lactic-coglycolic acid) films," *J. Biomed. Mater. Res.*, vol. 46, no. 2, pp. 236–244, 1999.
- [95] K. W. Leong, B. C. Brott, and R. Langer, "Bioerodible polyanhydrides as drug-carrier matrices. I: Characterization, degradation, and release characteristics," *J. Biomed. Mater. Res.*, vol. 19, no. 8, pp. 941–955, Oct. 1985.

- [96] A. J. Kirby, "Hydrolysis and Formation of Esters of Organic Acids," *Compr. Chem. Kinet.*, vol. 10, pp. 57–202, Jan. 1972.
- [97] A. Belbella, C. Vauthier, H. Fessi, J.-P. Devissaguet, and F. Puisieux, "In vitro degradation of nanospheres from poly(D,L-lactides) of different molecular weights and polydispersities," *Int. J. Pharm.*, vol. 129, no. 1–2, pp. 95–102, 1996.
- [98] S. M. Li, H. Garreau, and M. Vert, "Structure-property relationships in the case of the degradation of massive aliphatic poly-(α-hydroxy acids) in aqueous media," *J. Mater. Sci. Mater. Med.*, vol. 1, no. 3, pp. 123–130, 1990.
- [99] S. J. De Jong, E. R. Arias, D. T. S. Rijkers, C. F. Van Nostrum, J. J. Kettenes-Van Den Bosch, and W. E. Hennink, "New insights into the hydrolytic degradation of poly(lactic acid): Participation of the alcohol terminus," *Polymer (Guildf)*., vol. 42, no. 7, pp. 2795–2802, 2001.
- [100] K. Makino, H. Ohshima, and T. Kondo, "Mechanism of hydrolytic degradation of poly(L-lactide) microcapsules: effects of pH, ionic strength and buffer concentration," *J. Microencapsul.*, vol. 3, no. 3, pp. 203–212, Jan. 1986.
- [101] G. Schliecker, C. Schmidt, S. Fuchs, and T. Kissel, "Characterization of a homologous series of D,L-lactic acid oligomers; a mechanistic study on the degradation kinetics in vitro," *Biomaterials*, vol. 24, no. 21, pp. 3835–3844, 2003.
- [102] A. Finniss, S. Agarwal, and R. Gupta, "Retarding hydrolytic degradation of polylactic acid: Effect of induced crystallinity and graphene addition," *J. Appl. Polym. Sci.*, vol. 133, no. 43, pp. 1–8, 2016.
- [103] R. P. Batycky, J. Hanes, R. Langer, and D. A. E. §x, "A Theoretical Model of Erosion and Macromolecular Drug Release from Biodegrading Microspheres," *J. Pharm. Sci.*, vol. 86, no. 12, pp. 1464–1477, 1997.
- [104] C. Shih, "A Graphical Method for the Determination of the Mode of Hydrolysis of Biodegradable Polymers," *Pharm. Res. An Off. J. Am. Assoc. Pharm. Sci.*, vol. 12, no. 12, pp. 2036–2040, 1995.
- [105] Fabiola, "Hydrolytic Degradation of Poly (lactic acid) and Poly (lactic acid) Nanocomposites by Water-Ethanol Solutions Fabiola Maria Iñiguez Franco A Comprehensive Examination Material Doctor of Philosophy Packaging," 2016.
- [106] S. Lyu *et al.*, "Kinetics and Time-Temperature Equivalence of Polymer Degradation," *Biomacromolecules*, vol. 8, no. 7, pp. 2301–2310, 2007.
- [107] J. H. Jung, M. Ree, and H. Kim, "Acid-and base-catalyzed hydrolyses of aliphatic polycarbonates and polyesters," *Catal. today*, vol. 115, no. 1–4, pp. 283–287, 2006.
- [108] A. Göpferich, "Mechanisms of polymer degradation and erosion," in *The Biomaterials:* Silver Jubilee Compendium, vol. 17, no. 2, Elsevier, 1996, pp. 117–128.

- [109] H. Tsuji and Y. Ikada, "Properties and Morphology of Poly( L-lactide). II. Hydrolysis in Alkaline Solution," *Polymer (Guildf)*., vol. 36, no. 1, pp. 59–66, 1997.
- [110] X. Yuan, A. F. T. Mak, and K. Yao, "In vitro degradation of poly(L-lactic acid) fibers in phosphate buffered saline," *J. Appl. Polym. Sci.*, vol. 85, no. 5, pp. 936–943, 2002.
- [111] X. Yuan, A. F. T. Mak, and K. Yao, "Comparative observation of accelerated degradation of poly(l-lactic acid) fibres in phosphate buffered saline and a dilute alkaline solution," *Polym. Degrad. Stab.*, vol. 75, no. 1, pp. 45–53, 2002.
- [112] S. K. Saha and H. Tsuji, "Effects of molecular weight and small amounts of D-lactide units on hydrolytic degradation of poly(L-lactic acid)s," *Polym. Degrad. Stab.*, vol. 91, no. 8, pp. 1665–1673, 2006.
- [113] C. C. Chu, "A Comparison of the Effect of pH on the Biodegradation of Two Synthetic Absorbable Sutures," *Ann. Surg.*, vol. 195, no. 1, pp. 55–59, 1982.
- [114] M. Vert, S. Li, and H. Garreau, "More about the degradation of LA/GA-derived matrices in aqueous media," *J. Control. Release*, vol. 16, no. 1–2, pp. 15–26, 1991.
- [115] J. HELLER, "Controlled Drug Release from Poly(ortho esters)," *Ann. N. Y. Acad. Sci.*, vol. 446, no. 1, pp. 51–66, Jun. 1985.
- [116] F. Codari, S. Lazzari, M. Soos, G. Storti, M. Morbidelli, and D. Moscatelli, "Kinetics of the hydrolytic degradation of poly(lactic acid)," *Polym. Degrad. Stab.*, vol. 97, pp. 2460–2466, 2012.
- [117] C. F. Van Nostrum, T. F. J. Veldhuis, G. W. Bos, and W. E. Hennink, "Hydrolytic degradation of oligo(lactic acid): a kinetic and mechanistic study," *Polymer (Guildf)*., vol. 45, no. 20, pp. 6779–9787, 2004.
- [118] S. Lazzari, F. Codari, G. Storti, M. Morbidelli, and D. Moscatelli, "Modeling the pH-dependent PLA oligomer degradation kinetics," *Polym. Degrad. Stab.*, vol. 110, pp. 80–90, 2014.
- [119] L. Fabrice, P. Roberto, I. Valentina, A. Haroutioun, and V. Vincent, "Poly(Lactic Acid)-Based Nanobiocomposites with Modulated Degradation Rates," *Materials (Basel).*, vol. 11, no. 10, pp. 1–19, 2018.
- [120] M. P. Balaguer, C. Aliaga, C. Fito, and M. Hortal, "Compostability assessment of nanoreinforced poly(lactic acid) films," *Waste Manag.*, vol. 48, pp. 143–155, 2016.
- [121] P. Stloukal, A. Kalendova, H. Mattausch, S. Laske, C. Holzer, and M. Koutny, "The influence of a hydrolysis-inhibiting additive on the degradation and biodegradation of PLA and its nanocomposites," *Polym. Test.*, vol. 41, pp. 124–132, Feb. 2015.
- [122] D. N. Bikiaris, "Nanocomposites of aliphatic polyesters: An overview of the effect of different nanofillers on enzymatic hydrolysis and biodegradation of polyesters," *Polym.*

- Degrad. Stab., vol. 98, no. 9, pp. 1908–1928, Sep. 2013.
- [123] S. Benali, S. Aouadi, A.-L. Dechief, M. Murariu, and P. Dubois, "Key factors for tuning hydrolytic degradation of polylactide/zinc oxide nanocomposites," *Nanocomposites*, vol. 1, no. 1, pp. 51–61, Feb. 2015.
- [124] Y. Aso, S. Yoshioka, A. Li Wan Po, and T. Terao, "Effect of temperature on mechanisms of drug release and matrix degradation of poly(d,l-lactide) microspheres," *J. Control. Release*, vol. 31, no. 1, pp. 33–39, Aug. 1994.
- [125] M. Deng *et al.*, "Effect of load and temperature on in vitro degradation of poly(glycolide-co-l-lactide) multifilament braids," *Biomaterials*, vol. 26, no. 20, pp. 4327–4336, Jul. 2005.
- [126] N. A. Weir, F. J. Buchanan, J. F. Orr, D. F. Farrar, and G. R. Dickson, "Degradation of poly-L-lactide. Part 2: Increased temperature accelerated degradation," *Proc. Inst. Mech. Eng. Part H J. Eng. Med.*, vol. 218, no. 5, pp. 321–330, May 2004.
- [127] A. M. Reed and D. K. Gilding, "Biodegradable polymers for use in surgery poly(glycolic)/poly(lactic acid) homo and copolymers: 2. In vitro degradation," *Polymer* (*Guildf*)., vol. 22, no. 4, pp. 494–498, Apr. 1981.
- [128] C.C.Chu, "Classification and General Characteristics of Suture Materials," Wound Clos. Biomater. DeVices, pp. 182–183, 1997.
- [129] N. T. Lotto, M. R. Calil, C. G. F. Guedes, and D. S. Rosa, "The effect of temperature on the biodegradation test," *Mater. Sci. Eng. C*, vol. 24, no. 5, pp. 659–662, Nov. 2004.
- [130] C. M. Agrawal, D. Huang, J. P. Schmitz, and K. A. Athanasiou, "Elevated Temperature Degradation of a 50:50 Copolymer of PLA-PGA," *Tissue Eng.*, vol. 3, no. 4, pp. 345–352, Dec. 1997.
- [131] H. Planck et al., Degradation Phenomena on Polymeric Biomaterials. 1991.
- [132] H. Tsuji, T. Ono, T. Saeki, H. Daimon, and K. Fujie, "Hydrolytic degradation of poly(ε-caprolactone) in the melt," *Polym. Degrad. Stab.*, vol. 89, no. 2, pp. 336–343, Aug. 2005.
- [133] A. Torres, S. M. Li, S. Roussos, and A. M. Vert, "Screening of Microorganisms for Biodegradation of Poly(Lactic Acid) and Lactic Acid-Containing Polymers," 1996.
- [134] I. Grizzi, H. Garreau, S. Li, and M. Vert, "Hydrolytic degradation of devices based on poly(DL-lactic acid) size-dependence," *Biomaterials*, vol. 16, no. 4, pp. 305–311, Mar. 1995.
- [135] G. Li, H. Garreau, and M. Vert, "Structure-property relationships in the case of the degradation of massive poly(-hydroxy acids) in aqueous media. Part 3 Influence of the morphology of poly(L-/actic acid)," *J. Mater. Sci. Mater. Med.*, vol. 1, no. 4, pp. 198–206, 1990.

- [136] K. G. Ho, A. L. Pometto, and P. N. Hinz, "Effects of temperature and relative humidity on polylactic acid plastic degradation," *J. Environ. Polym. Degrad.*, vol. 7, no. 2, pp. 83–92, 1999.
- [137] K. Jamshidi, S.-H. Hyon, and Y. Ikada, "Thermal characterization of polylactides," *Polymer (Guildf).*, vol. 29, no. 12, pp. 2229–2234, Dec. 1988.
- [138] M. K. Mitchell and D. E. Hirt, "Degradation of PLA fibers at elevated temperature and humidity," *Polym. Eng. Sci.*, vol. 55, no. 7, pp. 1652–1660, Jul. 2015.
- [139] W. L. Tham, B. T. Poh, Z. A. Mohd Ishak, and W. S. Chow, "Water Absorption Kinetics and Hygrothermal Aging of Poly(lactic acid) Containing Halloysite Nanoclay and Maleated Rubber," *J. Polym. Environ.*, vol. 23, no. 2, pp. 242–250, 2015.
- [140] C. Migliaresi, L. Fambri, and D. Cohn, "A study on the in vitro degradation of poly(lactic acid)," *J. Biomater. Sci. Polym. Ed.*, vol. 5, no. 6, pp. 591–606, Jan. 1994.
- [141] H. A. Von Ream, R. L. Cleek, S. G. E&in+, and A. G. Mikos, "Degradation of polydispersed poly(L-lactic acid) to modulate lactic acid release," *Biomaterials*, vol. 16, no. 6, pp. 441–447, 1995.
- [142] S. K. Saha and H. Tsuji, "Hydrolytic Degradation of Amorphous Films of L-Lactide Copolymers with Glycolide and D-Lactide," *Macromol. Mater. Eng.*, vol. 291, no. 4, pp. 357–368, Apr. 2006.
- [143] E. Çelikkaya, E. B. Denkbaş, and E. Pişkin, "Poly(DL-lactide)/poly(ethylene glycol) copolymer particles. I. Preparation and characterization," *J. Appl. Polym. Sci.*, vol. 61, no. 9, pp. 1439–1446, Aug. 1996.
- [144] H. Pistner, D. R. Bendi, J. Mühling, and J. F. Reuther, "Poly (1-lactide): a long-term degradation study in vivo: Part III. Analytical characterization," *Biomaterials*, vol. 14, no. 4, pp. 291–298, Jan. 1993.
- [145] H. Tsuji, "Hydrolytic degradation," in *Poly(lactic acid): synthesis, structures, properties, processing, and applications,* New Jersey: John Wiley & Sons, Inc, 2010, pp. 345–381.
- [146] M. Vert, "Degradation of Polymeric Biomaterials with Respect to Temporary Therapeutic Applications: Tricks And Treats," in *Degradable Materials*, CRC Press, 2018, pp. 11–38.
- [147] K. Fukushima, J. L. Feijoo, and M.-C. Yang, "Comparison of abiotic and biotic degradation of PDLLA, PCL and partially miscible PDLLA/PCL blend," *Eur. Polym. J.*, vol. 49, no. 3, pp. 706–717, Mar. 2013.
- [148] H. Tsuji and Y. Ikada, "Blends of aliphatic polyesters. II. Hydrolysis of solution-cast blends from poly(L-lactide) and poly(ε-caprolactone) in phosphate-buffered solution," *J. Appl. Polym. Sci.*, vol. 67, no. 3, pp. 405–415, 2002.
- [149] H. Tsuji and T. Ishizaka, "Blends of aliphatic polyesters. VI. Lipase-catalyzed hydrolysis

- and visualized phase structure of biodegradable blends from poly( $\epsilon$ -caprolactone) and poly(L-lactide)," *Int. J. Biol. Macromol.*, vol. 29, no. 2, pp. 83–89, 2001.
- [150] A. P. Kumar, D. Depan, N. Singh Tomer, and R. P. Singh, "Nanoscale particles for polymer degradation and stabilization—Trends and future perspectives," *Prog. Polym. Sci.*, vol. 34, no. 6, pp. 479–515, Jun. 2009.
- [151] P. B. Messersmith and E. P. Giannelis, "Synthesis and Characterization of Layered Silicate-Epoxy Nanocomposites," *Chem. Mater.*, vol. 6, no. 10, pp. 1719–1725, Oct. 1994.
- [152] Y. Kojima *et al.*, "Mechanical properties of nylon 6-clay hybrid," *J. Mater. Res.*, vol. 8, no. 5, pp. 1185–1189, 2019.
- [153] P. C. Lebaron, Z. Wang, and T. J. Pinnavaia, "Polymer-layered silicate nanocomposites: an overview," *Appl. Clay Sci.*, vol. 15, no. 1–2, pp. 11–29, 1999.
- [154] † Masami Okamoto, \*, † Pham Hoai Nam, † Pralay Maiti, † Tadao Kotaka, ‡ and Naoki Hasegawa, and A. Usuki‡, "A House of Cards Structure in Polypropylene/Clay Nanocomposites under Elongational Flow," *Nano Lett.*, vol. 16, no. 6, pp. 295–298, 2001.
- [155] † Masami Okamoto, \* *et al.*, "Biaxial Flow-Induced Alignment of Silicate Layers in Polypropylene/Clay Nanocomposite Foam," *Nano Lett.*, vol. 1, no. 9, pp. 503–505, 2001.
- [156] M. Alexandre and P. Dubois, "Polymer-layered silicate nanocomposites: preparation, properties and uses of a new class of materials," *Mater. Sci. Eng.*, vol. 28, no. 1–2, pp. 1–63, 2000.
- [157] J.-M. Raquez, Y. Habibi, M. Murariu, and P. Dubois, "Polylactide (PLA)-based nanocomposites," *Prog. Polym. Sci.*, vol. 38, no. 10–11, pp. 1504–1542, 2013.
- [158] K. Müller *et al.*, "Review on the Processing and Properties of Polymer Nanocomposites and Nanocoatings and Their Applications in the Packaging, Automotive and Solar Energy Fields," *Nanomaterials*, vol. 7, no. 4, p. 74, Mar. 2017.
- [159] S. Sinha Ray and M. Okamoto, "Biodegradable polylactide and its nanocomposites: Opening a new dimension for plastics and composites," *Macromol. Rapid Commun.*, vol. 24, no. 14, pp. 815–840, 2003.
- [160] S. V. N. T. Kuchibhatla, A. S. Karakoti, D. Bera, and S. Seal, "One dimensional nanostructured materials," *Prog. Mater. Sci.*, vol. 52, no. 5, pp. 699–913, Jul. 2007.
- [161] M. Kotal and A. K. Bhowmick, "Polymer nanocomposites from modified clays: Recent advances and challenges," *Prog. Polym. Sci.*, vol. 51, pp. 127–187, 2015.
- [162] N. Bitinis, M. Hernandez, R. Verdejo, J. M. Kenny, and M. A. Lopez-Manchado, "Recent Advances in Clay/Polymer Nanocomposites," *Adv. Mater.*, vol. 23, no. 44, pp. 5229–5236, Nov. 2011.

- [163] H. M. C. de Azeredo, "Nanocomposites for food packaging applications," *Food Res. Int.*, vol. 42, no. 9, pp. 1240–1253, 2009.
- [164] S.-L. Bee, M. A. A. Abdullah, S.-T. Bee, L. T. Sin, and A. R. Rahmat, "Polymer nanocomposites based on silylated-montmorillonite: A review," *Prog. Polym. Sci.*, vol. 85, pp. 57–82, 2018.
- [165] A. Pratheep Kumar, D. Depan, N. Singh Tomer, and R. P. Singh, "Nanoscale particles for polymer degradation and stabilization-Trends and future perspectives," *Prog. Polym. Sci.*, vol. 34, no. 6, pp. 479–515, 2009.
- [166] A. Arora and G. W. Padua, "Review: Nanocomposites in food packaging," *J. Food Sci.*, vol. 75, no. 1, pp. 43–49, 2010.
- [167] Y. Xi, R. L. Frost, H. He, T. Kloprogge, and T. Bostrom<sup>†</sup>, "Modification of Wyoming Montmorillonite Surfaces Using a Cationic Surfactant," *Langmuir*, vol. 21, no. 19, pp. 8675–8680, 2005.
- [168] L. Betega De Paiva, A. R. Morales, and F. R. Valenzuela Díaz, "Organoclays: Properties, preparation and applications," *Appl. Clay Sci.*, vol. 42, no. 1–2, pp. 8–24, 2008.
- [169] M. M. Reddy, S. Vivekanandhan, M. Misra, S. K. Bhatia, and A. K. Mohanty, "Biobased plastics and bionanocomposites: Current status and future opportunities," *Prog. Polym. Sci.*, vol. 38, no. 10–11, pp. 1653–1689, 2013.
- [170] P. M. S. Souza, A. R. Morales, M. A. Marin-Morales, and L. H. I. Mei, "PLA and Montmorilonite Nanocomposites: Properties, Biodegradation and Potential Toxicity," *J. Polym. Environ.*, vol. 21, no. 3, pp. 738–759, 2013.
- [171] H. He, L. Ma, J. Zhu, R. L. Frost, B. K. G. Theng, and F. Bergaya, "Synthesis of organoclays: A critical review and some unresolved issues," *Appl. Clay Sci.*, vol. 100, no. C, pp. 22–28, 2014.
- [172] K. J. Shah, M. K. Mishra, A. D. Shukla, T. Imae, and D. O. Shah, "Controlling wettability and hydrophobicity of organoclays modified with quaternary ammonium surfactants," *J. Colloid Interface Sci.*, vol. 407, pp. 493–499, Oct. 2013.
- [173] Kinjal J. Shah, Atindra D. Shukla, Dinesh O. Shah, and Toyoko Imae, "Effect of organic modifiers on dispersion of organoclay in polymer nanocomposites to improve mechanical properties," *Polymer (Guildf).*, vol. 97, pp. 525–532, 2016.
- [174] B. Vergnes and W. Lertwimolnum, "Impact of processing conditions on the Morphology, Structure and Properties of Polymer-Organoclay Nanocomposites," in *Polymer Nanocomposite Research Advances*, Nova Science Publishers, Inc., 2008, pp. 51–75.
- [175] F. M. I. Franco, "Hydrolytic Degradation of Poly (lactic acid) and Poly (lactic acid) Nanocomposites by Water-Ethanol Solutions," 2016.

- [176] B. Zidelkheir and M. Abdelgoad, "Effect Of Surfactant Agent Upon The Structure Of Montmorillonite," *J. Therm. Anal. Calorim.*, vol. 94, no. 1, pp. 181–187, 2008.
- [177] A. A. Shokri, S. E. Zamani, and N. P. Company, "Melt Compounding of Polylactide/Organoclay: Structure and Properties of Nanocomposites," *J. Polym. Sci. B. Polym. Phys.*, vol. 44, no. 23, pp. 3392–3405, 2006.
- [178] L. Jiang, J. Zhang, and M. P. Wolcott, "Comparison of polylactide/nano-sized calcium carbonate and polylactide/montmorillonite composites: Reinforcing effects and toughening mechanisms," *Polymer (Guildf)*., vol. 48, pp. 7632–7644, 2007.
- [179] Biqiong Chen *et al.*, "A critical appraisal of polymer–clay nanocomposites," *Chem. Soc. Rev.*, vol. 37, no. 3, pp. 568–594, 2008.
- [180] S. Nazaré, B. K. Kandola, and A. R. Horrocks, "Flame-retardant unsaturated polyester resin incorporating nanoclays," *Polym. Adv. Technol.*, vol. 17, no. 4, pp. 294–303, Apr. 2006.
- [181] X. Kornmann, L. A. Berglund, J. Sterte, and E. P. Giannelis, "Nanocomposites based on montmorillonite and unsaturated polyester," *Polym. Eng. Sci.*, vol. 38, no. 8, pp. 1351–1358, 1998.
- [182] I. Mironi-Harpaz, M. Narkis, and A. Siegmann, "Nanocomposite systems based on unsaturated polyester and organo-clay," *Polym. Eng. Sci.*, vol. 45, no. 2, pp. 174–186, Feb. 2005.
- [183] D. Adame and G. W. Beall, "Direct measurement of the constrained polymer region in polyamide/clay nanocomposites and the implications for gas diffusion," *Appl. Clay Sci.*, vol. 42, no. 3–4, pp. 545–552, 2009.
- [184] K. Pathakoti, M. Manubolu, and H.-M. Hwang, "Nanostructures: Current uses and future applications in food science," *J. Food Drug Anal.*, vol. 25, no. 2, pp. 245–253, 2017.
- [185] E. Picard, E. Espuche, and R. Fulchiron, "Effect of an organo-modified montmorillonite on PLA crystallization and gas barrier properties," *Appl. Clay Sci.*, vol. 53, no. 1, pp. 58–65, 2011.
- [186] M. C. Tang, S. Agarwal, F. D. Alsewailem, H. J. Choi, and R. K. Gupta, "A model for water vapor permeability reduction in poly(lactic acid) and nanoclay nanocomposites," *J. Appl. Polym. Sci.*, vol. 135, no. 30, p. 46506, Aug. 2018.
- [187] N. Ogata, G. Jimenez, H. Kawai, and T. Ogihara, "Structure and thermal/mechanical properties of poly(l-lactide)-clay blend," *J. Polym. Sci. Part B Polym. Phys.*, vol. 35, no. 2, pp. 389–396, Jan. 1997.
- [188] Guo-Xiang Zou, Xin Zhang, Cai-Xia Zhao, and Jinchun L, "The crystalline and mechanical properties of PLA/layered silicate degradable composites," *Polym. Sci. Ser. A*, vol. 54, no. 5, pp. 393–400, 2012.

- [189] M. Nanotechnology, S.-M. Lai, S.-H. Wu, G.-G. Lin, and T.-M. Don, "Unusual mechanical properties of melt-blended poly(lactic acid) (PLA)/clay nanocomposites," *Eur. Polym. J.*, vol. 52, pp. 193–206, 2014.
- [190] D. Lewitus, A. S. Mccarthy, A. A. Ophir, and A. S. Kenig, "The Effect of Nanoclays on the Properties of PLLA-modified Polymers Part 1: Mechanical and Thermal Properties," *J. Polym. Environ.*, vol. 14, no. 2, pp. 171–177, 2006.
- [191] S. Sinha Ray, K. Yamada, M. Okamoto, and K. Ueda, "New polylactide-layered silicate nanocomposites. 2. Concurrent improvements of material properties, biodegradability and melt rheology," *Polymer (Guildf)*., vol. 44, no. 3, pp. 857–866, 2002.
- [192] S. Sinha Ray, K. Yamada, M. Okamoto, Y. Fujimoto, A. Ogami, and K. Ueda, "New polylactide/layered silicate nanocomposites. 5. Designing of materials with desired properties," *Polymer (Guildf).*, vol. 44, no. 21, pp. 6633–6646, 2003.
- [193] A. Araújo, G. Botelho, M. Oliveira, and A. V Machado, "Influence of clay organic modifier on the thermal-stability of PLA based nanocomposites," *Appl. Clay Sci.*, vol. 88–89, pp. 144–150, 2014.
- [194] K. Fukushima, D. Tabuani, M. Dottori, I. Armentano, J. M. Kenny, and G. Camino, "Effect of temperature and nanoparticle type on hydrolytic degradation of poly(lactic acid) nanocomposites," *Polym. Degrad. Stab.*, vol. 96, no. 12, pp. 2120–2129, 2011.
- [195] F. Iñiguez-Franco, R. Auras, M. Rubino, K. Dolan, H. Soto-Valdez, and S. Selke, "Effect of nanoparticles on the hydrolytic degradation of PLA-nanocomposites by water-ethanol solutions," *Polym. Degrad. Stab.*, vol. 146, no. September, pp. 287–297, 2017.
- [196] P. K. Roy, M. Hakkarainen, and A.-C. Albertsson, "Nanoclay effects on the degradation process and product patterns of polylactide," *Polym. Degrad. Stab.*, vol. 97, no. 8, pp. 1254–1260, 2012.
- [197] K. P. Rajan, S. P. Thomas, A. Gopanna, A. Al-Ghamdi, and M. Chavali, "Polyblends and Composites of Poly (Lactic Acid) (PLA): A Review on the State of the Art," *J. Polym. Sci. Eng.*, vol. 1, pp. 1–15, 2018.
- [198] M. A. Paul, C. Delcourt, M. Alexandre, P. Degée, F. Monteverde, and P. Dubois, "Polylactide/montmorillonite nanocomposites: Study of the hydrolytic degradation," *Polym. Degrad. Stab.*, vol. 87, no. 3, pp. 535–542, 2005.
- [199] K. Fukushima, E. Giménez, L. Cabedo, J. M. Lagarón, and J. L. Feijoo, "Biotic degradation of poly(DL-lactide) based nanocomposites," *Polym. Degrad. Stab.*, vol. 97, no. 8, pp. 1278–1284, 2012.
- [200] S. Sinha Ray, K. Yamada, M. Okamoto, and K. Ueda, "Control of biodegradability of polylactide via nanocomposite technology," *Macromol. Mater. Eng.*, vol. 288, no. 3, pp. 203–208, 2003.

- [201] S. S. Ray, K. Yamada, M. Okamoto, A. Ogami, and K. Ueda, "New polylactide/layered silicate nanocomposites, 4. Structure, properties and biodegradability," *Compos. Interfaces*, vol. 10, no. 4–5, pp. 435–450, 2003.
- [202] A. Araújo, M. Oliveira, R. Oliveira, G. Botelho, and A. V. Machado, "Biodegradation assessment of PLA and its nanocomposites," *Environ. Sci. Pollut. Res.*, vol. 21, no. 16, pp. 9477–9486, 2014.
- [203] P. Moraes *et al.*, "PLA and Montmorilonite Nanocomposites: Properties, Biodegradation and Potential Toxicity," *J. Polym. Environ.*, vol. 21, no. 3, pp. 738–759, 2013.
- [204] Y. H. Lee *et al.*, "Electrospun dual-porosity structure and biodegradation morphology of Montmorillonite reinforced PLLA nanocomposite scaffolds," *Biomaterials*, vol. 26, no. 16, pp. 3165–3172, Jun. 2005.
- [205] Sang-Rock Lee *et al.*, "Microstructure, tensile properties, and biodegradability of aliphatic polyester/clay nanocomposites," *Polymer (Guildf).*, vol. 43, no. 8, pp. 2495–2500, 2002.
- [206] E. Castro-Aguirre, R. Auras, S. Selke, M. Rubino, and T. Marsh, "Enhancing the biodegradation rate of poly(lactic acid) films and PLA bio-nanocomposites in simulated composting through bioaugmentation," *Polym. Degrad. Stab.*, vol. 154, pp. 46–54, 2018.
- [207] E. Castro-aguirre, R. Auras, S. Selke, M. Rubino, and T. Marsh, "Impact of Nanoclays on the Biodegradation of Poly (lactic acid) Nanocomposites," vol. 2, pp. 1–24, 2017.

#### **CHAPTER 3**

### **MATERIALS & METHODS**

# 3.1 Direct Measurement Respirometric & Hydrolysis Materials

Poly(lactic acid), PLA 2003D (L-lactic acid content of 96%) obtained from NatureWorks® LLC (Minnetonka, MN, USA) with weight average molecular weight ( $M_w$ ) of  $2.23 \pm 0.04 \times 10^5$  Da and number average molecular weight ( $M_n$ ) of  $1.14 \pm 0.07 \times 10^5$  Da was used as the main resin in this study. To study in detail the effect of nanoclays and surfactant on the biodegradation of PLA, organomodified montmorillonite nanoclay Nanomer® I.34 TCN, hereafter referred to as OMMT was obtained from Nanocor (Hoffman Estates, Illinois, USA). It contains about 80 % montmorillonite (MMT) and is modified by 20% of surfactant stearyl bis(2-hydroxyethyl) methyl ammonium chloride. The mean particle size of the clay was 14-18  $\mu$ m as described by Nanocor. Standard nanoclay polymer grade montmorillonite PGW, hereafter referred to as MMT was obtained from Sigma Aldrich (Illinois, USA). Table 3.1 shows main reported properties of these nanoclays.

Table 3.1. Physical data of organomodified clay [1].

Nanoclay	Surfactant	Surfactant Content (wt %)	X- ray diffraction $(d001)^a$ (Å)	Max Processing Temperature <sup>b</sup> (°C)
Nanomer I.34 TCN	Stearyl bis(2- hydroxyethyl) Methyl Ammonium Chloride	20	18 - 22	270
MMT	-	-	-	-

 $a d_{001}$  is the interplanar spacing in the layered structure of montmorillonite.

The surfactant stearyl bis(2-hydroxyethyl) methyl ammonium chloride is no longer manufactured, so a surfactant with similar chemistry tallow (b – hydroxyethyl) dimethyl ammonium chloride, (where T is an alkyl group with approximately 65% C<sub>18</sub>H<sub>37</sub>, 30% C<sub>16</sub>H<sub>33</sub>, 5% C<sub>14</sub>H<sub>29</sub>, the anion that is bound to the cation is a chloride anion) was obtained from Haihang Industry Co. Ltd (Jinan, China). The surfactant is hereafter referred to as QAC. For the hydrolysis test, water (HPLC grade) was supplied by J.T. Baker (Center Valley, PA, USA). Tetrahydrofuran (THF) was procured from Pharmco-Aaper, Shelbyville, KY.

## 3.2 Production of Masterbatches

Masterbatches of PLA-OMMT, PLA-MMT and PLA-QAC were produced. PLA pellets along with both the clays (i.e., OMMT and MMT) were dried at 50°C for 24 hours in a vacuum oven (Sheldon Manufacturing, Inc; Cornelius, OR, USA) to remove moisture before processing. Hand premixed PLA-MMT (5% w/w), PLA-OMMT (7% w/w) - 7% w/w of OMMT was added

<sup>&</sup>lt;sup>b</sup> Maximum recommended processing temperature for the extrusion process.

to have approximately the same amount of MMT, and PLA-QAC (20% w/w) were introduced in the feed throat of a co-rotating Century ZSK 30 twin screw extruder (Century Extruders, Traverse city, MI) having a length to diameter (L/D) ratio of 42:1 and 30 mm in diameter. The temperature profile of the twin screw extruder from the feed throat to die was set at 140/150/160/160/160/170/170/170/160/160°C. All the masterbatches were processed at the above-mentioned temperatures at a screw speed of 100 rpm corresponding to a residence time of 2 min. The extrudate coming out of the circular die was passed through a water bath for cooling and then pelletized and stored in freezer at around -21°C.

## 3.3 Production of Nanocomposite Films

The PLA-OMMT, PLA-MMT and PLA-QAC masterbatches along with the PLA resin were vacuum dried at 50°C for 24 hours to remove moisture before further processing. A 15.875 mm single screw RandCastle RCP-0625 Multi-Layer Cast film extruder (Randcastle Extrusion Systems, Inc; Cedar Grove, New Jersey, USA) with length to diameter (L/D) ratio of 24:1 was used to cast PLA-OMMT, PLA-MMT, PLA-QAC and PLA films. Before processing the films, the extruder was cleaned thoroughly using LDPE resin to avoid any contamination. The extrusion temperatures were set to 193, 229, 229, 229, 229, 204, 204°C for zone 1, 2, 3, transfer tube, adapter, feed block and die, respectively with screw rotation speed of 40 rpm for PLA film. The extruded film passed through a slit die opening of 1.168 mm and then over the chilled rollers. The chill roller was placed 0.8" from the die and the temperature was fixed at 15°C. The film was quenched by the chill roller and transported to a winding station using a nip roller. The speed of the chill and the nip roller was set at 40 rpm. The winding unit was placed at a distance of 34" from the die and the winding roller was operated at a speed of 12 rpm. Table 3.2 shows the extrusion conditions for different films in the order of processing.

Table 3.2. Processing conditions for cast film extrusion.

Extrusion Conditions				
Materials	rials Temperature Profile (°C) (Zone 1 to Die)		Nip Roller (rpm)	Winding Roller (rpm)
PLA	193/229/229/229/229/204/204	35	40	15
PLA-OMMT	139/150/160/160/160/170/160	30	30	12
PLA-MMT	139/150/160/160/160/170/160	30	40	12
PLA-QAC	132/143/152/152/152/163/160	30	40	12

### 3.4 Material characterization

# 3.4.1 Differential scanning calorimetry (DSC)

The glass transition temperature ( $T_g$ ), melting temperature ( $T_m$ ), crystallization temperature ( $T_c$ ), enthalpy of cold crystallization process ( $\Delta H_c$ ) and total enthalpy of melting peaks( $\Delta H_m$ ) were determined using a Q100 differential scanning calorimeter (TA Instruments, New Castle, DE, USA). The DSC cell was purged using nitrogen gas, flowing at a constant rate of 70 mL/min. A set of heating and cooling cycles were carried to wipe out the thermal history of the sample. The samples weighing between 5 -10 mg were cooled to 5°C, and then heated to 180°C at a rate of  $10^{\circ}$ C/min and then cooled back to 5°C using nitrogen. The thermograph obtained was analyzed using the software Thermal Universal Analysis 2000, V4.5 (TA Instruments, Delaware, USA). The first heat curves of the films are reported. The percentage crystallinity (%  $X_c$ ) was calculated from the heat of fusion using the equation 1.

$$\% \chi_c = \left(\frac{\Delta H m - \Delta H c}{\Delta H^{\circ} m \left(1 - \frac{\% wt \ filler}{100}\right)}\right) \times 100$$
 Equation 3

where  $\Delta H_c$  (J/g) is cold crystallization enthalpy,  $\Delta H_m$  (J/g) is the heat of fusion for 100% crystalline PLA (93 J/g) [2] and  $\% wt_{filler}$  is the weight percentage of the filler. The measurements were carried out in triplicates.

## 3.4.2 Thermogravimetric Analysis (TGA)

To determine the heat stability, the content of surfactant and clays in the PLA-OMMT, PLA-MMT and PLA-QAC films, was determined by thermogravimetric analysis. The films were characterized using a Q-50 thermogravimetric analyzer (TA Instruments Inc, USA). Samples weighing between 5-10 mg, were heated under dynamic mode from room temperature to 600°C at a ramp rate of 10°C/min under a high purity nitrogen atmosphere (70 mL/min) to avoid thermoxidative degradation and the weight loss was recorded using the software Thermal Universal Analysis 2000, V4.5 (TA Instruments, Delaware, USA).

## 3.4.3 Carbon, Hydrogen and Nitrogen analysis (CHN Analyzer)

Elemental analysis of the different test materials was carried out using a PerkinElmer 2400 Series II CHNS/O Elemental Analyzer (PerkinElmer Inc., Shelton, CT, USA). Samples were weighed in the range of 2-3 mg and 3 measurements were recorded for each sample. The basic working principle involves burning the sample at high temperature of 925°C in an oxygen rich environment, where carbon is converted to carbon dioxide, nitrogen to nitrogen oxides, hydrogen to water and sulphur to sulphur dioxide. The combustion products are carried by inert gas helium and passed over copper located at the base of the combustion chamber. This copper is used to collect any leftover oxygen or nitrogen that might had not been taken up during the initial

combustion phase. The gases then travel through the absorbent traps and only carbon dioxide, water, hydrogen, nitrogen and sulphur dioxide are left behind.

## 3.4.4 Size Exclusion Chromatography (SEC)

The test materials were collected at pre-determined intervals of time throughout the experiments to determine  $M_w$  and  $M_n$ . Approximately (10  $\pm$  1 mg) of test materials were dissolved in 5mL of high pressure liquid chromatography (HPLC) grade tetrahydrofuran (THF) (Pharmco-Aaper, Shelbyville, KY, USA) at ambient temperatures for 24h. Once the samples were dissolved, the solution was then filtered through a 0.45µm poly(tetrafluoroethylene) (PTFE) (Simsii Inc., Irvine, CA, USA) syringe filter. A gel permeation chromatograph (GPC) (Waters1515, Waters, Milford, MA, USA) equipped with a Waters<sup>®</sup> 1515 isocratic pump, a Waters<sup>®</sup> 717 autosampler, a series of Waters<sup>®</sup> Styragel columns (HR4, HR3, and HR 2 each 7.8mm x 300mm), and a Waters<sup>®</sup> 2414 refractive index detector interface with Waters® Breeze software (Waters, Milford, MA, USA) was used. Each sample was run for a total of 50 min. THF was used as a mobile phase, 100µL of sample was injected, and eluted at a flow rate of 1mL/min. The temperature of the column and detector was 35°C. A calibration curve was made using external polystyrene standards-Shodex STD KIT SM-105 (Showa denko, Japan), with  $M_w$  in the range of 1.37 x  $10^3$  to 2.48 x 10<sup>6</sup> Da and calculated using a 5<sup>th</sup> order polynomial equation. The weight average molecular weight  $(M_w)$ , number average molecular weight  $(M_n)$ , viscosity average molecular weight (Mv)and polydispersity index (PI) of the samples were determined using the Waters® Breeze GPC software v2. The Mark –Houwink constants for the correction to absolute  $M_w$  were K = 0.0164 mL/g and  $\alpha = 0.704$ . Values of dilute PLA solution at 35°C were used to obtain the absolute values from the relative values. Triplicate measurements were carried out for each sample.

### 3.4.5 Digital Micrometer

The thickness of the PLA, PLA-OMMT, PLA-MMT and PLA-QAC films was measured using a digital micrometer model N# 49-70-01-0001 (Testing Machines Inc, New Castle, DE, USA). Ten measurements were recorded for each sample.

## **3.4.6 Scanning Electron Microscopy (SEM)**

A scanning electron microscope SEM JOEL 6610LV (JEOL, Tokyo, Japan) was used to observe the surface morphology and measure the thickness of PLA-OMMT and PLA-MMT films. The film specimens were first immersed in liquid nitrogen, and a clean single cut was made using sterilized razor blades. These fractured samples were then mounted on aluminum stubs using adhesive tapes and were set aside in a glass vacuum desiccator for a day. An Emscope SC500 sputter coater (Emscope Laboratories, Ashford, UK) was used to gold coat the samples before analyzing to increase the conductivity of the samples. The samples were studied and imaged with magnifications in the range of 5X to 50,000X using an accelerating voltage of 30kV. The thicknesses of PLA-OMMT and PLA-MMT films were also determined using the SEM since the nanoclays dispersed in the film hinder the actual measurement done using a micrometer. Nanoclays form a bump like structure, which gives inaccurate determination when measured using a micrometer.

## 3.4.7 X-ray diffraction study (XRD)

X-ray diffraction measurements were carried out for PLA-MMT, and PLA-OMMT films using a Bruker AXS D8 Advance X-ray diffractometer (Bruker Co., Billerica, MA, USA) equipped with a Gobel Mirror filtered Cu Kα radiation source set at 40 kV and 100 mA. The samples were

scanned, and the data was recorded in a  $2\theta$  range of  $2^{\circ}$  to  $40^{\circ}$  at a scan rate of  $0.20^{\circ}$ /min and an increment of  $0.01^{\circ}$ .

## 3.5 Biodegradation Test

An in-house Direct Measurement Respirometric system (DMR) located in the School of Packaging, East Lansing, MI was used to assess the aerobic degradation of the test materials. DMR is capable of simultaneously running up to 30 samples (in triplicates, 95 bioreactors) under controlled composting conditions ( $58 \pm 2^{\circ}$ C,  $50 \pm 5\%$  RH) as per ASTM D5338[3] and ISO 14855[4] standards. The CO<sub>2</sub> evolved from the bioreactors is measured using a non-dispersive infrared gas analyzer (NDIR).

The prime components of the DMR system include:

- Scrubbing system: To reduce the CO<sub>2</sub> concentration from 400 to below 30 ppm
- Environmental chamber: To control the temperature of the bioreactors. The operating range is -23°C (10°F) to 60°C (140°F), and therefore can replicate the required temperatures for simulating composting conditions (58 ± 2°C). A relative humidity generator (mix of dry and water saturated air) is used to obtain the desired relative humidity for the system.
- Bioreactor: Test materials are housed in with the media of interest. Daily maintenance to allow injection of water and optimum aeration.
- Measurement device: The carbon dioxide concentration of the exhaust air coming from each jar is measured using a non-dispersive infrared gas analyzer (NDIR model LI-820) (Licor Inc., Lincoln, NE).

 Control software: A control software is used to control the switching system and measurement devices such as NDIR, RH/Temperature sensor to record and measure the test variables.

Throughout, the testing period the flow rate of air passing through each bioreactor was maintained at 40 sccm. Water was injected on a regular basis to maintain the moisture content of the medias used and to prevent drying. The blank bioreactors carried only the solid media (*i.e.* compost, vermiculite and inoculated vermiculite). Cellulose powder was used as a positive reference material since it is well known to be easily biodegradable. For data analysis, firstly the CO<sub>2</sub> evolved from each bioreactor was calculated, followed by average cumulative CO<sub>2</sub> and % mineralization.

## 3.5.1 Moisture Analyzer

The moisture content of the compost was determined using a moisture content analyzer, model MX-50 (A&D Company, Tokyo, Japan). Five samples of compost were randomly tested, and the average was obtained. The moisture content of the compost was determined as 25.22%.

## 3.5.2 Preparation of inoculum solution

Dry compost was mixed with deionized water (20% wt./vol.), stirred and allowed to settle down for 30 min and filtered through a sieve with 1 mm mesh to obtain the compost extract as previously explained by Castro-Aguirre et al. 2013[5]. This compost extract was then combined with a mineral solution in the ratio 1:1 to prepare the inoculum solution for vermiculite as shown in Table 3.3.

Table 3.3. Detailed composition of 1L mineral solution

1L of mineral solution	
KH <sub>2</sub> PO <sub>4</sub> , g	1
MgSO <sub>4</sub> , g	0.5
CaCl <sub>2</sub> (10% sol), mL	1
NaCl (10% sol), mL	1
Trace-element solution, mL	1
1L of trace-element solution, mg	
H <sub>3</sub> BO <sub>3</sub>	500
Kl	100
FeCl <sub>3</sub>	200
MnSO <sub>4</sub>	400
$(NH_4)_6MO_7O_{24}$	200
FeSO <sub>4</sub>	400

# 3.5.3 Biodegradation in compost

The bioreactors were placed in the environmental chamber which was set to conditions  $58 \pm 2^{\circ}\text{C}$ ,  $50 \pm 5\%$  RH to simulate the composting conditions. Each bioreactor was supplied with  $CO_2$  free water saturated air at a flow rate of  $40 \pm 2$  sccm (i.e. cm<sup>3</sup>/min at standard temperature and pressure). The bioreactors were stuffed with 400g of compost mixed rigorously with 8g of test material filling up to of volume of the bioreactors thereby allowing sufficient headspace. The test materials were cut into small squares of 1 cm x 1 cm and analyzed in triplicates. Blank bioreactors (compost only) were also assessed in triplicates. The bioreactors were nurtured in the dark until the data showed a plateau in  $CO_2$  evolution.

### 3.5.4 Biodegradation in vermiculite

Apart from compost, biodegradation test was also carried out in inoculated and non-inoculated vermiculite to take into account the priming effect of compost and also to separate the abiotic and biotic phases of biodegradation process. Vermiculite was mixed with inoculum solution in the ratio of 1:4 to prepare inoculated vermiculite and with distilled water in the same ratio to prepare non-inoculated vermiculite. The bioreactors were filled with 400g of compost mixed rigorously with 8g of test material filling up to of volume of the bioreactors thereby allowing sufficient headspace and subjected to testing conditions  $58 \pm 2^{\circ}\text{C}$ ,  $50 \pm 5\%$  RH.

# 3.6 Hydrolysis Test

The abiotic phase of biodegradation was the test materials was evaluated by cutting into disks of 2.0 cm in diameter and threaded 10 disks onto a stainless-steel wire separated by glass beads and placed in a glass vial. Water (HPLC grade) (J.T. Baker, Center Valley, PA, USA) previously pre-conditioned at  $60^{\circ}$ C was added to the vial. The experiment was conducted at  $60^{\circ}$ C using the migration cell, in accordance with ASTM D4754-11 [6]. The total surface area of disk to volume of water was  $1.81 \text{ cm}^2/\text{mL}$ . Samples were recovered at pre-determined specific time intervals to determine the Mn,  $M_w$  and crystallinity as mentioned above. Figure 3.1 shows the setup that was used to conduct hydrolysis.

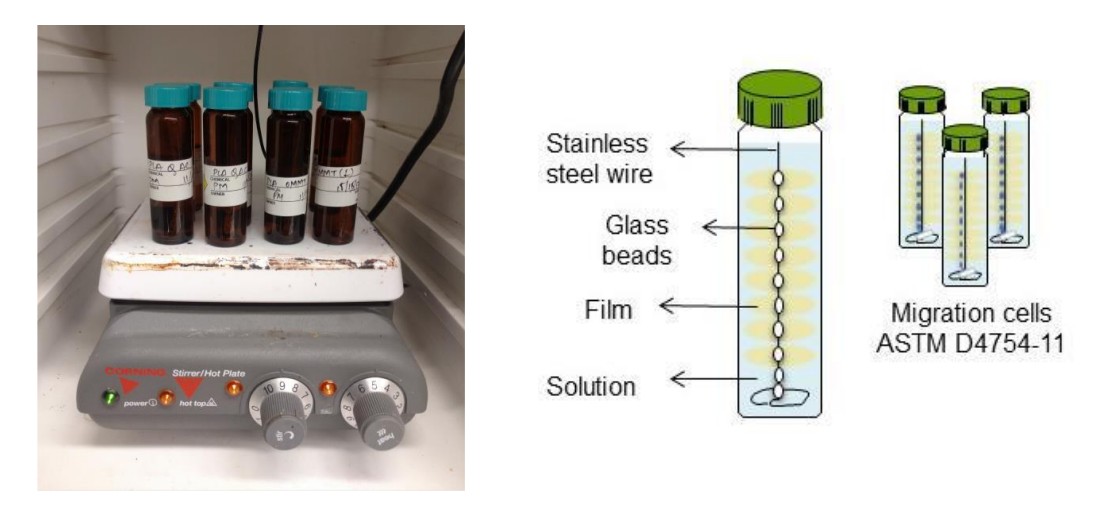


Figure 3.1 Hydrolysis setup in the lab and migration cell, partially reproduced from [7].

REFERENCES

### REFERENCES

- [1] Nanocor, "Nanomer ® I. 34TCN General Description: Product Data \*: Application Guideline: Processing Guideline:," 1918.
- [2] F. Iñiguez-Franco *et al.*, "Concurrent solvent induced crystallization and hydrolytic degradation of PLA by water-ethanol solutions," *Polym. (United Kingdom)*, vol. 99, pp. 315–323, 2016.
- [3] "ASTM Standard D5338-15, Standard test method for determining aerobic biodegradation of plastic materials under controlled composting conditions, West Conshohocken, PA.," 2015.
- [4] "Determination of the ultimate aerobic biodegradability of plastic materials under controlled composting conditions Method by analysis of evolved carbon dioxide Part 1: General method," 2012.
- [5] E. Castro, "Design And Construction Of A Medium-Scale Automated Direct Measurement Respirometric System To Assess Aerobic Biodegradation Of Polymers," 2013.
- [6] ASTM International, "ASTM Standard D4754-18, Standard Test Method for Two-Sided Liquid Extraction of Plastic Materials Using FDA," 2003.
- [7] F. M. I. Franco, "Hydrolytic Degradation of Neat and Modified Poly(lactic acid) with Nanoparticles and Chain extenders by Water-Ethanol solution," 2018.

### **CHAPTER 4**

### **RESULTS & DISCUSSIONS**

#### 4.1 Initial Characterization of the films

The films were initially characterized for their molecular weight, thickness, crystallinity and amount of clay present in PLA-OMMT and PLA-MMT films before introducing in the DMR. The characterization was essential as one of the main objectives of this thesis was to produce films in the same range of molecular weight, crystallinity and thickness with a variation of no more than  $\pm$  10%.

### 4.1.1 Initial Molecular weight

PLA, PLA-QAC, PLA-OMMT, and PLA-MMT films were subjected to size exclusion chromatography. Table 4.1 presents the molecular weights  $M_n$  for all the films.

Table 4.1. Initial molecular weight of PLA, PLA-OMMT & PLA-MMT & PLA-QAC films

Materials	$M_n$ , $kDa$	$M_w$ , $kDa$
PLA	$109.76 \pm 3.14^{a}$	$185.54 \pm 9.35^{a}$
PLA-QAC	$87.59 \pm 4.22^{b}$	$128.63 \pm 4.85^{b}$
PLA-OMMT	$114.26 \pm 11.81^{a}$	$170.42 \pm 5.80^{a}$
PLA-MMT	$111.07 \pm 3.97^{a}$	160.41 ± 5.69 <sup>a</sup>

*Values with different letter are statistically different* ( $\alpha = 0.05$  *Tukey-Kramer Test*)

The  $M_n$  of PLA, PLA-OMMT and PLA-MMT were not significantly different.  $M_n$  of PLA-QAC films was significantly lower than the other films. This reduction in  $M_n$  can be attributed to the presence of surfactant, which acts as a plasticizer, promoting chain scission, and possible shortening of the PLA chains during the melt processing.

# **4.1.2** Initial Thickness

The thickness of all four films was measured first using a digital micrometer and then using SEM, since the clay particles dispersed formed a bump like structure in PLA-OMMT and PLA-MMT films hindering the thickness measurement using a digital micrometer. Figure 4.1 shows the SEM micrographs. Table 4.2 shows the thickness measured by micrometer and SEM.

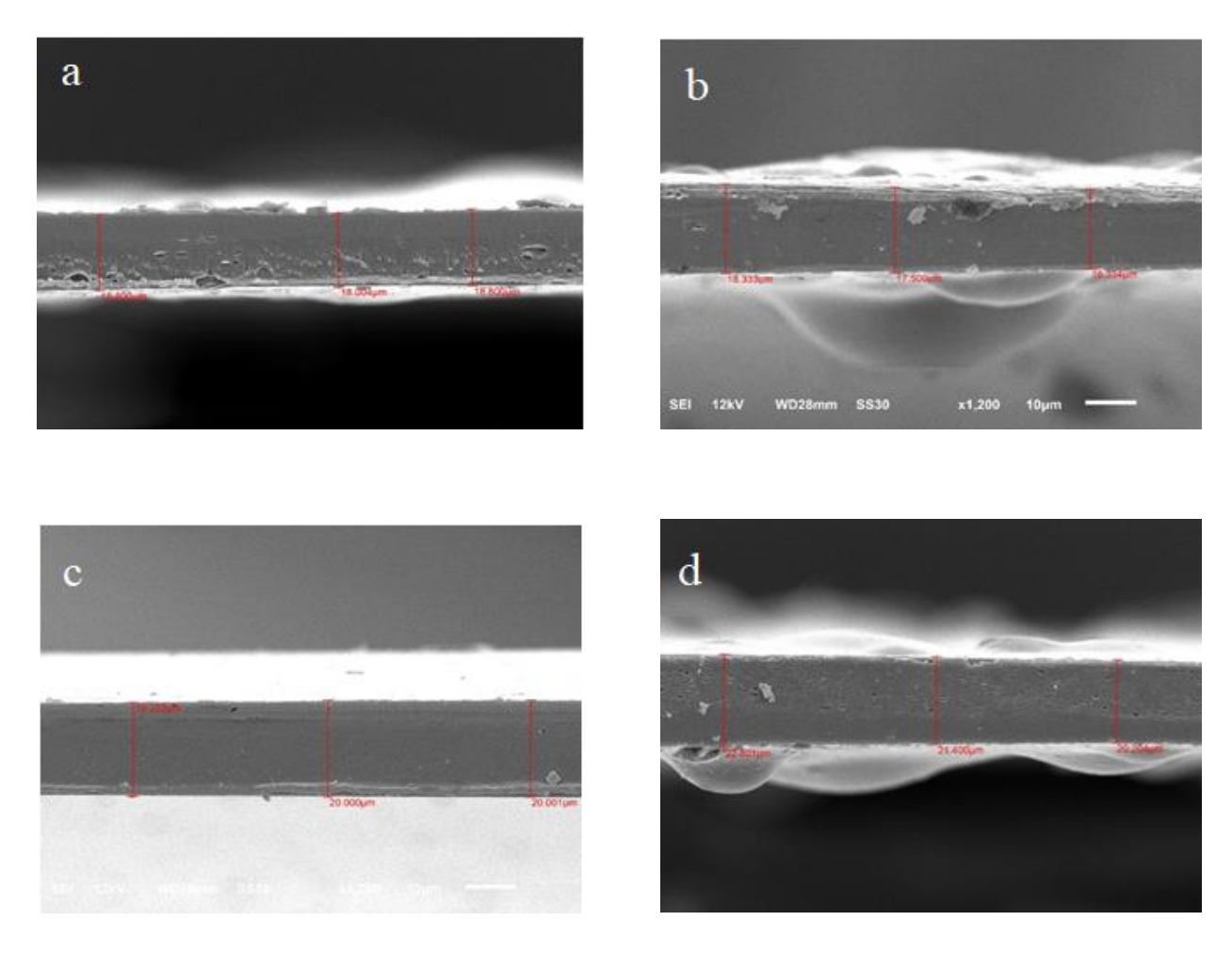


Figure 4.1. SEM micrographs of a) PLA, b) PLA -MMT, c) PLA-QAC and d) PLA-OMMT.

Table 4.2. Micrometer and SEM thickness t for all the films.

Materials	Micrometer - Thickness (μm)	SEM - Thickness (µm)
PLA	$19.30 \pm 1.27^{a}$	$19.78 \pm 0.39^a$
PLA-QAC	$19.03 \pm 1.69^{a}$	$18.97 \pm 3.81^{a}$
PLA-OMMT	$71.12 \pm 6.35^{b}$	$21.47 \pm 1.30^{a}$
PLA-MMT	$77.72 \pm 8.16^{a}$	$17.39 \pm 1.01^{a}$

Values with different letter are statistically different ( $\alpha = 0.05$  Tukey-Kramer Test)

There was no significant difference between the four films thicknesses as measured by SEM.

# 4.1.3 Crystallinity

Table 4.3 presents the crystallinity of the produced films by cast extrusion. There was no significant variation in the crystallinity among the PLA-C, PLA-OMMT, PLA-MMT and PLA-QAC films. All the films were mostly amorphous.

Table 4.3. Crystallinity  $\chi_c$  (%) for all the films.

Materials	χc (%)
PLA	$3.7\pm4.7^a$
PLA- OMMT	$1.7 \pm 1.2^{a}$
PLA-MMT	$2.3 \pm 2.1^{a}$
PLA-QAC	$1.0\pm1.0^{\rm a}$

*Values with different letter are statistically different* ( $\alpha = 0.05$  *Tukey-Kramer Test*)

### **4.1.4** Amount of Nanoclay

As previously described, to evaluate the effect of clay (MMT), organomodified clay (OMMT) and surfactant (QAC) on the biodegradation of PLA, four films PLA-MMT (5% wt. of MMT), PLA-OMMT (5% wt. of OMMT), PLA-QAC (20% wt. of QAC) and PLA were produced. The amount of surfactant was determined by performing thermogravimetric analysis on OMMT

powder, thus helping to determine the amount of QAC to be added. Table 4.4 shows the amount of carbon (C), hydrogen (H) and nitrogen (N) content in QAC, OMMT and MMT as determined by elemental analysis. The table also presents the amount of carbon, hydrogen and nitrogen in all four films. By subtracting the C, H, and N wt % of PLA from the PLA-MMT, PLA-OMMT and PLA-QAC films, the amount of MMT, OMMT and QAC present in the films was calculated.

Table 4.4. Amounts of carbon, hydrogen & nitrogen content determined by CHNS/O Elemental Analyzer (%)

Materials	C , wt %	H, wt %	N, wt %
QAC	$17.02 \pm 0.02$	$2.23 \pm 0.07$	$0.86 \pm 0.02$
OMMT	$17.21 \pm 0.02$	$3.48 \pm 0.02$	$0.86 \pm 0.01$
MMT	$0.19 \pm 0.04$	$1.26\pm0.08$	$0.00 \pm 0.02$
PLA	$51.21 \pm 0.14$	$5.81 \pm 0.03$	$0.04 \pm 0.01$
PLA-QAC	$50.45 \pm 0.27$	$5.65 \pm 0.03$	$0.06 \pm 0.01$
PLA-OMMT	$49.06 \pm 0.02$	$5.55 \pm 0.01$	$0.05 \pm 0.01$
PLA-MMT	$48.53 \pm 0.09$	$5.47 \pm 0.01$	$0.04 \pm 0.00$

Figure 4.2 shows the DSC curve for PLA-OMMT film. Table shows tabulates the results from thermal properties for PLA, PLA-QAC, PLA-OMMT and PLA-MMT film. Figure 4.3 shows the TGA of the produced films. The percentages mentioned for PLA-OMMT, PLA-MMT and PLA-QAC films indicate the amount of OMMT, MMT and QAC present in the films. Thermogravimetric analysis helps to corroborate the CHN results.

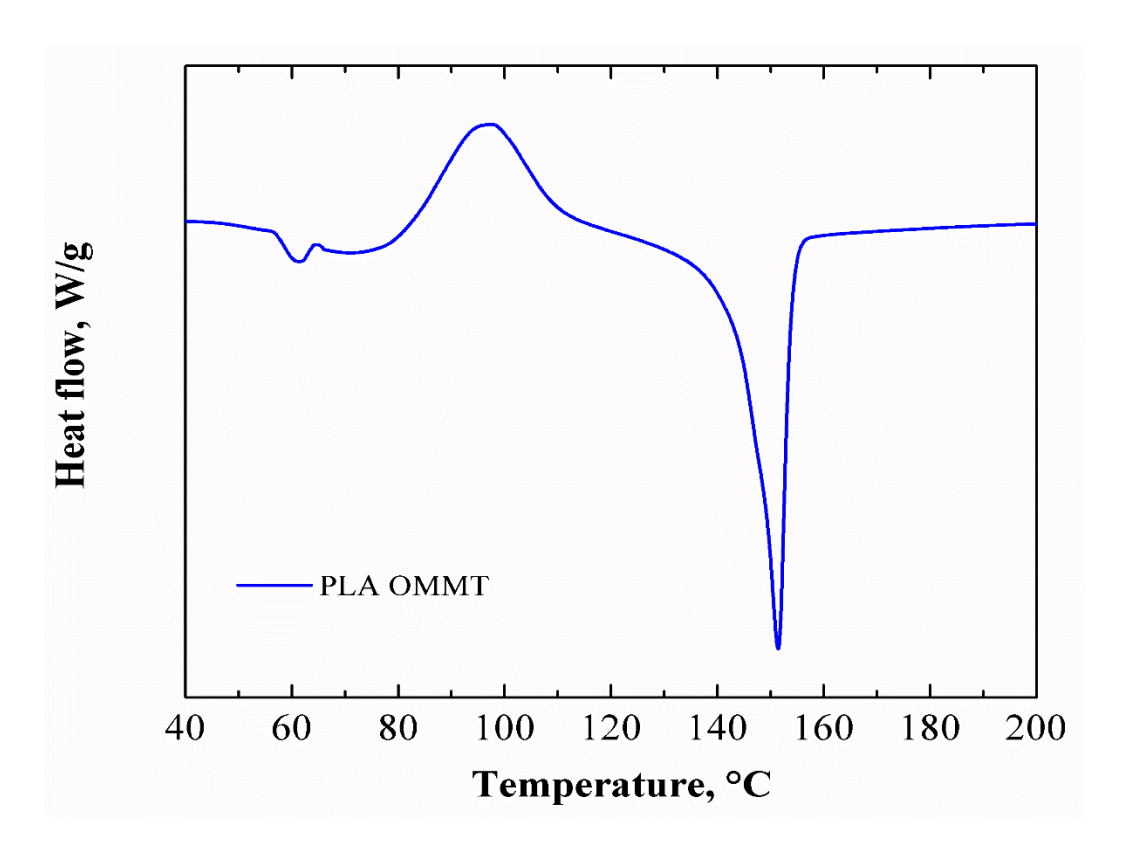


Figure 4.2. DSC curve for PLA OMMT film.

Table 4.5. Thermal properties of PLA, PLA-QAC, PLA-MMT and PLA-OMMT films.

Materials	Tg, °C	Tm, °C	Tc, °C	χc, %
PLA	61.57	151.83	93.49	2.0
PLA-QAC	58.54	146.46	106.68	0.82
PLA-OMMT	59.12	151.44	96.93	2.66
PLA-MMT	60.66	149.68	116.53	3.82

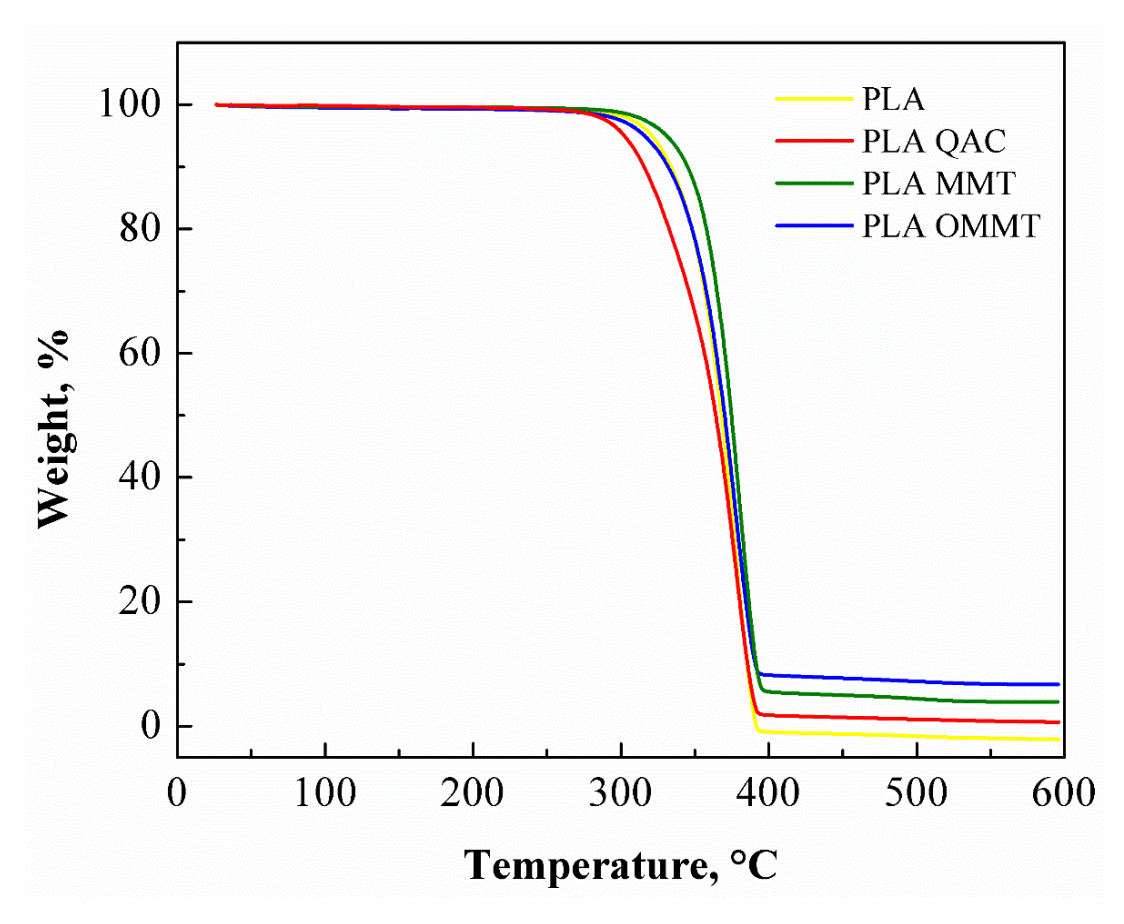


Figure 4.3. TGA of PLA, PLA-QAC, PLA-MMT and PLA-OMMT films.

## 4.1.5 Characterization of PLA OMMT films

XRD is generally used to evaluate the presence of nanoclays and its dispersion in the PLA matrix. Figure 4.4 reveals the XRD patterns of OMMT clay powder, PLA-OMMT and PLA C films. The diffraction peak at  $2\theta = 4.76$  ° for OMMT clay corresponds to the gallery distance (*d*-spacing) of 18.53 Å. The diffraction peak was observed at  $2\theta = 7.2$  ° (*d*-spacing 11.23 Å) for MMT. The shift of peak from 7.2 ° (*d*-spacing 11.23 Å) to at  $2\theta = 4.76$  ° (*d*-spacing 18.53 Å) shows that modification took place by means of ion exchange of the surfactant. It was essential to understand if the resulting layered silicate nanocomposite was either exfoliated or intercalated.

The shift of the peak to  $2\theta = 2.44$  ° (*d*-spacing 36.16 Å) *i.e.*, to the left of pristine clay, was observed for PLA-OMMT film indicating that intercalation has occurred as seen in

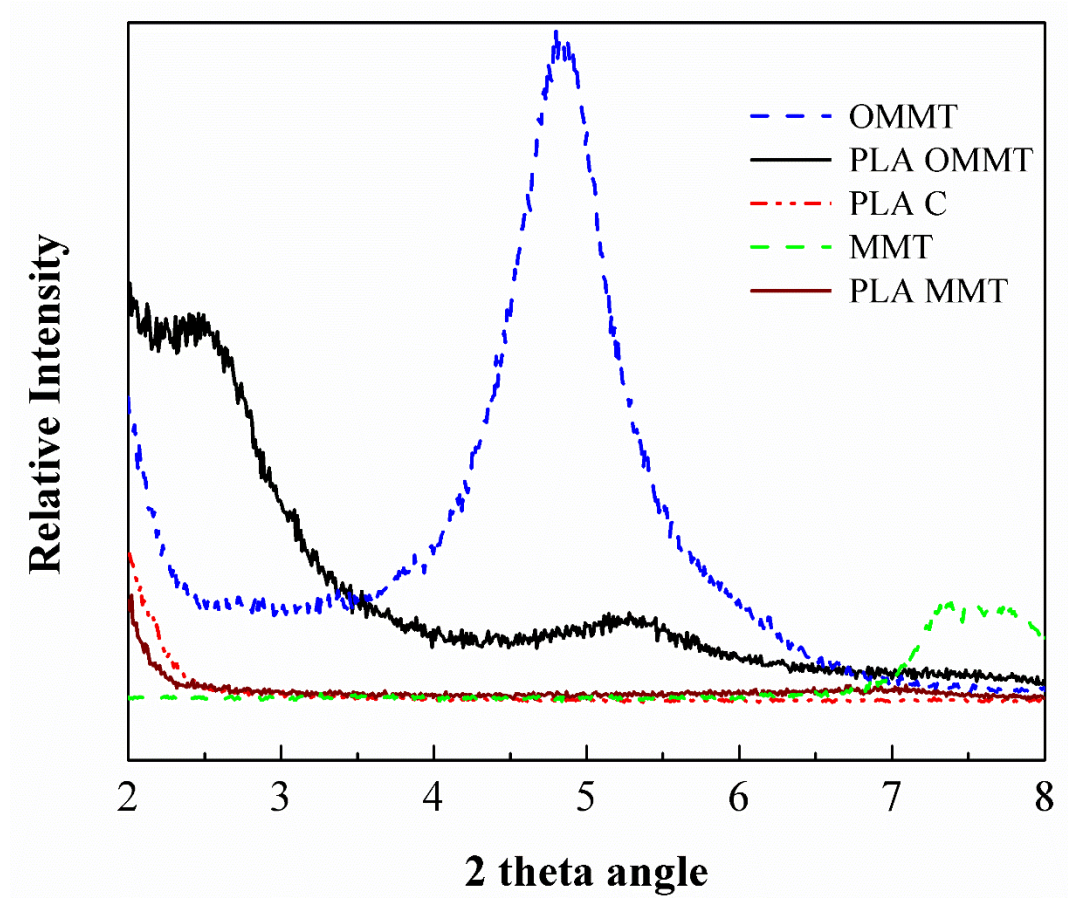


Figure 4.4. XRD spectra for OMMT and MMT clay powder ,PLA-OMMT, PLA-MMT and PLA films.

Intercalation takes place when the polymer chains partially infiltrate between the silicate layers of the clay, which is demonstrated by the shift of the peak to a smaller angle and increase in interlayer spacing. Exfoliation is observed due to the complete delamination and random dispersion of layered silicate within the polymer matrix, which is demonstrated by the absence of the peak in the resulting nanocomposite film. The PLA-OMMT film was therefore intercalated and not exfoliated. In general, full exfoliation is difficult to achieve, usually a mixture of

intercalated and exfoliated structures is observed in the resulting nanocomposites. These are referred to as disordered morphology or orderly exfoliated morphology [3].

# 4.2 Biodegradation: CO<sub>2</sub> evolution and mineralization

The biodegradability of PLA, PLA-QAC, PLA-MMT and PLA-OMMT films was evaluated in an in-house built DMR system in which temperature, air flow rate, RH were monitored to determine the CO<sub>2</sub> evolution from each bioreactor. As per ASTM D5338 [4] and ISO 14855 [5] standards, temperature and pH were steady at 58°C and 7 respectively. To evaluate the effect of nanoclays and surfactant on the biodegradation of PLA, the four films were introduced in compost, inoculated and non-inoculated vermiculite.

# **4.2.1 Biodegradation in Compost**

Figure 4.5 shows the cumulative  $CO_2$  evolution and % mineralization curves. The % mineralization indicates the relationship between the actual amount of  $CO_2$  evolved from the test material and the theoretical amount of  $CO_2$  that can be evolved from the same test material. The values are represented as average  $\pm$  standard deviation.

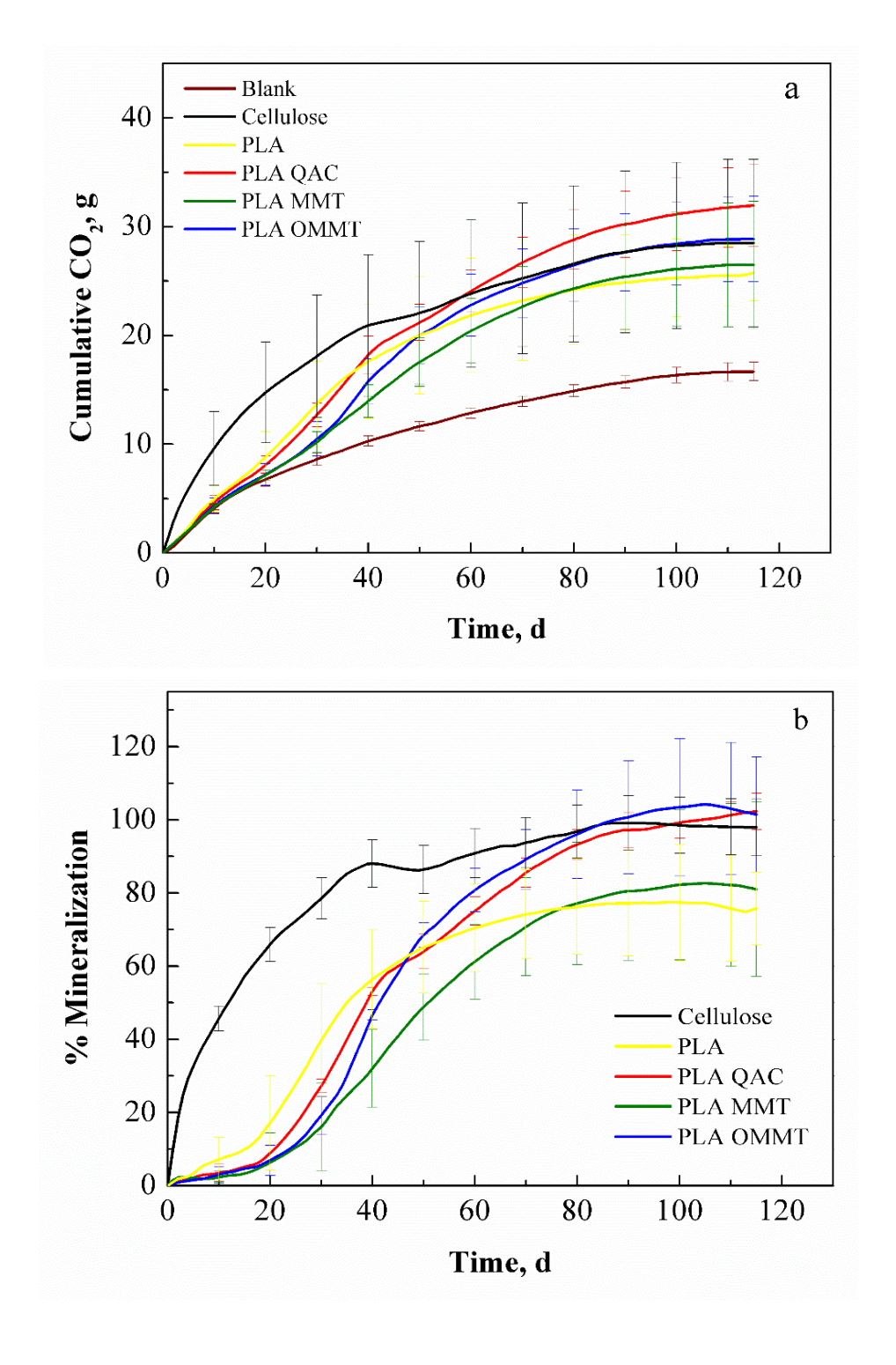


Figure 4.5. CO<sub>2</sub> evolution (a) and % Mineralization (b) of PLA, PLA-OMMT, PLA-MMT and PLA-QAC films in compost.

The lag phase was determined from the graph when a steep increase in the evolution of  $CO_2$  was determined. A lag phase of around 15 days was observed for PLA, whereas lag time of around 18 days was observed for PLA-MMT, PLA-OMMT and PLA-QAC films. This averse behavior in the difference of lag phase for PLA OMMT and PLA MMT with respect to PLA could be attributed to the lower water transmission due to no significant difference in the starting initial molecular weight. The dispersed silicate layers present a torturous path for the diffusing water molecules by increasing the effective path length and time thereby delaying the effective abiotic phase [1]. Though PLA QAC had lower starting initial molecular weight  $M_{n0}$  ( $\leq$  100 kDa), no difference was seen in the lag phase, as compared to the other films. The amount of  $CO_2$  evolved from bioreactors for PLA-OMMT and PLA-QAC, varied from 28.9  $\pm$  3.9 g and 31.9  $\pm$  3.7 g, whereas for PLA-MMT and PLA ranged from 26.5  $\pm$  5.8 g and 25.7  $\pm$  2.6 g respectively through the end of the test. A maximum average mineralization of 101.4 % was reached by PLA OMMT by the end of the test (120 days). Cellulose reached a maximum mineralization of 102.9% whereas, PLA-QAC, PLA-MMT and PLA reached 102.3%, 81% and 75.6% after 115 days, respectively.

The mineralization of PLA-OMMT and PLA-QAC was higher as compared to PLA-MMT and PLA by the end of the test. This faster degradation can be attributed to the presence of hydroxyl groups in the clay organic modifiers (QAC), which improves the relative hydrophilicity of the nanoclay surface (OMMT). The surfactant (QAC) used in this study is ammonium salt with two alkyl tails, having hydroxyl group attached to either the ammonium head or tallow tail, which further improves the hydrophilicity of the matrix [1]. This allows easy permeation of the water molecules in the polymer matrix, thereby triggering hydrolytic degradation [4-8].

The mineralization values above 100% for PLA-OMMT, PLA-QAC and cellulose indicate the presence of priming effect, which results from the enhanced mineralization of the indigenous

organic carbon present in the compost, in addition to the CO<sub>2</sub> evolution coming from the conversion of carbon present in the test material [9].

By the end of the test, the mineralization of PLA with respect to PLA-OMMT, PLA-MMT and PLA-QAC films was not significantly different. The large error bars indicate a greater variation among the replicates, which has been previously reported [10,11]. Though no significant difference was observed among all the films, a significant enhancement in mineralization was observed in PLA-OMMT and PLA-QAC films as compared to PLA-MMT and PLA films after one month. This can be attributed to the dihydroxy hydrogenated tallow tails which absorb moisture from the compost and enhance the hydrolysis of the PLA matrix [12]. Therefore, until one month we see a similar trend in all the films. A pronounced difference and steep increase in slope was found in PLA-OMMT, PLA-QAC films with respect to PLA and PLA-MMT due to the above mentioned behavior.

### 4.2.2 Biodegradation in Non-inoculated & Inoculated Vermiculite

The PLA, PLA-QAC, PLA-MMT and PLA-OMMT films were introduced in non-inoculated vermiculite to avoid the priming effect as observed with the compost media [9,13,14]. Since vermiculite is an inert, solid media there is no background indigenous carbon available, as in case of compost. This also leads to low variation among replicates of the samples tested for cumulative CO<sub>2</sub> evolution and % mineralization.

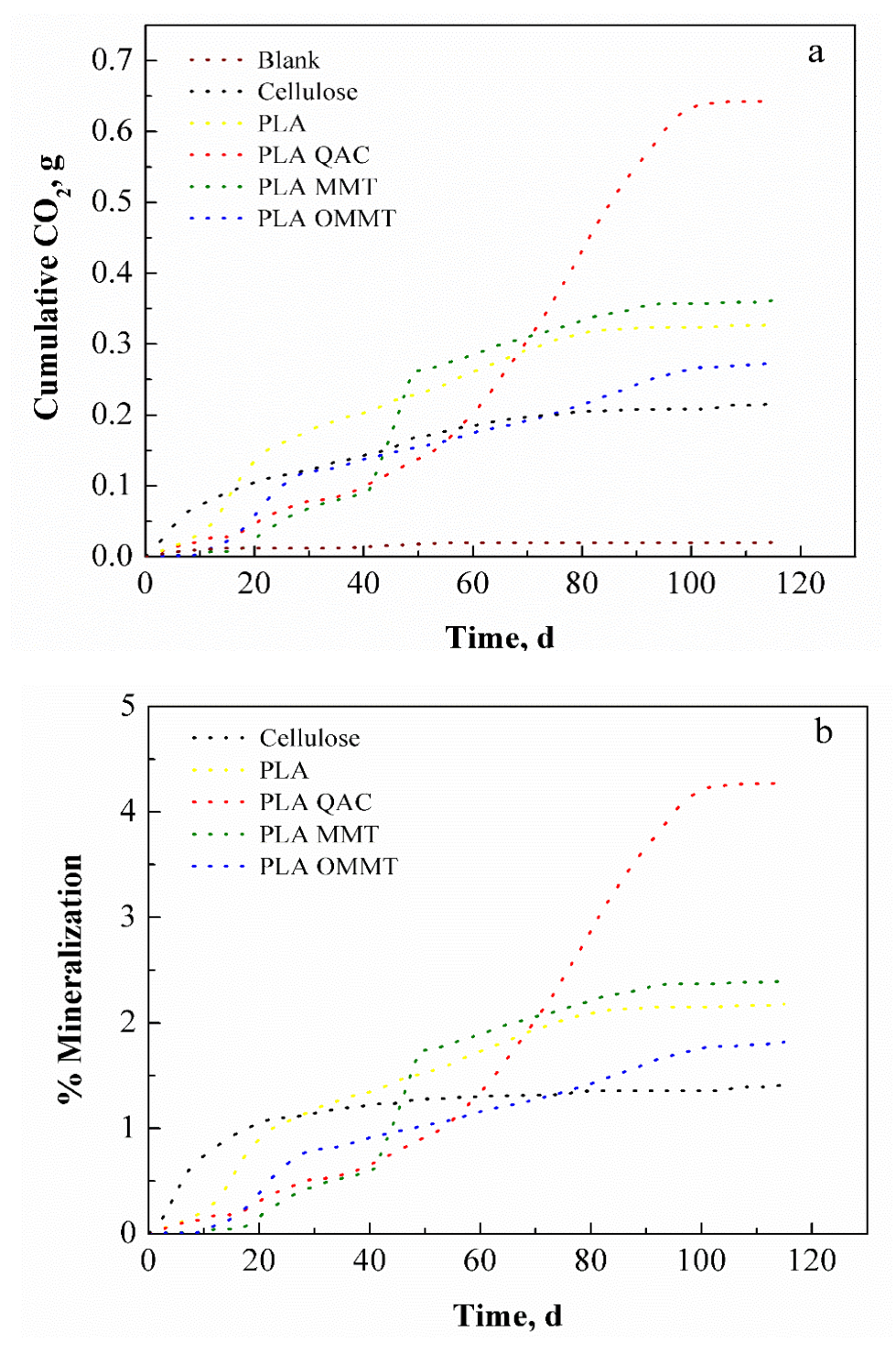
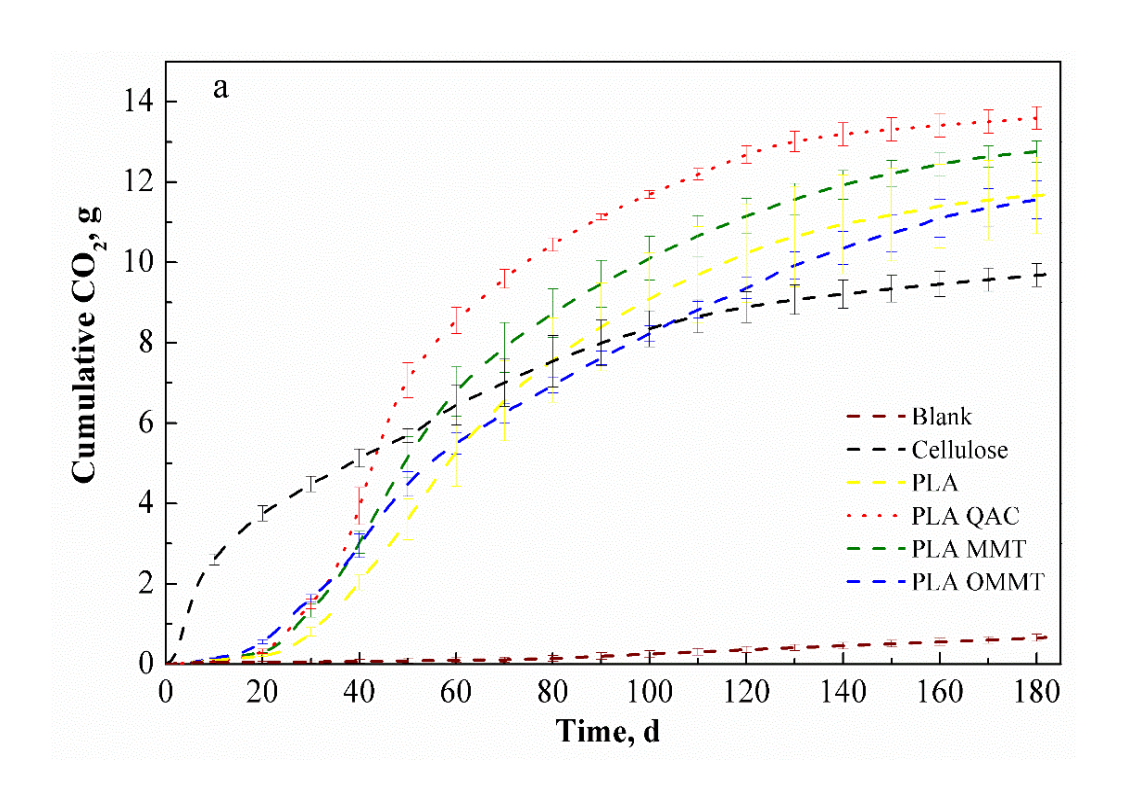


Figure 4.6. CO<sub>2</sub> evolution (a) and % Mineralization (b) of PLA, PLA-OMMT, PLA-MMT and PLA-QAC films in non-inoculated vermiculite.



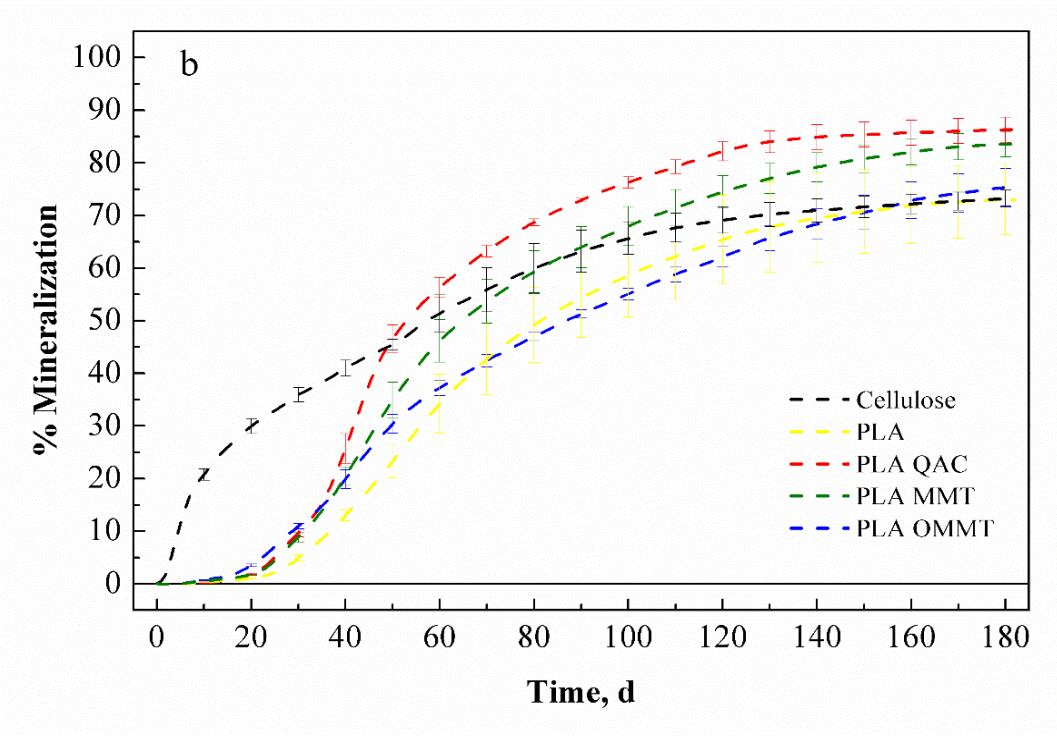


Figure 4.7. CO<sub>2</sub> evolution (a) and % Mineralization (b) of PLA, PLA-OMMT, PLA-MMT and PLA-QAC films in inoculated vermiculite.

Figure 4.7 shows that there was significant difference in the mineralization of PLA-QAC and PLA, whereas no significant difference was observed with respect to PLA-OMMT and PLA-MMT films by the end of the test (183 days). This can be attributed to the lower initial molecular weight of the PLA-QAC film  $M_{n0}$  ( $\leq$  100 kDa).

PLA control achieved a maximum mineralization of 73 % by 183 days, whereas PLA-QAC reached the same mineralization in 90 days and reached a maximum average mineralization of 86.4% by the end of the test. PLA-OMMT and PLA-MMT achieved a maximum average mineralization of 75.5% and 83.6% respectively. Cellulose reached a mineralization of 73.3% by the end of the test. A difference in lag phase with respect to compost was seen in case of PLA. PLA-MMT and PLA-QAC exhibited a lag time of around 20 days while PLA-OMMT and PLA control showed a lag time of around 15 and 25 days. This was in accordance to the values reported in the literature before [10]. PLA-QAC produced  $13.6 \pm 0.3$  g of CO<sub>2</sub>, whereas PLA-OMMT, PLA-MMT and PLA produced  $11.6 \pm 0.5$  g,  $12.8 \pm 0.3$  g and  $11.7 \pm 1$  g of CO<sub>2</sub>.

After 60 days and until the end of the test, PLA control seems to produce more CO<sub>2</sub> than PLA-OMMT, but the difference is negligible. Same trend is observed in the mineralization curve. The increase in the mineralization of PLA-QAC compared to PLA-OMMT and PLA after day 45 could be attributed to the hydroxyl groups present in the surfactant. By the end of the test, no significant difference was observed in the mineralization of PLA, PLA-OMMT, PLA-MMT and PLA-QAC. It is significant to refer that long testing periods are needed in this case since the biodegradation proceeds at a slower rate in inoculated vermiculite as compared to compost. Figure 4.5 also shows the results for testing the samples in non-inoculated vermiculite to evaluate abiotic degradation. As anticipated, the abiotic degradation test did not show any remarkable CO<sub>2</sub> evolution. No significant difference was seen in mineralization values.

# 4.3 Molecular weight

# 4.3.1 Molecular Weight distribution

Figure 4.8 shows the initial molecular weight distribution for (MWD) for PLA, PLA-OMMT, PLA-MMT and PLA-QAC. As stated previously, there was no significant difference in the starting initial molecular weight  $M_n$ , thickness and crystallinity for all the samples.

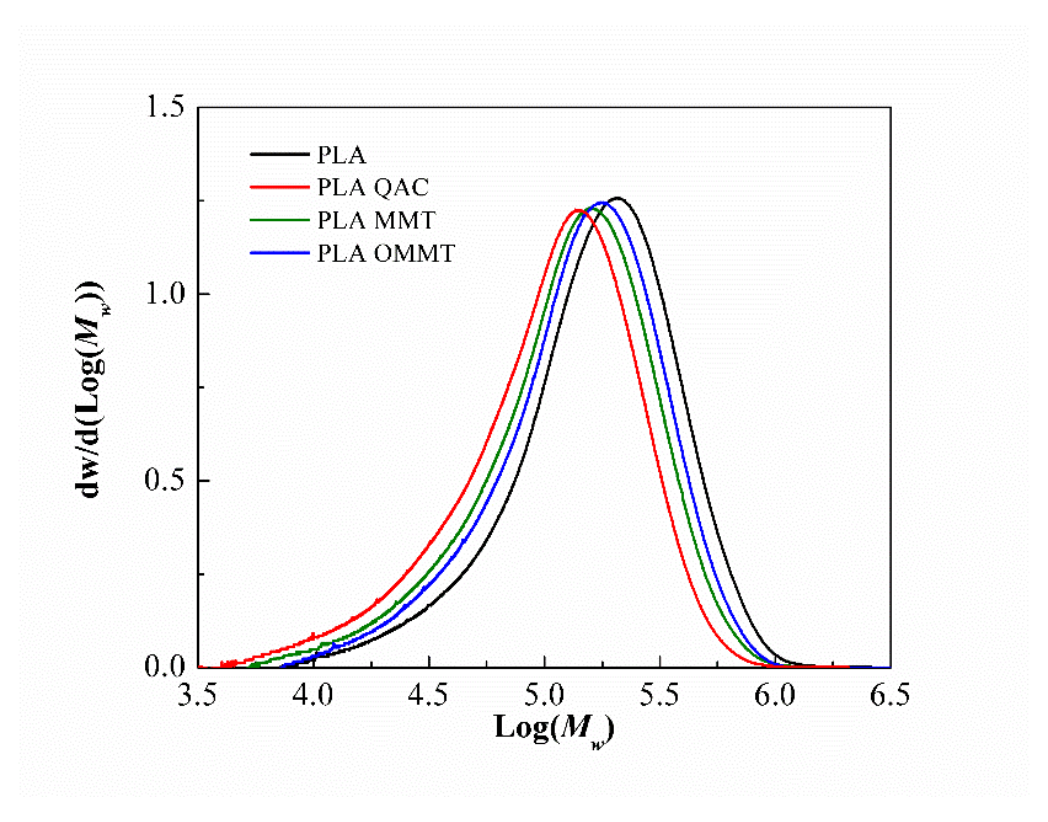


Figure 4.8. Initial molecular weight distribution for PLA, PLA-OMMT, PLA-MMT and PLA-QAC films.

Figure 4.9 shows the molecular weight distribution for PLA as a function of time during the biodegradation test until day 30.

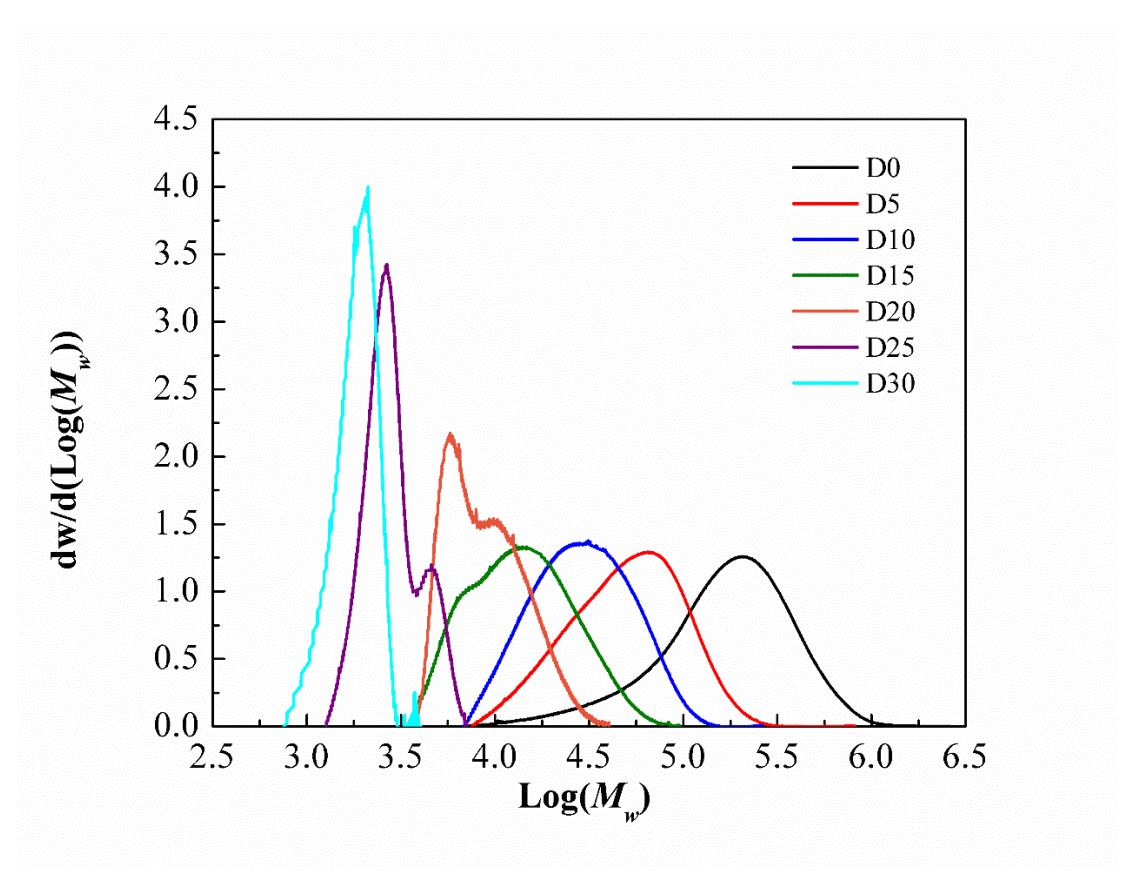


Figure 4.9. Change in molecular weight distribution for PLA film in Compost.

A change from monomodal to multimodal distribution is observed starting increasingly at day 15 until day 30. To carry out the kinetics analysis, deconvolution of the peaks was necessary due to the observed multimodal behavior for PLA, PLA-OMMT, PLA-MMT and PLA-QAC films. Fityk 0.9.8, a curve fitting and data analysis program, was used to perform the deconvolution using a log normal function, to fit such irregular functions [10,17,18]. Figure 4.10. shows an example as to how the deconvolution was carried out for PLA in compost media for days 5,10,15 and 20 respectively.

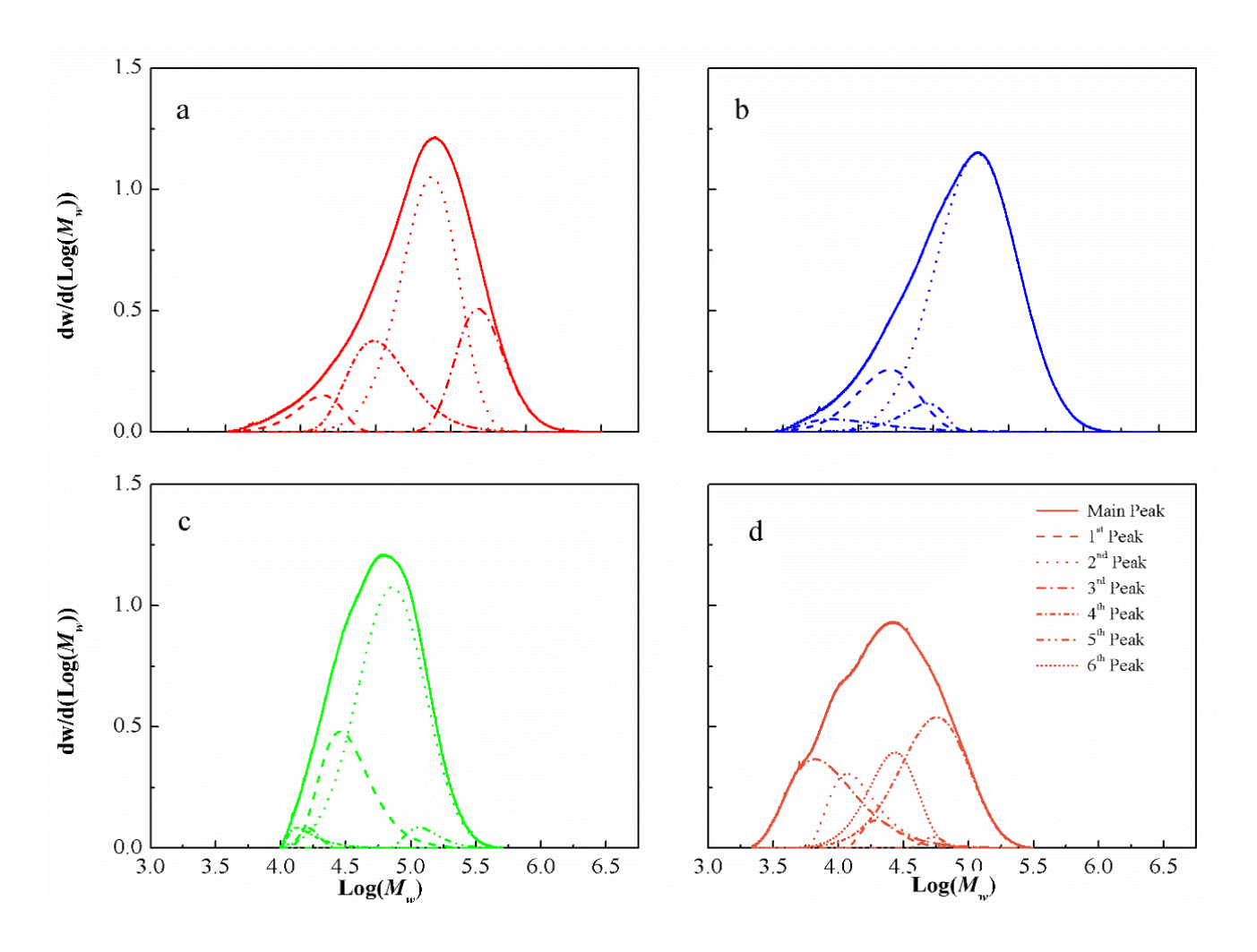


Figure 4.10. Deconvolution of PLA peaks at days a) 5, b) 10, c) 15, d) 20 in Compost media.

To determine the main peak of the molecular weight distribution (MWD), the area fraction methodology was used. Once the deconvolution was performed, the peak having the largest area was selected as the main peak for each case to determine the  $M_n$  reduction rate constant (k). The methodology is illustrated below in Figure 4.11 which shows PLA control as an example.

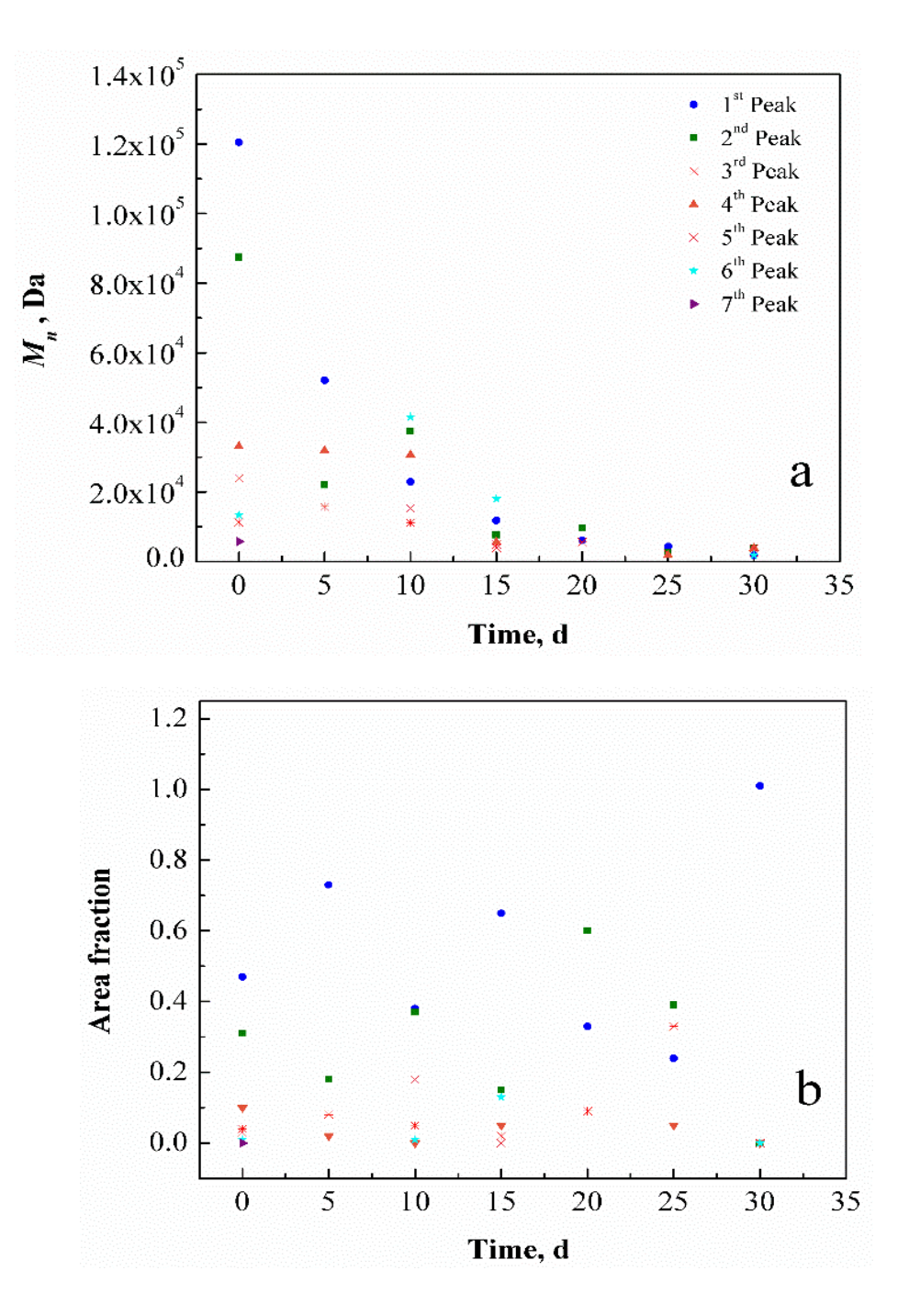
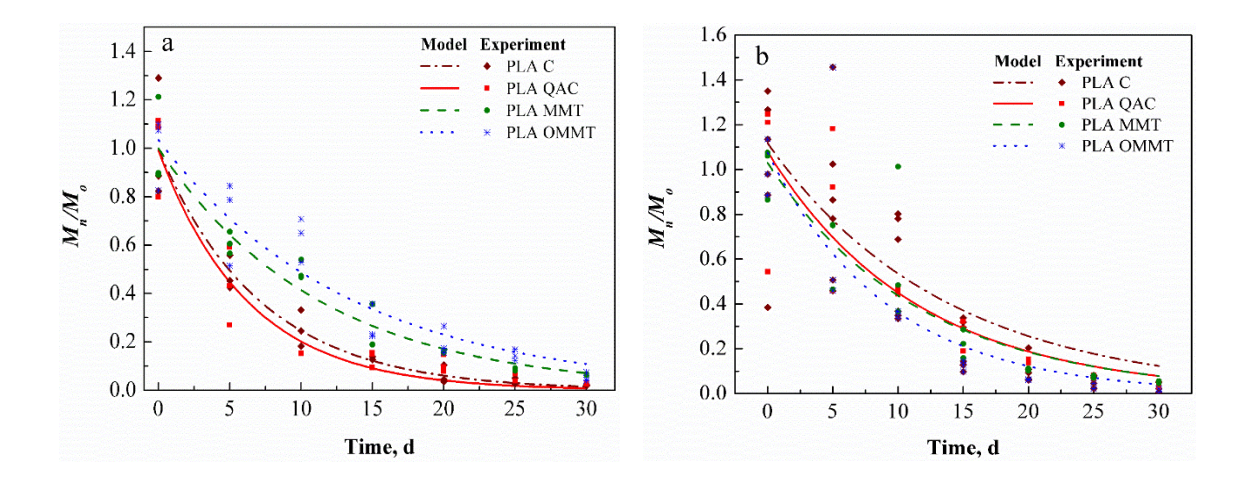


Figure 4.11 a)  $M_n$  and b) area fraction as function for PLA in compost after performing deconvolution

Figure 4.11 a shows  $M_n$  calculated after deconvolution of different peaks while Figure 4.11 b shows the area fraction for the different peaks until day 30. The first peak is seen as the main contributor until day 15, but for day 20 & 25 peak 2 has the highest area fraction again followed by first peak for day 30. The same methodology was employed to PLA-OMMT, PLA-MMT and PLA-QAC films. The main peaks were selected individually for all the films for each day until day 30 for determining k. The deconvolution was also performed for day 0.

To study the effect of nanoclays on the biodegradation of PLA, PLA-OMMT, PLA-MMT and PLA-QAC films and to track the changes in the molecular weight, samples were collected every five days from all the medias and a first order reaction relationship was fitted to the experimental data. Figure 4.12 shows  $M_n$  as a function of time for all the films tested in the three media.



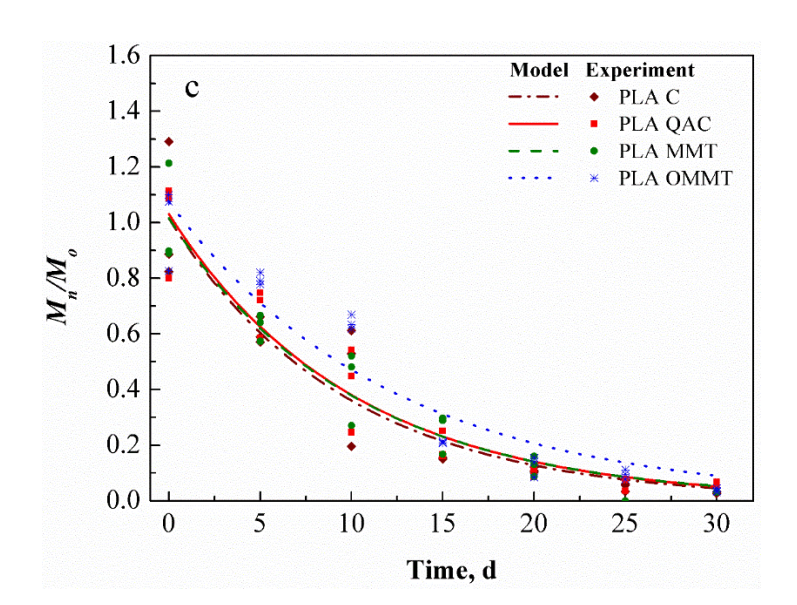


Figure 4.12. Molecular weight reduction as a function of time for PLA, PLA-OMMT, PLA-MMT and PLA-QAC films in (a) compost media, (b) inoculated vermiculite and (c) non inoculated vermiculite. Fitting of first order reaction:  $M_n = M_{no} \exp(-kt)$ , where  $M_n$  is the number average molecular weight at time t,  $M_{no}$  is the initial  $M_n$  and k is the rate constant.

Table 4.6. presents the rate constant k (d<sup>-1</sup>) for PLA, PLA-OMMT, PLA-MMT and PLA-QAC exposed to different medias.

<i>k</i> (	$(d^{-1})$	for	films	in	different	medias
------------	------------	-----	-------	----	-----------	--------

Films	Compost	Vermiculite	Inoculated Vermiculite
PLA	$0.1397 \pm 0.0138^{a,A}$	$0.1035 \pm 0.0120^{a,B}$	$0.0735 \pm 0.0137^{a,C}$
PLA MMT	$0.0822 \pm 0.0067^{b,A}$	$0.0986 \pm 0.0085^{a,B}$	$0.0857 \pm 0.0125^{a,AB}$
PLA OMMT	$0.0751 \pm 0.0075^{b,A}$	$0.0959 \pm 0.0077^{a,B}$	$0.1087 \pm 0.0211^{a,AB}$
PLA QAC	$0.1589 \pm 0.0164^{a,A}$	$0.0996 \pm 0.0086^{a,B}$	$0.0874 \pm 0.0149^{a,B}$

Values with different lowercase letters in a column and values with different uppercase letters in a row are statistically different ( $\alpha = 0.05$  Tukey-Kramer Test)

The degradation of PLA in compost environment is known to proceed by two dominant stages: abiotic and biotic degradation. During the dominant abiotic phase of PLA degradation, high molecular weight chains are reduced to low molecular weight lactic acid oligomers and monomers [15]. This phase is typically dominant before lag time – which is defined as the time in days, from the start of test until the time of activation of the degrading micro-organisms is achieved. During the lag time, the degree of biodegradation for the degrading material achieved is about 10% of the maximum level of biodegradation. The lag phase proceeds by hydrolytic degradation where cleavage of ester linkages takes place due to their high affinity towards water. The second step which is the biotic degradation proceeds by the assimilation of the low molecular weight chains to CO<sub>2</sub>, water and biomass. The addition of nanoclays has been reported to enhance the rate at which biodegradation proceeds [6,10].

A significant difference in the  $M_n$  reduction was observed in compost media for PLA film with respect to PLA-OMMT and PLA-MMT films which challenges the studies done so far with nanoclay as seen in Table 4. This studies imply that addition of nanoclay enhances the

biodegradation, but no control was exercised over the initial molecular weight ( $M_n$ ) and thickness (t) [14,18]. The higher rate for PLA-QAC can be attributed to the low starting molecular weight with respect to all films, and also due to the presence of two alkyl (tallow) tails [1]. QAC may induce a plasticization effect by promoting chain movements and increasing the free space available thereby allowing faster diffusion of water into the amorphous region [1,16]. However, no significant difference was seen with respect to the degradation rate for PLA, PLA-OMMT and PLA-MMT films in inoculated and uninoculated vermiculite. This can be attributed to the same initial conditions of molecular weight and thickness considering that at high molecular weight, there is less segmental mobility of backbone chains and limited access to the hydroxyl groups and hydrophilic terminal carboxyl groups for the water to access. The nanoclays may be acting as a barrier thereby producing a torturous path and delaying the water diffusion into the PLA matrix, thereby restricting the chain movements and hence no difference in the rate of hydrolysis as compared to pure PLA [5].

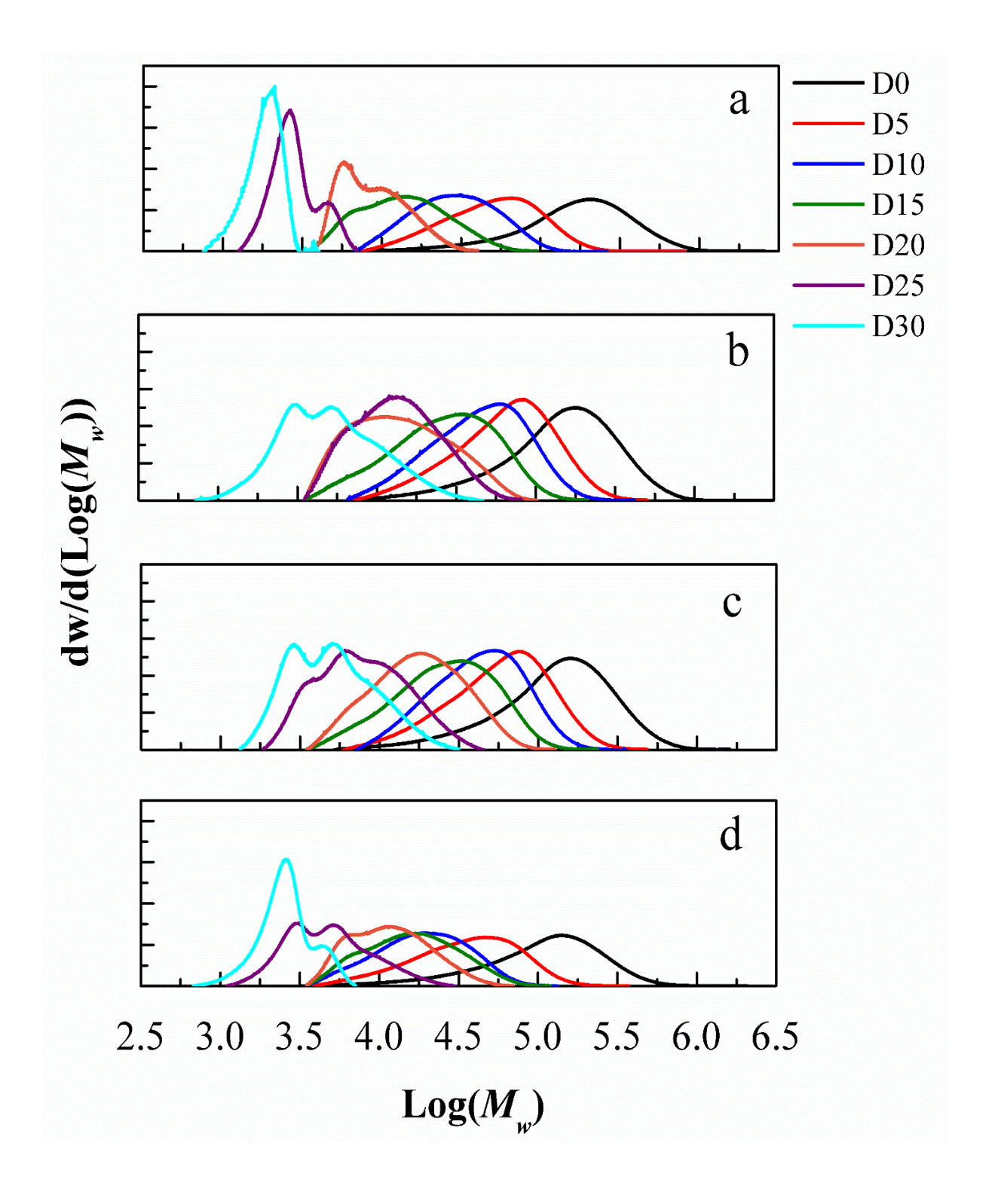


Figure 4.13. Change in molecular weight distribution for a) PLA b) PLA-OMMT c) PLA-MMT and d) PLA-QAC films in compost.

Figure 4.13. illustrates the changes in the molecular weight distribution for PLA, PLA-OMMT, PLA-MMT and PLA-QAC films in compost media for the biodegradation test until day 30, since it was difficult to retrieve samples after that. The decrease in molecular weight is depicted by shifting of the peak to the left. This behavior is observed during the hydrolytic degradation i.e. abiotic phase and is mainly accredited to the chain scission happening in the bulk of the polymer matrix and not only on the surface [10,14,16]. The bulk erosion happening can be corroborated by the fact that the main peak of all the molecular distribution curves shift to the left i.e. low molecular weight and does not remain at the same place as hydrolysis proceeds [14]. Bulk erosion takes place homogenously wherein the water diffusion is faster as compared to polymer degradation. As the hydrolysis proceeds, due to the bulk erosion random cleavage of ester bonds take place generating carboxylic acid end groups that further catalyse the degradation process thus producing an autocatalytic effect and making it self-sustaining [6]. A broadening of peaks is also observed over time, indicating an increase in PDI. Around day 20, the molecular weight distribution becomes bimodal. The main peak is replaced by a small shoulder at the original molecular weight and one comparatively large shoulder at lower molecular weight. As the biodegradation proceeds, the peak corresponding to high molecular weight vanishes leaving behind a sharper peak for low molecular weight fraction [19]. This can be attributed to the formation of more stable crystalline structure due to the realignment of shorter molecular weight chains [20]. The sharper peaks are formed due to the degradation of amorphous regions, since the hydrolytic chain cleavage is known to preferentially take place in amorphous regions. This behavior is more pronounced for PLA and PLA-QAC films and less for PLA-OMMT and PLA-MMT films. It could be due to the slower formation of crystalline regions. It has been reported that OMMT may act as a nucleating agent, due to its large surface area, enhancing the degradation of amorphous region, which in turn increases the crystallinity (put in the table no of crystallinity). The crystalline regions are known to be resistant to hydrolysis since they restrict the diffusion of water [4,14]. This can be the plausible explanation for the blunt and wide peaks seen at day 30. A whitening effect was also observed in PLA, PLA-OMMT, PLA-MMT and PLA-QAC films because of the increased crystallinity thereby producing a change in the refractive index of the polymer, in the initial hydrolysis phase [8,14,21]. It is also essential to understand the effect this nanoclays have on the microorganisms, since a difference was seen with respect to CO<sub>2</sub> evolution between PLA, PLA-OMMT, PLA-MMT and PLA-QAC films. For example, Edgar et al. has suggested that PLA-OMMT shows significantly more biofilm formation as compared to PLA while PLA-QAC shows the lowest, which might be due to the inhibiting action of the surfactant.

# 4.4 Hydrolysis

Many factors are involved when it comes to the abiotic and biotic degradation in compost environment like temperature, pH, microorganisms, oxygen and water availability *etc.* [239] and play a crucial role in the breakdown of the material. Abiotic or hydrolytic degradation has been identified as the rate determining step for biodegradation of PLA [4,22]. Therefore, to study the abiotic phase and investigate the impact of nanoclays and surfactant in detail, hydrolysis was run in parallel at 58±2°C in the same DMR setting for PLA, PLA-OMMT, PLA-MMT and PLA-QAC films. Samples were collected on day 0, 2, 4, 7, 10, 14, 21, 30, 45. No samples could be collected for PLA and PLA-MMT on day 60. So, data only until day 45 is reported.

## 4.4.1 Molecular Weight

The deduction of molecular weight was based on deconvolution of peaks as mentioned before. Figure 4.14 shows  $M_n$  as a function of time for PLA, PLA-OMMT, PLA-MMT and PLA-QAC films in water at 60°C. This hydrolysis experiment was run in parallel with the biodegradation tests. For all the films, the molecular weight decreased over 60 days due to the hydrolytic degradation of PLA. Table 4.8 presents the rate constant k (d<sup>-1</sup>) for PLA, PLA-OMMT, PLA-MMT and PLA-QAC exposed to water. As seen no significant difference was observed in the hydrolytic degradation rate among all the films. This could be attributed to no significant difference in the initial molecular weight  $(M_{no})$  and thickness (t) of the films. This results are not in agreement with the results published so far [4,6,22] since nanoclays (OMMT) have been reported to ease the diffusion of water in the PLA matrix due to the hydroxylated tallow tails and surfactant (QAC) is known to plausibly act as a plasticizer thereby inducing chain movements and paving way for diffusion of water, to start the cleavage of ester bonds. Fabiola et al. reported otherwise as opposed to the findings so far, that inspite of the difference in the initial molecular weight due to the incorporation of nanoclays, still no significant reduction in  $M_n$  and thus no difference in the hydrolytic degradation rates of PLA, PLA-OMMT, PLA-MMT and PLA-QAC films was found.

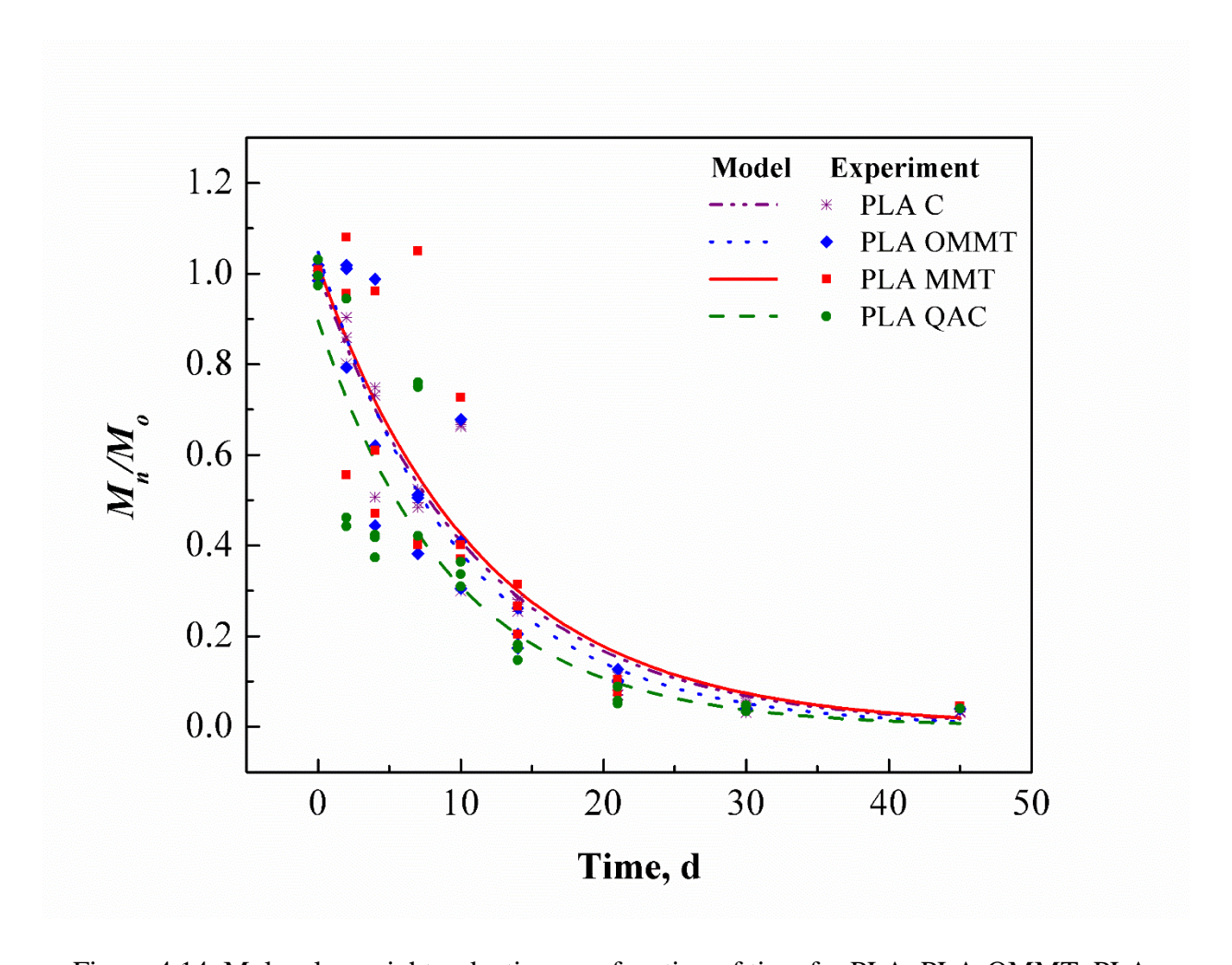


Figure 4.14. Molecular weight reduction as a function of time for PLA, PLA-OMMT, PLA-MMT and PLA-QAC films in water at 60°C. Fitting of first order reaction:  $M_n = M_{no} \exp(-kt)$ , where  $M_n$  is the number average molecular weight at time t,  $M_{no}$  is the initial  $M_n$  and k is the rate constant.

Table 4.7. Rate constants for PLA, PLA-QAC, PLA-OMMT & PLA-MMT films in water at 60°C.

k (d <sup>-1</sup> ) for films in different medias					
Films	Water	Non-inoculated Vermiculite			
PLA	$0.0895 \pm 0.0080^{a,A}$	$0.1035 \pm 0.0120^{a,A}$			
PLA-MMT	$0.0874 \pm 0.0139^{a,A}$	$0.0986 \pm 0.0085^{a,A}$			
PLA-OMMT	$0.1002 \pm 0.0110^{a,A}$	$0.0959 \pm 0.0077^{a,A}$			
PLA-QAC	$0.1060 \pm 0.0174^{a,A}$	$0.0996 \pm 0.0086^{a,A}$			

Values with different lowercase letters in a column and values with different uppercase letters in a row are statistically different ( $\alpha = 0.05$  Tukey-Kramer Test)

Figure 4.15 illustrates the changes in the molecular weight distribution for PLA, PLA-OMMT, PLA-MMT and PLA-QAC films exposed to water for the hydrolysis test until day 45. Deconvolution was performed using the peak area methodology as explained before. The rates mentioned in Table 4.7 were calculated after performing the deconvolution of the multimodal peaks. As the hydrolytic degradation proceeds, the molecular weight distribution shifts to the left indicating the evolution of low molecular weight chains resulting from the diffusion of water into the PLA matrix. The broadness of the peaks increased over time and several sharp peaks were observed by the end of the test. Trimodal and bimodal peaks were observed starting day 21, indicating the presence of different molecular weight chains. The  $M_n$  at this point for PLA, PLA-OMMT, PLA-MMT and PLA-QAC was 9 kDa, 10 kDa, 8 kDa and 6 kDa respectively. Comparing the MWD for PLA, PLA-OMMT, PLA-MMT and PLA-QAC films in water and uninoculated vermiculite at 58°C, much sharper peaks were observed for PLA-OMMT and PLA-MMT films for day 30, indicating the degradation of amorphous regions. As the amorphous regions degrade,

the remaining low molecular weight chains realign themselves into a more definite compact structure.

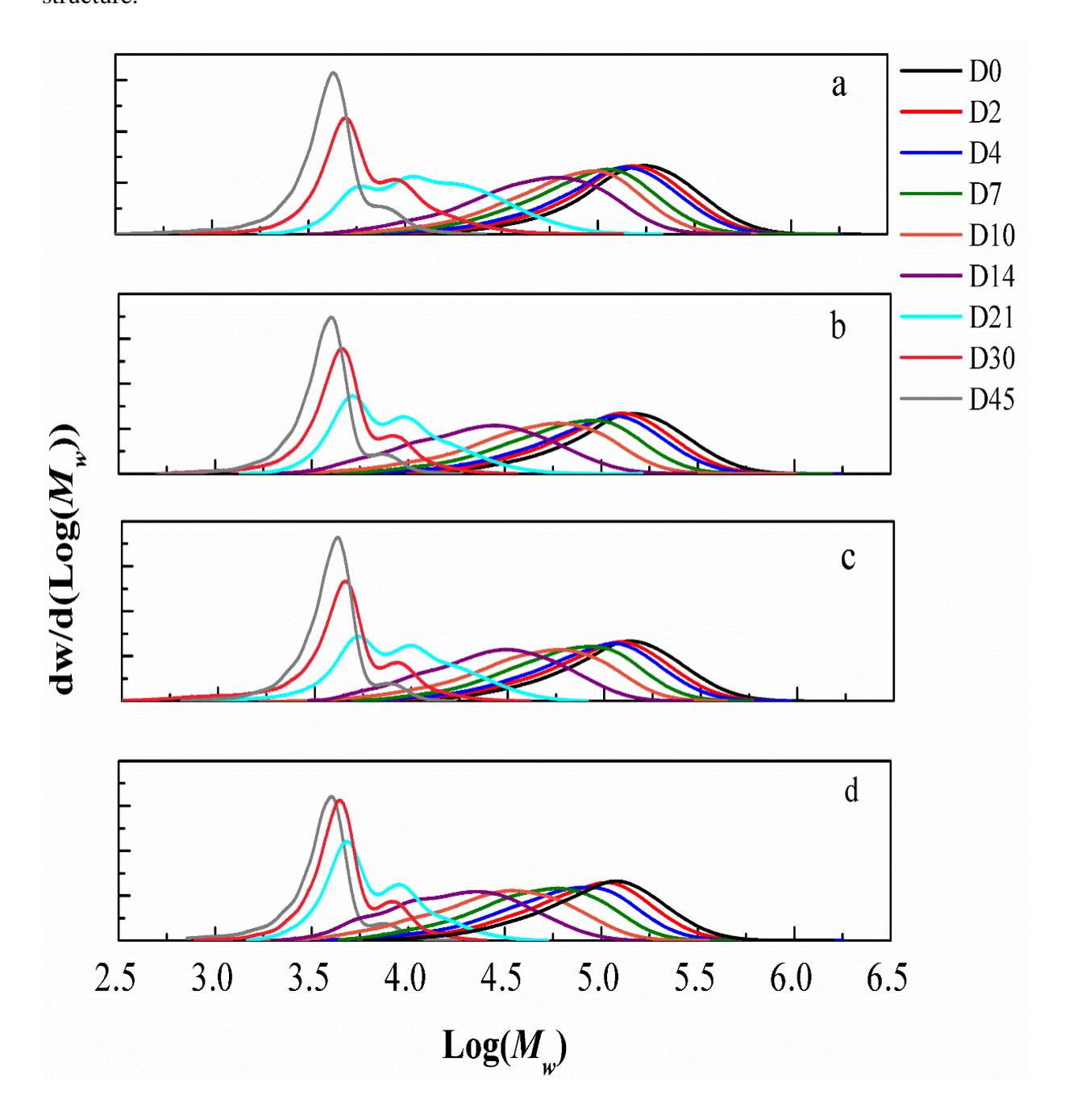


Figure 4.15. Change in molecular weight distribution for a) PLA b) PLA-OMMT c) PLA-MMT and d) PLA-QAC films in water at 60°C.

In addition to water diffusion, in case of PLA-QAC films, the free QAC available could act as a plasticizer further enhancing the release of low molecular weight chains and oligomers. The PLA-OMMT films apart from the presence of hydroxyl group of silicates are known to increase the wettability of the surface, thus promoting the hydrolytic degradation of PLA ester bonds [4]. The release and accumulation of hydrolysis by-products such as oligomers and monomers, reduce the pH of the water which in turn promotes autocatalytic reaction thus sustaining the hydrolytic degradation. However, by the end of the test no statistical difference was detected in the hydrolysis rate for PLA, PLA-OMMT, PLA-MMT and PLA-QAC films, this could be due to the lower diffusivity of water through the PLA-OMMT and PLA-MMT films.

# 4.5 Crystallinity evolution during hydrolysis

The DSC technique was used to assess the crystallinity of the PLA, PLA-OMMT, PLA-MMT and PLA-QAC films during hydrolytic degradation in water at  $60^{\circ}$ C. The changes in  $T_g$ ,  $T_m$  and  $T_c$  along with the percent crystallinity was also determined. Figure 4.16 depicts the DSC thermograms for PLA, PLA-OMMT, PLA-MMT and PLA-QAC before and after being hydrolyzed by water at various time intervals.

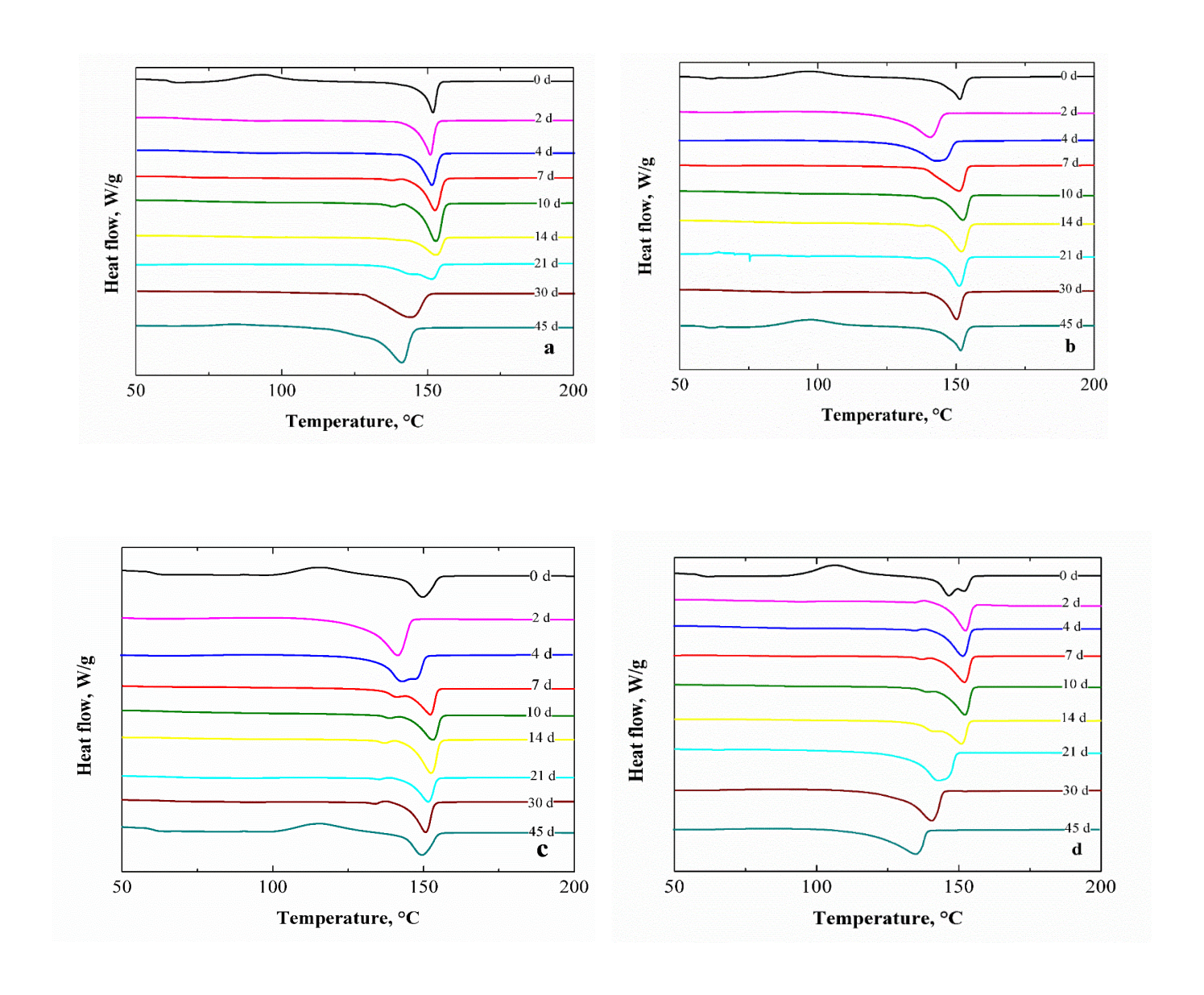


Figure 4.16. DSC thermograms of a) PLA b) PLA-OMMT c) PLA-MMT and d) PLA-QAC in water at  $60^{\circ}$ C (1st cycle). The numbers on the thermogram indicate the day immersed.

All the film samples on day 0, before exposure showed a  $T_{cc}$  (cold crystallization) peak, but the peak disappeared once the films disks were introduced in water. This peak can be pertained to the crystallization induced due to the reorganization of amorphous phase into new crystalline regions during the immersion process [23,24]. The melting peak is observed at around 153°C,

corresponding to the melting of newly developed crystalline fractions resulting from the chain movements due to higher temperature. As, the hydrolysis proceeds, the cold crystallization peak disappears. This disappearance can be attributed to the formation of locally organized structures meaning that PLA has been completely crystallized in the PLA and PLA-nanoclay films during the cooling process thereby further preventing the occurrence of cold crystallization peak [4]. The nanoclays acts as a nucleating agent thereby assisting the progress of crystallization [25-28], by increasing the diffusion of water due to the hydrophilic nature and resulting improved chain segmental mobility. Double melting peaks are also observed in PLA, PLA-OMMT, PLA-MMT and PLA-QAC films during the DSC heating process which indicate towards the formation of two different crystalline structure, but this behavior is not uniform and mostly occurrence of one peak is observed after day 21. Due to the lower  $M_n$  and  $M_w$ , only one peak is observed starting day 21. This formed crystalline structure is unstable since the peak disappears after day 21. Of the double peaks, the higher  $T_m$  can be ascribed to the melting of primary and more stable crystal formation while low  $T_m$  can be assigned to the melting of less stable and reorganized crystals. Fabiola et. Al has suggested the formation of  $\alpha$ -form crystals which also reflects only one melting peak over time [20]. This single peak indicates the crystals melt directly without undergoing recrystallization. As the hydrolysis proceeds,  $T_m$  is shifted slightly to low temperatures in PLA and PLA-QAC films, though the heating enthalpy seems to increase with time. Also, a small endothermic peak is seen at day 45 for PLA-OMMT and PLA-MMT films at 95°C and 125°C. This can be elucidated by the rearrangement of some amorphous segments into polymer crystallization due to the chain mobility which would have been increased, right before the melting commenced. The pH was also monitored when the samples were retrieved. A severe drop was observed until value 2 indicating the media turning acidic from neutral. In acidic condition, the hydrolysis proceeds by chain

scission forming small molecular weight oligomers, giving lactide units in the end of the hydrolysis [29]. Table 5 depicts the change in crystallinity by the end of the test at day 45.

Table 5 Crystallinity for PLA, PLA-QAC, PLA-OMMT & PLA-MMT films in water at 60°C at end of hydrolysis (45 days).

Material	Crystallinity (χ <sub>c</sub> ) , %	
PLA C	$60 \pm 1.15^{a}$	
PLA OMMT	$66\pm2.52^a$	
PLA MMT	$67 \pm 5.13^{a}$	
PLA QAC	$53 \pm 11.01^{a}$	

*Values with different letter are statistically different* ( $\alpha = 0.05$  *Tukey-Kramer Test*)

The development in the global crystallinity of the PLA, PLA-OMMT, PLA-MMT and PLA-QAC films can be calculated from cold crystallization and heating enthalpies. Initially as mentioned in Table, the crystallinity was between 1 and 4% before the start of hydrolysis. PLA-OMMT and PLA-MMT showed the highest crystallinity values among all indicating that the clays in fact act as a nucleating agent, thereby facilitating the degradation of amorphous region by enhancing the diffusion of water molecules through the galleries. The increase in crystallinity for PLA and PLA-QAC films could be ascribed to decrease in molecular weight due to the chain scission reaction occurring due to the plasticisation of PLA by water, accompanied by the lactic acid oligomers that provide enough mobility so that the polymer chains can organise and crystallize further.

- [1] S. M. Mohomane, "Preparation and Characterization of Polychloroprene/modified Clay Nanocomposites," 2010.
- [2] G. Ozkoc and S. Kemaloglu, "Morphology, biodegradability, mechanical, and thermal properties of nanocomposite films based on PLA and plasticized PLA," *Journal of Applied Polymer Science*, vol. 114, no. 4. pp. 2481–2487, 2009.
- [3] H. M. C. de Azeredo, "Nanocomposites for food packaging applications," *Food Res. Int.*, vol. 42, no. 9, pp. 1240–1253, 2009.
- [4] ASTM International, "ASTM D5338-15: Standard Test Method for Determining Aerobic Biodegradation of Plastic Materials Under Controlled Composting Conditions, Incorporating Thermophilic Temperatures," in *ASTM Standards*., 2015, pp. 1–7.
- [5] I. Standard, "ISO 14855-2: Determination of the ultimate aerobic biodegradability of plastic materials under controlled composting conditions Method of analysis of evolved carbon dioxide," 2018.
- [6] P. Song, L. Sang, L. Zheng, C. Wang, K. Liu, and Z. Wei, "Insight into the role of bound water of a nucleating agent in polymer nucleation: A comparative study of anhydrous and monohydrated orotic acid on crystallization of poly(l-lactic acid)," *RSC Adv.*, vol. 7, no. 44, pp. 27150–27161, 2017.
- [7] S.-R. Lee *et al.*, "Microstructure, tensile properties, and biodegradability of aliphatic polyester/ clay nanocomposites," *Polymer (Guildf).*, vol. 43, pp. 2495–2500, 2002.
- [8] M. A. Paul, C. Delcourt, M. Alexandre, P. Degée, F. Monteverde, and P. Dubois, "Polylactide/montmorillonite nanocomposites: Study of the hydrolytic degradation," *Polym. Degrad. Stab.*, vol. 87, no. 3, pp. 535–542, 2005.
- [9] A. V. Machado, A. Araújo, and M. Oliveira, "Assessment of polymer-based nanocomposites biodegradability," *Biodegrad. Polym. Vol. 1 Adv. Biodegrad. Study Appl.*, pp. 166–196, 2015.
- [10] K. Fukushima, E. Giménez, L. Cabedo, J. M. Lagarón, and J. L. Feijoo, "Biotic degradation of poly(DL-lactide) based nanocomposites," *Polym. Degrad. Stab.*, vol. 97, no. 8, pp. 1278–1284, 2012.
- [11] G. Bellia, M. Tosin, and F. Degli-Innocenti, "Test method of composting in vermiculite is unaffected by the priming effect," *Polym. Degrad. Stab.*, vol. 69, no. 1, pp. 113–120, 2000.
- [12] E. Castro-aguirre, R. Auras, S. Selke, M. Rubino, and T. Marsh, "Impact of Nanoclays on the Biodegradation of Poly (lactic acid) Nanocomposites," vol. 2, pp. 1–24, 2017.
- [13] G. Kale, T. Kijchavengkul, R. Auras, M. Rubino, S. E. Selke, and S. P. Singh, "Compostability of bioplastic packaging materials: An overview," *Macromol. Biosci.*, vol.

- 7, no. 3, pp. 255–277, 2007.
- [14] S. Sinha Ray, K. Yamada, M. Okamoto, and K. Ueda, "Control of biodegradability of polylactide via nanocomposite technology," *Macromol. Mater. Eng.*, vol. 288, no. 3, pp. 203–208, 2003.
- [15] G. Bellia, M. Tosin, G. Floridi, and F. Degli-Innocenti, "Activated vermiculite, a solid bed for testing biodegradability under composting conditions," *Polym. Degrad. Stab.*, vol. 66, no. 1, pp. 65–79, 1999.
- [16] H. Tsuji and Y. Ikada, "Blends of crystalline and amorphous poly(lactide) .3. Hydrolysis of solution-cast blend films," *J. Appl. Polym. Sci.*, vol. 63, pp. 855–863, 1997.
- [17] K. Fukushima, C. Abbate, D. Tabuani, M. Gennari, and G. Camino, "Biodegradation of poly(lactic acid) and its nanocomposites," *Polym. Degrad. Stab.*, vol. 94, no. 10, pp. 1646–1655, 2009.
- [18] M. A. Paul, C. Delcourt, M. Alexandre, P. Degée, F. Monteverde, and P. Dubois, "Polylactide/montmorillonite nanocomposites: Study of the hydrolytic degradation," *Polym. Degrad. Stab.*, vol. 87, no. 3, pp. 535–542, 2005.
- [19] Fabiola, "Hydrolytic Degradation of Poly (lactic acid ) and Poly (lactic acid ) Nanocomposites by Water-Ethanol Solutions," 2016.
- [20] M. Wojdyr, "Fityk: A general-purpose peak fitting program," *J. Appl. Crystallogr.*, vol. 43, no. 5 PART 1, pp. 1126–1128, 2010.
- [21] A. Perejón, P. E. Sánchez-Jiménez, J. M. Criado, and L. A. Pérez-Maqueda, "Kinetic Analysis of Complex Solid-State Reactions. A New Deconvolution Procedure," *J. Phys. Chem. B*, vol. 115, no. 8, pp. 1780–1791, 2011.
- [22] M. Hakkarainen, A. C. Albertsson, and S. Karlsson, "Weight losses and molecular weight changes correlated with the evolution of hydroxyacids in simulated in vivo degradation of homo- and copolymers of PLA and PGA," *Polym. Degrad. Stab.*, vol. 52, no. 3, pp. 283–291, 1996.
- [23] F. Iñiguez-Franco *et al.*, "Concurrent solvent induced crystallization and hydrolytic degradation of PLA by water-ethanol solutions," *Polym. (United Kingdom)*, vol. 99, pp. 315–323, 2016.
- [24] M. P. Balaguer, C. Aliaga, C. Fito, and M. Hortal, "Compostability assessment of nanoreinforced poly(lactic acid) films," *Waste Manag.*, vol. 48, pp. 143–155, 2016.
- [25] L. Husrov *et al.*, "Identification of important abiotic and biotic factors in the biodegradation of poly(l-lactic acid)," *Int. J. Biol. Macromol.*, vol. 71, pp. 155–162, 2014.
- [26] P. Kucharczyk, E. Hnatkova, Zdenekdvorak, and V. Sedlarik, "Novel aspects of the degradation process of PLA based bulky samples under conditions of high partial pressure of water vapour," *Polym. Degrad. Stab.*, vol. 98, no. 1, pp. 150–157, 2013.
- [27] E. Picard, E. Espuche, and R. Fulchiron, "Effect of an organo-modified montmorillonite on PLA crystallization and gas barrier properties," *Appl. Clay Sci.*, vol. 53, no. 1, pp. 58–

- 65, 2011.
- [28] E. Rudnik and D. Briassoulis, "Comparative Biodegradation in Soil Behaviour of two Biodegradable Polymers Based on Renewable Resources," *J. Polym. Environ.*, vol. 19, no. 1, pp. 18–39, 2011.
- [29] S. J. De Jong, E. R. Arias, D. T. S. Rijkers, C. F. Van Nostrum, J. J. Kettenes-Van Den Bosch, and W. E. Hennink, "New insights into the hydrolytic degradation of poly(lactic acid): Participation of the alcohol terminus," *Polymer (Guildf)*., vol. 42, no. 7, pp. 2795–2802, 2001.

#### **CHAPTER 5**

### CONCLUSIONS & RECOMMENDATIONS

#### 5.1 Conclusions

As an alternative to the ever-growing demand of petroleum-based conventional polymers, due to issues such as plastic waste management, global warming and limited availability etc. biobased polymers that are biodegradable and sustainable have garnered great interest in the scientific community. One such polymer is poly(lactic acid) (PLA), which has been promoted for its advantages such as biodegradability, zero toxicity, and excellent barrier to flavor and aroma. But certain drawbacks such as poor mechanical and thermal properties, and low flexibility have limited its commercial applications in many sectors such as packaging and automotive industries. One of the main challenges faced by PLA-based materials is that PLA degrades at a slower pace as compared to other organic wastes during composting, which affect its admittance into the industrial composting facilities. Nanoclays in low concentration are known to enhance PLA properties as well as improve PLA biodegradability. According to the previous studies assessing the effect of nanoclays on the PLA biodegradation, claims were made which concluded that nanoclays, in fact increase the biodegradability of PLA in composting environment due to the increasing water sorption producing more chain cleavages. But no control was exercised over the initial weight average molecular number  $(M_n)$ , crystallinity, and thickness of the films, which are known to have a huge impact on the biodegradation. Therefore, it was crucial to understand how nanoclays behave and whether they enhance the biodegradation of the PLA matrix if Mn, crystallinity, and thicknesses are controlled and kept constant among samples [1–4].

So, the first objective of this research was to produce films with the same  $M_n$ , crystallinity, and thickness. These parameters are known to heavily influence the hydrolysis and biodegradation phenomena [5–7]. The results indicated that PLA films and PLA added with nanoclays with the same  $M_n$ , crystallinity, and thicknesses were produced. Controlling these parameters ensured that that they do not exert any influence during the hydrolysis and biodegradation tests and skew the results in favor of nanoclays.

The second phase was conducted to gauge and understand the role of surfactant and nanoclays on the biodegradation of PLA. For this, hydrolysis test was conducted in water at  $58 \pm 2^{\circ}$ C to decouple the abiotic phase of biodegradation in PLA and PLA nanocomposites films [8]. The results showed that the degradation rate constants for PLA and PLA nanocomposites films were not significantly different. The DSC results indicated an increase in crystallinity for PLA and PLA nanocomposites films at the end of the test, implying a recrystallization of the samples and preponderant biodegradation of the amorphous region. Further research needs to be conducted to understand the crystallization effect of samples during hydrolytic degradation.

The final phase focused on understanding the effect of surfactant and nanoclays on the biodegradation process. For this PLA and PLA nanocomposites films were evaluated in inoculated and non-inoculated vermiculite, and a simulated compost environment ( $58 \pm 2^{\circ}$ C,  $50 \pm 5\%$  RH) with an in-house DMR setup by analyzing the evolved CO<sub>2</sub> [9]. No reduction in lag phase of biodegradation was observed for PLA due to the addition of nanoclays. For the compost media, PLA films with QAC showed higher mineralization as compared to PLA nanocomposites films. This was attributed to the two alkyl tails in the surfactant structure, acting as a plasticizer and improving the hydrophilicity of PLA. The non-inoculated and inoculated vermiculite media gave

similar results. Along with  $CO_2$  evolution,  $M_n$  was tracked throughout the biodegradation process and as the results disclosed, nanoclays did not enhance the biodegradation rate of PLA.

#### **5.2 Recommendations**

The future work should focus on having a better control on the film processing conditions even though it is very challenging. Strict control exercised over the processing conditions can eliminate flaws that may be introduced into the samples and have a major impact on the final results. In depth studies should be done to further investigate and better understand the biodegradation mechanism and the interaction and effect of surfactant and nanoclays.

The hydrolysis test should be conducted at different temperatures and in different solutions to assess the effect of nanoclays and surfactant. Deconvolution of the multimodal peaks is necessary and should be explored in further detail to decouple the different molecular weight fractions and underlying mechanism of the hydrolysis process.

- [1] A. P. Gupta and V. Kumar, "New emerging trends in synthetic biodegradable polymers-Polylactide: A critique," *Eur. Polym. J.*, vol. 43, no. 10, pp. 4053–4074, 2007.
- [2] H. Liu and J. Zhang, "Research progress in toughening modification of poly(lactic acid)," *J. Polym. Sci. Part B Polym. Phys.*, vol. 49, no. 15, pp. 1051–1083, 2011.
- T. Wu, T. Xie, and G. Yang, "Preparation and characterization of poly(ε-caprolactone)/Na +-MMT nanocomposites," *Appl. Clay Sci.*, vol. 45, no. 3, pp. 105–110, 2009.
- [4] M. P. Balaguer, C. Aliaga, C. Fito, and M. Hortal, "Compostability assessment of nanoreinforced poly(lactic acid) films," *Waste Manag.*, vol. 48, pp. 143–155, 2016.
- [5] Q. Zhou and M. Xanthos, "Nanoclay and crystallinity effects on the hydrolytic degradation of polylactides," *Polym. Degrad. Stab.*, vol. 93, no. 8, pp. 1450–1459, 2008.
- [6] S. K. Saha and H. Tsuji, "Effects of molecular weight and small amounts of D-lactide units on hydrolytic degradation of poly(L-lactic acid)s," *Polym. Degrad. Stab.*, vol. 91, no. 8, pp. 1665–1673, 2006.
- [7] G. Li, H. Garreau, and M. Vert, "Structure-property relationships in the case of the degradation of massive poly(-hydroxy acids) in aqueous media. Part 3 Influence of the morphology of poly(L-/actic acid)," *J. Mater. Sci. Mater. Med.*, vol. 1, no. 4, pp. 198–206, 1990.
- [8] ASTM International, "ASTM Standard D4754-18, Standard Test Method for Two-Sided Liquid Extraction of Plastic Materials Using FDA," 2003.
- [9] ASTM International, "ASTM D5338-15: Standard Test Method for Determining Aerobic Biodegradation of Plastic Materials Under Controlled Composting Conditions, Incorporating Thermophilic Temperatures," in *ASTM Standards.*, 2015, pp. 1–7.